

AN EVALUATION OF VARIABLES AFFECTING GOLD EXTRACTION AT A
MINERAL PROCESSING PLANT OPERATED IN A SUB-ARCTIC ENVIRONMENT

A
THESIS

Presented to the Faculty
of the University of Alaska Fairbanks

in Partial Fulfillment of the Requirements
for the Degree of

DOCTOR OF PHILOSOPHY

By

John T. Hollow, B.S.

Fairbanks, Alaska

May 2006

UMI Number: 3240326

Copyright 2007 by
Hollow, John T.

All rights reserved.

INFORMATION TO USERS

The quality of this reproduction is dependent upon the quality of the copy submitted. Broken or indistinct print, colored or poor quality illustrations and photographs, print bleed-through, substandard margins, and improper alignment can adversely affect reproduction.

In the unlikely event that the author did not send a complete manuscript and there are missing pages, these will be noted. Also, if unauthorized copyright material had to be removed, a note will indicate the deletion.

UMI[®]

UMI Microform 3240326

Copyright 2007 by ProQuest Information and Learning Company.

All rights reserved. This microform edition is protected against
unauthorized copying under Title 17, United States Code.

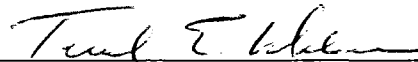
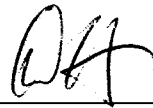
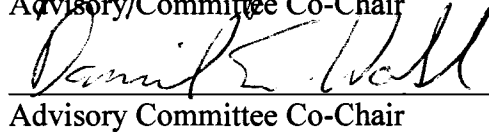

ProQuest Information and Learning Company
300 North Zeeb Road
P.O. Box 1346
Ann Arbor, MI 48106-1346

AN EVALUATION OF VARIABLES AFFECTING GOLD EXTRACTION AT A
MINERAL PROCESSING PLANT OPERATED IN A SUB-ARCTIC ENVIRONMENT

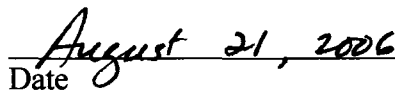
By

John T. Hollow

RECOMMENDED:


Advisory Committee Co-Chair
Advisory Committee Co-Chair
Chair, Department of Mining and Geological Engineering

APPROVED:


Dean, College of Engineering and Mines
Dean of the Graduate School
Date

Abstract

The Fort Knox Mine, located 25 miles northeast of Fairbanks, Alaska, is operated in a sub-Arctic environment. Since process slurry temperatures cycle seasonally with air temperature, the mine presents a unique opportunity to measure the impact of slurry temperature on process performance under full scale plant conditions. This thesis analyzes an energy balance approach to model the seasonal variations in slurry temperature throughout the Fort Knox mill.

The mill utilizes both gravity concentration and cyanidation for gold recovery. Models were developed to accurately predict the impact of slurry temperature on cyanide leach, carbon adsorption and cyanide destruction kinetics. The energy balance model, combined with the kinetics models, was used to accurately predict the gold recovery and subsequently to justify the installation of a tailings wash thickener to recovery heat from the mill tailings. A substantial portion of this thesis is dedicated to the development of these models, analysis of the post expansion plant performance, and summarizing project economics.

Gold in the Fort Knox deposit is generally less than 100 microns in size and contained in quartz veins and along shears within the host granite, at an average gold grade of 0.8 g/metric ton. In April 2001, the mill began processing ore from a satellite ore deposit, the True North Mine, as a blend with Fort Knox ore. The gold grade in the True North deposit averages 1.5 g/metric ton and can be associated with pyrite, arsenopyrite and stibnite.

An unexpected drop in gold recovery resulted from processing the blended ore and was the subject of an extensive laboratory evaluation. Laboratory results suggested that the leach kinetics of the coarse gold particles were significantly impacted, when the blended ore was processed, and that the impact could be reduced, or eliminated, with the addition of lead nitrate. Subsequently, a lead nitrate addition scheme was implemented at the Fort Knox mill. A portion of this thesis is dedicated to a review of the laboratory

program, an evaluation of the environmental impacts and a summary of plant performance, when utilizing lead nitrate at the Fort Knox Mine.

Table of Contents

	Page
Signature Page	i
Title Page	ii
Abstract	iii
Table of Contents	v
List of Figures	ix
List of Tables	xiii
Acknowledgements.....	xv
Chapter 1 Thesis Introduction.....	1
1.1 General Introduction.....	1
1.2 Overview of Chapters.....	2
References	5
Chapter 2 The Effect of Pb(NO₃)₂ Addition on the Processing of Blended Fort Knox and True North Ores at the Fort Knox Mine	6
2.1 Abstract.....	6
2.2 Introduction	6
2.3 Gold Loss in the Tailing Solution.....	9
2.4 Testing of Mill Leach Feed Material (APRIL 24-29)	10
2.5 Testing of Mill Tailings Material (APRIL 24-29).....	12
2.6 Environmental Implications of Lead Nitrate Addition.....	15
2.7 Conclusions	18
References	19

Chapter 3 Optimizing Cyanidation Parameters for Processing of Blended Fort Knox and True North Ores at the Fort Knox Mine	23
3.1 Abstract.....	23
3.2 Introduction	24
3.3 CANMET Laboratory Investigation.....	27
3.3.1 Leachable Gold Content	28
3.3.2 Effect of Pre-treatment.....	29
3.3.3 Effect of Lead Nitrate Addition.....	31
3.3.4 Effect of Cyanide Concentration	32
3.3.5 Effect of Dissolved Oxygen Concentration.....	33
3.3.6 Effect of Slurry pH.....	34
3.3.7 Effect of Antimony on Gold Extraction	35
3.4 Fort Knox Laboratory Results.....	36
3.4.1 Effect of Lead Nitrate Addition on Leaching Fort Knox Ore.....	37
3.4.2 Effect of Lead Nitrate Addition on Leaching True North Ore	38
3.4.3 Effect of Lead Nitrate Addition on Blend of Fort Knox and True North Ores.....	38
3.4.4 Effect of Antimony and Lead Nitrate Addition	40
3.5 Comparison Fort Knox and CANMET Results.....	42
3.6 Discussion.....	44
3.7 Conclusions	45
3.8 Acknowledgements	46
References	46
Chapter 4 Modeling the Influence of Slurry Temperature on Gold Leach and Adsorption Kinetics at the Fort Knox Mine, Fairbanks, Alaska	48
4.1 Abstract.....	48
4.2 Introduction	48
4.3 Model Development.....	54
4.3.1 Gold Dissolution in Cyanide Solution.....	54
4.3.2 Effect of Temperature on Leach Slurry Rheology.....	57
4.3.3 Effect of Temperature on Leach Oxygen Concentration.....	59

4.3.4	Effect of Temperature on Gold Leach Rate.....	62
4.3.5	Effect of Temperature on CIP Circuit Efficiency.....	69
4.4	Model Predictions and Discussion	72
4.5	Conclusions	76
	References	77
Chapter 5 Modeling the Influence of Slurry Temperature on the Cyanide Destruction Plant at the Fort Knox Mine, Fairbanks, Alaska.....		81
5.1	Abstract.....	81
5.2	Introduction	81
5.2.1	Process Description.....	82
5.2.2	Process Chemistry.....	83
5.2.3	Cyanide Analytical Techniques	86
5.2.4	Plant Performance	88
5.3	Model Development.....	90
5.4	Conclusions and Recommendations	106
5.5	Supplemental Work - 2001	107
	References	111
Chapter 6 The Development of an Energy Balance Model to Predict the Economic Impact of Installing a Tailings Wash Thickener at the Fort Knox Mine, Fairbanks Alaska.....		112
6.1	Abstract.....	112
6.2	Introduction	112
6.2.1	Ambient Air Temperature.....	114
6.2.2	Precipitation.	114
6.2.3	Snow Pack.....	114
6.2.4	Water Supply Reservoir (WSR) Water Temperature	115
6.2.5	Tailings Storage Facility (TSF) Water Temperature	116
6.3	Energy Balance Temperature Model.....	117
6.3.1	Ore Temperature Determinations	119
6.3.2	Ore Moisture Content.	120

6.3.3 Grinding Circuit Heat Input	122
6.3.4 Grinding Circuit Heat Losses.....	122
6.3.5 Model Verses Actual Leach Feed Temperature.....	122
6.3.6 Heat Transfer from Leach and CIP Tanks	124
6.3.7 Heat Input to Leach/CIP Circuit	125
6.3.8 Heat Exchange Between the Atmosphere and Leach/CIP Circuit.....	125
6.4 Results and Discussion.....	131
6.4.1 Predicted Impact of TWT on Gold Recovery	136
6.4.2 Predicted Impact of TWT on Reagent Usage	139
6.5 TWT Project Schedule.....	141
6.6 TWT Project Cost.....	143
6.7 Post TWT Expansion Leach Gold Recovery.....	144
6.8 Post TWT Expansion Reagent Usage.....	148
6.9 Project Financial Analysis.....	154
6.10 Conclusions	155
References	156
Chapter 7 Recommendations for Future Work.....	158

List of Figures

	Page
Figure 2.1: Eh-pH equilibrium diagram for the Pb-S-H ₂ O system at.....	16
Figure 3.1: Fort Knox mill process flowsheet	25
Figure 3.2: Leachable gold of the blend sample from Fort Knox.....	29
Figure 3.3: Effect of pre-treatment, with and without lead nitrate,	30
Figure 3.4: Effect of lead nitrate addition on cyanidation, without.....	31
Figure 3.5: Effect of NaCN concentration on leaching of the	32
Figure 3.6: Effect of dissolved oxygen concentration on leaching of	33
Figure 3.7: Effect of slurry pH on cyanidation of the.....	34
Figure 3.8: Effect of stibnite concentration on gold recovery by	36
Figure 3.9: Comparison of the extraction of gold from Fort	37
Figure 3.10: Comparison of the extraction of gold from True	38
Figure 3.11: Comparison of plant performance and FGMI laboratory testing	39
Figure 3.12: Effect of antimony concentration in the feed	41
Figure 3.13: Effect of lead nitrate - comparison between laboratory and	43
Figure 4.1: Simplified flowsheet of the Fort Knox mill	50
Figure 4.2: Leach circuit and ambient air temperatures, °C (1999-2001)	51
Figure 4.3: Regression - Leach gold recovery vs. slurry temperature (1998-2001)	52
Figure 4.4: Regression - CIP solution gold loss vs. slurry temperature	52
Figure 4.5: Regression - Leach circuit lime addition vs. slurry temperature.....	53
Figure 4.6: Regression - Ratio of SO ₂ :NaCN vs. slurry temperature (1998-2001)	54
Figure 4.7: Summary of 1993 rheology studies on Fort Knox	58
Figure 4.8: Historical Fort Knox leach slurry [O ₂] vs. slurry	60
Figure 4.9: Theoretical rate controlling regions vs. slurry temperature	61
Figure 4.10: Historical Fort Knox leach/CIP circuit [NaCN] (2000-2006).....	62
Figure 4.11: Monthly cyanide soluble gold in solid tailings;(1997-2001)	63
Figure 4.12: Comparison of 2004 laboratory results and order (n)	65
Figure 4.13: Comparison of plant data and order (n) of	66

Figure 4.14: Comparison of plant data and order (n) of	66
Figure 4.15: Arrhenius plot - effect of slurry temperature on leach	68
Figure 4.16: Typical first-order rate relationship CIP profile.....	70
Figure 4.17: Arrhenius plot - effect of slurry temperature on CIP	71
Figure 4.18: Model error term vs. carbon advance rate	72
Figure 4.19: Comparison of plant solid tailings [Au] and predicted	73
Figure 4.20: Comparison of plant solution tailings [Au] and predicted	74
Figure 5.1: Simplified flowsheet of the Fort Knox Mine leach/CIP.....	82
Figure 5.2: Comparison of analytical techniques used to determine weak-acid.....	87
Figure 5.3: Comparison of detox feed slurry free cyanide concentration.....	88
Figure 5.4: Timeline of detox feed, detox control and detox.....	90
Figure 5.5: Relationship between [CN _{WAD}] measured in compliance and operator	93
Figure 5.6: Trend line of detox feed slurry pH at	94
Figure 5.7: Actual ABS addition rate vs. ABS addition rate	96
Figure 5.8: Trend line of actual and predicted ABS addition	96
Figure 5.9: Standardized residual timeline, Detox Model 2000	97
Figure 5.10: Actual ABS addition rate vs. ABS addition rate	99
Figure 5.11: Trend line of actual and predicted ABS addition	99
Figure 5.12: Standardized residual timeline, Detox Model 2000a	100
Figure 5.13: Actual ABS addition rate vs. ABS addition rate	101
Figure 5.14: Trend line of actual and predicted ABS addition	102
Figure 5.15: Standardized residual timeline, Detox Model 2000b	103
Figure 5.16: Actual ABS addition rate vs. ABS addition rate	105
Figure 5.17: Trend line of actual and predicted ABS addition	106
Figure 5.18: Standardized residual timeline, Detox Model 2000c	106
Figure 5.19: Trend line of Cu ²⁺ :SO ₂ addition rate ration.....	108
Figure 5.20: Trend line of actual and predicted ABS addition	110
Figure 5.21: Actual ABS addition rate vs. ABS addition rate	110
Figure 6.1: Ore temperature - model vs. themal scan data	120

Figure 6.2: Model input - Ore moisture content	121
Figure 6.3: Ore moisture content vs. precipitation.....	121
Figure 6.4: Actual and predicted leach feed slurry temperature.....	123
Figure 6.5: Actual vs. predicted leach feed slurry temperature	123
Figure 6.6: Historic leach/CIP circuit temperature	124
Figure 6.7: Historic temperature drop in leach/CIP tanks	125
Figure 6.8: Heat transfer coefficient model error trend.....	127
Figure 6.9: Error trend with model adjustment factor.....	128
Figure 6.10: Actual and predicted temperature drop in leach/CIP tanks	129
Figure 6.11: Actual and predicted CIP discharge slurry temperature	129
Figure 6.12: Actual vs. predicted CIP discharge slurry temperature	130
Figure 6.13: Simplified flowsheet for the proposed tailings thickener expansion.....	131
Figure 6.14: Baseline temperatures at the Fort Knox Mine	132
Figure 6.15: Effect of TWT underflow density on ΔT_w and ΔT_s	133
Figure 6.16: TWT effect on mill makeup water temperature.....	135
Figure 6.17: TWT effect on leach feed temperature	135
Figure 6.18: Temperature effect on solid gold loss.....	137
Figure 6.19: Temperature effect on solution gold loss.....	137
Figure 6.20: TWT effect on total leach gold recovery	138
Figure 6.21: TWT effect on NaCN addition in leach circuit.....	139
Figure 6.22: TWT effect on detox feed slurry $[CN_{WAD}]$	140
Figure 6.23: TWT effect on detox circuit ABS addition.....	141
Figure 6.24: TWT effect on detox circuit copper sulfate addition.....	141
Figure 6.25: Actual vs. predicted solid tailings $[Au]$	145
Figure 6.26: TWT effect on solution gold loss	145
Figure 6.27: TWT effect on solution tailings $[Au]$	146
Figure 6.28: TWT effect on leach gold recovery	147
Figure 6.29: NaCN addition vs. leach $[NaCN]$	148
Figure 6.30: TWT effect on detox circuit feed $[NaCN]$	149

Figure 6.31: TWT effect on leach discharge [NaCN].....	150
Figure 6.32: Lime addition vs. slurry temperature	150
Figure 6.33: Historic TSF water and final plant tailings [CN _{WAD}].....	152
Figure 6.34: TWT effect on CIP discharge [CN _{WAD}]	152
Figure 6.35: Effect of TSF [CN _{WAD}] on detox feed slurry	153

List of Tables

	Page
Table 2.1: Composite tailing solution and loaded carbon analysis, ppm.....	10
Table 2.2: Summary of bottle roll tests for mill leach	11
Table 2.3: Summary of gravity concentration tests performed on leach	12
Table 2.4: Sulfide mineral distribution in the gravity concentrates from	13
Table 2.5: Summary of leaching tests on gravity tailings.....	14
Table 2.6: Lead distribution in cyanidation tests without lead nitrate.....	16
Table 2.7: Lead distribution in cyanidation tests with lead nitrate	17
Table 2.8: MWMP test of True North composite cyanidation residue.....	18
Table 2.9: MWMP test of True North composite cyanidation residue.....	18
Table 3.1: Mineralogical and chemical analysis of the blend sample	27
Table 3.2: Effect of pretreatment on the cyanidation of the	30
Table 3.3: Actual plant and bottle roll test results on	40
Table 3.4: FGMI, CANMET laboratory results and actual plant performance	42
Table 4.1: Mill conditions evaluated	75
Table 4.2: Predicted mill grades and losses	75
Table 5.1: Critical dates in detox circuit operating history.....	89
Table 5.2: Regression statistics for the 2000 Detox Model	95
Table 5.3: Regression statistics for the 2000a Detox Model	98
Table 5.4: Regression statistics for the 2000b Detox Model	101
Table 5.5: Regression statistics for the 2000c Detox Model	104
Table 5.6: Regression statistics for the 2001 Detox Model	109
Table 6.1: Fort Knox Mine average air temperature, °C.....	114
Table 6.2: Fort Knox Mine average precipitation, cm.....	115
Table 6.3: Fort Knox Mine average snow fall, cm	115
Table 6.4: Fort Knox Mine mean WSR water temperature, °C	116
Table 6.5: Fort Knox Mine mean TSF water temperature, °C.....	117
Table 6.6: Baseline meteorological and water conditions used for the	133

Table 6.7:	Baseline operating parameters – TWT evaluation.....	134
Table 6.8:	Project schedule and key milestones	142
Table 6.9:	Project cost summary.....	143
Table 6.10:	Estimated increase in gold production and revenue from	146
Table 6.11:	Changes in reagent usage and reagent spending due.....	154
Table 6.12:	Summary of project financial analysis	154

Acknowledgments

The work presented in this thesis was made possible by the encouragement and patience of family and friends, I thank them for their involvement. I would also like to thank Dr. Steve Lin, Professor Dan Walsh, Dr. Ted Wilson and Dr. Dan White for their time commitment and guidance as my advisory committee. The quality of the publications resulting from this work is the direct result of the input and guidance of my committee Co-Chairmen, Professor Walsh and Dr. Lin. I would like to extend my sincere gratitude for their active participation in my research and development over the past ten years.

I would also like to thank the personnel at Fairbanks Gold Mining, Inc. for their ongoing support of the work and the confidence required to supply funding for the recommended process improvements. Without the implementation of the plant improvement projects, the validation of this work would have been incomplete.

CHAPTER 1

THESIS INTRODUCTION

1.1 GENERAL INTRODUCTION

With the renewed interest in hard rock mining in Alaska's interior and the increasing cost of energy, a better understanding of the variables affecting mineral processing plant performance is required. The Fort Knox Mine, located in the Fairbanks Mining District, 40-road km (25 miles) northeast of Fairbanks, Alaska, began commercial gold production in the first quarter of 1997. Through the combined effort of the metallurgical group at the Fort Knox Mine and faculty from the Mineral Industry Research Laboratory at the University of Alaska Fairbanks, more information on the subject has been developed.

The Fort Knox Mine is owned by Kinross Gold Corporation and operated by Fairbanks Gold Mining, Inc. (FGMI), a 100% owned subsidiary of Kinross Gold. The average annual temperature at the site is -3.6°C (26°F) with daily temperatures averaging -23.8°C (-10.9°F) in January and 15.8°C (60.4°F) in July. The mine is accessible year round from Fairbanks via the Steese Highway and 9.7 km (6 miles) of well-maintained gravel road.

The Fort Knox gold deposit was defined as a 91.3 million metric ton resource at a grade of 0.8 g/t Au and is hosted within a multi-phase granitic body with an elongated surface exposure. Gold is contained in milky-white quartz stockwork veins and veinlets, as well as along shears and fractures within the granite. The quartz filled shears contain evenly distributed gold, generally less than 100 microns in size, while the gold in the milky-white stockwork veins and veinlets is similar in size, but has a more erratic occurrence. The ore is free milling at a relatively coarse grind (65%-100 mesh), has a gravity recoverable gold (GRG) content of 30-65% and has relatively little sulfide mineralization.

The True North Mine is located 15 kilometers northeast of the Fort Knox Mine and was defined as a 6.4 million metric ton resource at an average grade of 1.5 g/t Au. Gold mineralization is more variable in the True North reserve with a GRG content less

than 4% and can be associated with sulfides. In April 2001, FGMI began blending and processing ore from the True North Mine at the Fort Knox mineral processing facility. Ore from the True North Mine was trucked to the Fort Knox mill, where it was blended with Fort Knox ore and represented approximately 20% of the annual material processed through the mill facility from 2001 through 2004.

The relatively consistent low grade ore processed under tightly controlled conditions through the Fort Knox mill provided for an opportunity to research variations in gold extraction and adsorption, as a function of controlled changes in solution chemistry. Additionally, the actual plant slurry temperatures cycle seasonally and presented a unique opportunity to measure the impact of this variable under full scale plant conditions.

The studies included in this thesis were selected, in order to improve the understanding of the impact of a sub-Arctic environment on gold plant performance. From this understanding, appropriate evaluations can be completed to optimize plant design and maximize operating efficiencies and profits.

1.2 OVERVIEW OF CHAPTERS

This thesis is divided into seven chapters; this introduction, five research related chapters, and the final chapter summarizing recommendations for related future research opportunities. Chapters 2, 3, 4 and 6 have been prepared as separate journal manuscripts. Each of these manuscripts has its own introduction, discussion of data, analysis, conclusions and references, which are specific to the individual chapters. The individual chapters are expanded versions of the published manuscripts and do not reflect the order in which the work was completed. The discussion, figures and tables in the thesis are presented in metric units, unless otherwise noted. Condensed versions of the chapters have been published.

Chapter 2 presents results of an investigation of the reduction in gold extraction experienced when Fairbanks Gold Mining, Inc. (FGMI) began processing a blend of True North ore and Fort Knox ore through the mill at Fort Knox. The primary objective of the

study was to identify the cause of the reduced gold extraction and identify alternative processing scenarios, that would minimize the negative effects of processing the blended ore.

The results indicated that the poor extraction was the result of a surface chemistry problem affecting gold particles due to the dissolution of minerals contained in True North ore. The extraction was substantially improved through the addition of lead nitrate and elevated cyanide concentrations in leach. The work from Chapter 2 was presented at the Annual SME Meeting in Cincinnati, Ohio in February 2003, accepted for publication in June 2003, and published in *Minerals and Metallurgical Processing* (Hollow *et al.*, 2003a).

Chapter 3 is essentially a continuation of the work completed in Chapter 2. It focused on optimizing plant performance, when processing the blend of Fort Knox and True North ores. The work included further laboratory investigations and modeling of plant performance using various reagent schemes. The laboratory results correlated strongly with the plant performance and indicated the approach used in the lab was reliable.

A lead nitrate/cyanidation processing scheme was implemented in the Fort Knox mill in January, 2002. Applying the model to actual plant operating conditions over the initial 18 month period and predicting the gold extraction without the lead nitrate addition, indicates that the plant gold production was increased by 49,600 ounces, at an incremental cost of \$US32 per ounce due to the lead nitrate addition. The preliminary results contained in Chapter 3 were presented at Hydrometallurgy 2003 in Vancouver, B.C., Canada and published in the proceedings (Hollow *et al.*, 2003b). Additionally updated material from the chapter was presented at the 36th Annual Meeting of the Canadian Mineral Processors in Ottawa, Canada in January 2004 and published in the proceedings (Hollow *et al.*, 2004).

Chapter 4 describes the development of the gold leach and carbon adsorption models that accurately predict the impact of slurry temperature on circuit efficiencies.

The chapter contains a detailed review of the mechanism for gold dissolution in cyanide solution and a summary of modeling techniques successfully developed in the past. These models were then modified based on work completed over the last six years at Fort Knox to include temperature terms to predict plant performance.

Applying the mathematical models to baseline plant operating conditions indicates that gold extraction increases from 86.5% to 89.4%, when the plant slurry temperature increases from 10.0°C (typical temperature reached during winter operation at the Fort Knox mill) to 26.7°C (typical temperature reached during summer operation at the Fort Knox mill) and represents a difference in daily leach gold production of approximately 33 ounces. The work described in Chapter 4 was presented at the Annual SME Meeting in Salt Lake City, Utah in February 2005, accepted for publication in December 2005 and published in *Minerals and Metallurgical Processing* (Hollow *et al.*, 2006).

Chapter 5 describes the development of the cyanide destruction process model that measures the impact of slurry temperature on reaction equilibriums and kinetics. The work contained in Chapter 5 has not been formally presented nor published, but is included in the thesis and referenced in the manuscript summarizing the Fort Knox plant expansion in Chapter 6. Since the work contained in Chapter 5 was prepared as an internal Fort Knox Mine report, the discussion, figures and tables are presented in English units and is an exception to the other chapters in the thesis.

Chapter 6 describes the development of an energy balance model that accurately predicts plant slurry temperature resulting from variations in outdoor air temperature, process water temperature, mill process equipment and operational strategies. The chapter also contains the justification for installing a tailings wash thickener at Fort Knox and presents a summary of plant operating results for 38 months following the thickener installation, which validates the modeling work to date.

Applying the multiple process models developed by this thesis research to actual plant operating conditions and evaluating post expansion performance, indicates that gold

production was increased by 19,157 ounces, generating a \$7,365,000 increase in revenue, while decreasing operating costs by \$6,302,000, over a 38 month period. The work described in Chapter 6 will be presented at the Annual SME Meeting in Denver, Colorado in February 2007 and has been accepted, with minor revisions, for publication in *Minerals and Metallurgical Processing* (Hollow *et al.*, 2007).

Chapter 7 contains recommendations for future investigations, that could add to the research contained in this thesis.

REFERENCES

- Hollow, J.T., Hill, E.M., Lin, H.K., and Walsh, D.E., 2003a, *The effect of $Pb(NO_3)_2$ addition on the processing of blended Fort Knox and True North ores at the Fort Knox Mine*, Minerals and Metallurgical Processing, Vol. 20, No. 4, pp. 185-190.
- Hollow, J., Deschenes, G., Guo, H. and Hill, E., 2003b, *Optimizing cyanidation parameters for processing of blended Fort Knox and True North ores at the Fort Knox Mine*, Hydrometallurgy 2003 – Fifth International Conference in Honor of Professor Ian Ritchie, Vol. 1: Leaching and Solution Purification, pp. 21-34.
- Hollow, J., Deschenes, G., Guo, H., Fulton, M. and Hill, E., 2004, *Improvement of Gold Extraction at the Fort Knox Mine*, Proceedings, 36th Annual Meeting of the Canadian Mineral Processors, pp. 435-449.
- Hollow, J.T., Hill, E.M., Lin, H.K., and Walsh, D.E., 2006, *Modeling the influence of slurry temperature on gold leach and adsorption kinetics at the Fort Knox Mine, Fairbanks, Alaska*, Minerals and Metallurgical Processing, Vol. 23, No. 3, pp. 151-159.
- Hollow, J.T., Lin, H.K., Walsh, D.E. and White, D.M., 2007, *The Development of an energy balance model to predict the economic impact of installing a tailings wash thickener at the Fort Knox Mine, Fairbanks, Alaska*, Minerals and Metallurgical Processing, accepted for publication.

CHAPTER 2

THE EFFECT OF $\text{Pb}(\text{NO}_3)_2$ ADDITION ON THE PROCESSING OF BLENDED FORT KNOX AND TRUE NORTH ORES AT THE FORT KNOX MINE¹

2.1 ABSTRACT

Fairbanks Gold Mining, Inc. (FGMI) began blending and processing True North ore at their Fort Knox mill on April 12, 2001. Gold extraction subsequently dropped from 88% to 71% during the last week of April 2001. Twenty five percent of the gold values remaining in the leach tailings were gravity recoverable free gold. Significant quantities of stibnite and arsenopyrite were also identified in the tailings. In laboratory bottle roll tests, the gold extraction from a composite of leach circuit feed collected during the same period was 72.6%, when leached at an average NaCN concentration of 0.16 g/kg. The extraction increased to 82.4% with 0.5 g/kg NaCN and to 91.7% with 0.5 g/kg NaCN plus 0.075 g/kg $\text{Pb}(\text{NO}_3)_2$, respectively. A passivating layer, resulting from sulfide mineral dissolution, surrounded liberated gold particles and likely contributed to the reduced gold recovery. The gold recovery can be substantially increased by the addition of lead nitrate. Lead species remain in the solid residues after leaching and were not mobilized using Meteoric Water Mobility Procedure.

2.2 INTRODUCTION

Fairbanks Gold Mining, Inc. (FGMI) began blending and processing True North ore at their Fort Knox mill on April 12, 2001. The ore averaged 14.4% of the total mill throughput between April 12 and April 23. Gold recovery during this period (88%) was consistent with expected mill gold recovery. However, beginning on April 24, mill gold recovery dropped substantially below any values historically obtained with Fort Knox ore, and poor performance continued into May. Between April 24 and April 29, the

¹ Hollow, J.T., Hill, E.M., Lin, H.K., and Walsh, D.E., (2003), *Minerals and Metallurgical Processing*, Vol. 20, No. 4, pp. 185-190.

overall mill gold extraction was 71.1%, with no significant change in the percentage (16.4%) of True North ore blended in the mill feed.

During the last week of April, the cyanide concentration in the mill's leach circuit was increased substantially with a minimal impact on total gold recovery. Although NaCN was subsequently added to the grinding circuit, all cyanide addition was to the leach circuit during the late-April time frame encompassing this evaluation.

The True North ore contains sulfide minerals that are known to impact gold-leach kinetics and overall recovery. Stibnite (antimony sulfide), arsenopyrite, orpiment and realgar (arsenic sulfides) are examples of these minerals (Hedley and Howard, 1958; Habashi, 1967; Nicol *et al.*, 1987; Yannopoulos, 1991; Marsden and House, 1992). Numerous articles and research programs (Barsky *et al.*, 1934; Kameda, 1949; Fink and Putnam, 1950; Krudryk and Kellogg, 1954; Weischselbaum *et al.*, 1989; Jeffrey and Breuer, 2000; Tshilombo and Sandenbergh, 2001) have targeted the impact of sulfide and hydrosulfide ions on gold dissolution. In addition, substantial research has been performed on both synthetic and naturally occurring sulfide minerals to measure the retarding effect of sulfide ions on gold cyanidation (Hedley and Howard, 1958; Lorenzen and Van Deventer, 1992a, 1992b; Kondos *et al.*, 1995; Deschenes and Wallingford, 1995, 1998, 1999a, 1999b, 2000). Both sulfide and hydrosulfide ions are generated during the dissolution of sulfide minerals in cyanidation circuits.

Under laboratory conditions, it was found that the addition of 1,000 ppm stibnite completely stopped gold dissolution from a rotating gold disc that was submerged in 0.23 kg NaCN per ton solution at a pH of 10.5, with a dissolved oxygen concentration of 8 ppm (Liu and Yen, 1995). The same effect was also measured when the dissolved oxygen concentration was increased to 32 ppm. The retarding effect of the stibnite was attributed to neither cyanide nor oxygen depletion, but to the formation of a dark-brown colored film on the gold disc surface. The passivating effect of SbO^+ , generated during the oxidation of stibnite, on gold leaching has also been confirmed (Avraamides *et al.*, 2000).

The generally accepted theory is that sulfide ions released during the oxidation of the sulfide minerals form a passivating layer on the liberated gold surface, retarding and ultimately stopping the cyanidation process. Depending on the mineralogy of the sample, oxides, carbonates and cyanide complexes films may also retard the cyanidation kinetics (Lorenzen and Van Deventer, 1992a). A mathematical model based on the electrochemical mechanism for batch leaching of a particulate gold ore has been developed (Crundwell and Godorr, 1996). The model incorporates the formation of a passivating layer, which forms on the surface of the gold during the course of the reaction. Although no work was done to identify the chemistry of the film, the model produced a good description of the actual leaching curve for two South African ores, as well as test results previously published from leach tests conducted on a Canadian ore.

It has been shown that the presence of lead, mercury, bismuth, and, especially, thallium can have an accelerating effect on gold dissolution (Cathro and Koch, 1964; Chimenos *et al.*, 1997). Tshilombo and Sandenbergh (2001) found that lead was slightly more noble than gold in an aqueous cyanide solution and could be reduced to metallic lead on an anodically dissolving gold surface. They showed that at potentials where lead was in the form of a soluble lead species, the presence of lead increased the anodic dissolution of gold significantly. It has also been theorized that the heavy metal atoms are deposited on the surface of the gold and disrupt the formation of the passivating layer (Nicol, 1980; Jeffrey *et al.*, 1996; Deschenes *et al.*, 2000).

The accelerating effect of the above-mentioned heavy-metal ions has also been measured in the absence of sulfide ions (Jeffrey *et al.*, 1996). Thus, it can be assumed that the influence of these ions is somewhat independent of the chemical nature of the passivating film. A number of researchers also reported that lead can have a passivating effect when added in high concentrations and that the Pb:CN ratio can be an important variable in investigations (Kameda, 1949; Weichselbaum *et al.*, 1989; Lorenzen and Van Deventer, 1992b; Jeffrey *et al.*, 1996; Tshilombo and Sandenbergh, 2001). In addition, a passivating layer can be attributed to a buildup of the $[\text{AuCN}]_{\text{ads}}$ species (Cathro and Koch, 1964; MacArther, 1972; Thurgood *et al.*, 1981; Lin and Chen, 2001). The

formation of the $[\text{NaCN}]_{\text{ads}}$ was shown to be the intermediate step in the oxidation of Au to $\text{Au}(\text{CN})_2^-$.

To evaluate the cause of the reduced gold extraction at the Fort Knox mill during late April, the FGMI metallurgical department conducted a series of bottle-roll tests on grab samples of mill-tailing material. These tests were intended to determine the cyanide-soluble gold content remaining in the plant tailings. The results indicated that only 3% to 4% improvement in extraction could be realized at high leach cyanide concentrations and four to six additional hours of leaching. Preg-robbing tests and finer grinds were also evaluated, and neither was found to be a factor. Based on these preliminary findings, the additional studies described in the following sections of this paper were performed.

2.3 GOLD LOSS IN THE TAILING SOLUTION

Evident during the April 24-29 period was a significantly higher gold loss in tailing solution than would normally be expected for the given mill processing conditions. To identify the source of the reduced carbon circuit efficiency, composite, loaded carbon samples were collected from the circuit during the first two weeks of April (immediately prior to blending True North ore) and the last two weeks of April (while blending True North ore). The samples were analyzed to determine if any known carbon-fouling problem could be identified. In addition, a composite (April 24-29) CIP tailing solution sample was collected and sent to Intermountain Laboratories (IML) for analysis. Table 2.1 summarizes the major element concentrations for these carbon and solution samples.

The only major difference identified between the two carbon samples was a detectable level of arsenic for the samples collected after the start of True North ore processing. Although the overall carbon activity remained consistent, above normal gold losses in the tailing solution were measured during the late April period. These losses were later determined to be residual leaching from the solid in the sample buckets and not actual gold losses due to poor carbon-circuit performance. This indicated that significant

cyanide-soluble gold existed in the plant tailings, and this was the result of reduced gold dissolution kinetics in the leach circuit. The presence of antimony in the tailing solution, along with field observations by mine geologists, indicated that significant quantities of stibnite could have been present in the mill feed material.

Table 2.1 Composite tailing solution and loaded carbon analysis, ppm.

Sample	As	Sb	Ca	Cu	Fe	Mo	Po	Si	Na	Zn	Sulfate
Loaded Carbon ¹ 4/1-4/15	<1	<5	3866	91.0	18.0	<5	54.0	n.a.	212	25.0	n.a.
Loaded Carbon ¹ 4/16-4/31	2.0	<5	3698	96.0	7.0	<5	40.0	n.a.	171	22.0	n.a.
Tails Solution ² 4/24-4/29	1.0	6.3	97.1	7.54	0.65	0.4	12.1	9.5	122	0.38	225

¹32 element: SM3120 B ICP

²EPA 600/R94/111

2.4 TESTING OF MILL LEACH FEED MATERIAL (APRIL 24-29)

Although ore displaying poor gold recovery characteristics has been identified within Fort Knox ore reserves, historically the gold extraction for this material is typically 5% - 7% below normal operation - not the 15% - 20% experienced in late April. Therefore, to evaluate the effect of lead nitrate addition on the leach kinetics at various cyanide concentrations, a series of bottle roll cyanidation tests were conducted on a leach feed composite sample collected April 24-29, 2001. The results indicate that gold extraction rates are substantially improved with the addition of lead nitrate at all cyanide concentration levels evaluated. Table 2.2 summarizes these bottle roll tests results.

The results indicate that blended Fort Knox and True North ore is sensitive to cyanide concentrations. The tests yielded a gold extraction of 49.9%, when leached at a sodium cyanide concentration of 0.068 g NaCN per kg solution and yielded a gold extraction of 82.4% when leached at a sodium cyanide concentration of 0.455 g NaCN per kg solution. The impact of lead nitrate was significant in this bottle roll series, with

gold extraction increasing to 79.5% and 90.7%, respectively, for the above NaCN concentrations. All lead nitrate bottle-roll tests were performed in triplicate with the reported values being the average of the three tests. In separate cyanidation tests on straight True North ore, results of 24-hour bottle-roll tests indicate that gold extraction increases moderately through the addition of lead nitrate at all cyanide concentrations.

Table 2.2 Summary of bottle roll tests for mill leach feed material (April 24-29).

Test Number	Head Grade Au, mg/kg	Dissolved Oxygen, ppm	pH	[NaCN] g/kg solution	Pb(NO ₃) ₂ Addition g/kg ore	Gold Extraction, % Leach Time, hrs.				
						0*	2	4	6	20
Series 1	1.101	7.5	10.8	0.068	0.000	10.2	25.5	32.9	28.2	49.9
Series 2	1.142	7.5	10.8	0.068	0.136	9.9	48.9	61.9	n.a.	79.5
Series 3	1.125	7.5	10.8	0.173	0.000	10.0	29.9	37.6	46.1	72.6
Series 4	1.129	7.5	10.8	0.173	0.136	10.0	72.7	79.8	n.a.	85.0
Series 5	1.078	7.5	10.8	0.455	0.000	10.4	40.3	47.9	55.0	82.4
Series 6	1.047	7.8	10.8	0.455	0.136	10.8	60.4	72.1	n.a.	90.7
Series 7	1.054	7.8	11.0	0.455	0.068	10.7	55.6	70.0	n.a.	91.7

*Due to addition of cyanide in grinding circuits.

The results also indicate that gold extraction is slightly higher (91.7%) at a lead nitrate addition rate of 0.068 g/kg of ore, than it is at 0.136 g/kg, for the series 6 and 7 tests conducted at a NaCN concentration of 0.455 g/kg solution. Although this may not be a statistically significant increase in gold extraction, a number of the references (Kameda, 1949; Weichselbaum et al., 1989; Jeffrey et al., 1996; Deschenes and Wallingford, 1995; Tshilombo and Sandenbergh, 2001) indicate that excess lead nitrate addition can have a negative impact on gold extraction. Additional optimization work is planned to determine the relationship between gold extraction and lead nitrate addition.

Numerous references also indicate that the benefits associated with lead nitrate are ore dependent and optimum leach conditions need to be evaluated on an individual ore basis. Under experimental conditions, the effectiveness of lead nitrate addition was found to be a function of the gold particle size and shape. The lead nitrate addition rates

found in the literature (Kondos et al., 1995; Dechenes et al., 1995, 1998, 1999, 2000) range between 0.023 g/kg (0.05 lbs/st) ore to and 0.68 g/kg (1.50 lbs/st). In most cases, the greatest benefits were realized with addition rates in the 0.045 to 0.182 g/kg (0.10 to 0.40 lbs/st) range.

2.5 TESTING OF MILL TAILINGS MATERIAL (APRIL 24-29)

A test program was also performed on a 17-kg composite leach tailings sample from the April 24-29 period. To generate gravity concentrate and middlings products, the FGMI metallurgical department processed the 17-kg sample over a Gemini table at the Mineral Industry Research Laboratory (MIRL). The distribution of gold in the table products, shown in Table 2.3, indicates a substantial portion of the gold is gravity recoverable, reporting to the table concentrate and middling products.

Table 2.3 Summary of gravity concentration tests performed on leach tailings composite.

Sample	Au, mg/kg	Solid, wt %	Au, wt %
Leach Feed ¹	0.914	N.A.	N.A.
Leach Tails ¹	0.246	100.0	104.1
Leach Tails ²	0.235	100.0	100.0
Table Tails	0.167	96.3	66.2
Table Middling	0.750	2.7	8.6
Table Concentrate	5.858	1.0	25.2

¹ Weighted average fire assays from daily met balance.

² Back calculated from test results

A split of the table concentrate was sent to Hazen Research, Golden, Colorado, for detailed mineralogical characterization. The free gold was observed to be significantly larger than free gold particles examined during a previous mineralogical study. The previous study was performed on tailings from the Fort Knox mill, which at the time was processing Fort Knox ore displaying poorer gold-recovery characteristics, but unrelated and prior to processing True North ore (Hazen Research report, August 7, 2001).

The test results indicate that 25% of the gold lost to leach tailings is gravity recoverable. Microscopic examination of the free gold particles showed that the gold surface was tarnished in color. Since all the metallurgical work performed on the True North ore to date indicates that less than 5% of the total gold is gravity recoverable, it is likely that the free gold associated with the poor recovery period originated from the Fort Knox ore. The Fort Knox mill experienced typical gravity circuit performance during the timeframe when the composite leach tailings were collected. It is likely that the increase in gravity recoverable gold remaining in the leach tailings is due to fouling of the surface of free gold, that would normally be leached when processing straight Fort Knox ore, and not due to a lower efficiency in the gravity circuit. This theory is also supported by the increase in the average gold particle size of free gold in the tailings experienced when processing blended ore.

Table 2.4 Sulfide mineral distribution in the gravity concentrates from the True North blend and Fort Knox poor recovery ore leach tailings samples.

Mineral	True North Blend. April 24-29)	Straight Fort Knox (poor recovery ore)
Arsenopyrite	3.99	0.38
Bismuthinite	1.90	0.26
Chalcopyrite	0.00	0.12
Galena	0.22	0.16
Molydenite	0.23	0.06
Pyrite	86.24	97.30
Pyrrhotite	0.23	0.96
Sphalerite	0.23	0.75
Stibnite	6.84	0.00
Tetradymite	0.12	0.01
Total	100.00	100.00

Hazen Project 008-0778, September 28,2001

A mineralogical study was conducted to characterize the mode of occurrence of gold values (in addition to free gold) and the sulfide mineralization accompanying the gold in the gravity concentrate. Results of X-ray backscatter electron (XBSE) and image analyses of 4,008 particles, given in Table 2.4, indicate that stibnite is the second most abundant sulfide mineral after pyrite. Stibnite accounts for 6.84% of the sulfide mineral content and approximately 3% of the total weight of the gravity concentrate produced from the leach residue sample. The other common sulfide mineral of significant concentration is arsenopyrite. However, arsenopyrite is much less likely to cause a dramatic drop in gold recovery under cyanide leach conditions (Hedley and Howard, 1958; Deschenes et al., 2002). A suite of sulfide minerals from a sample of straight Fort Knox ore, displaying poor recovery characteristics, is also presented in Table 2.4.

Bottle-roll tests were also performed on the table tailings. The 24-hour leach program included triplicate bottle rolls, with and without lead nitrate addition. The results, presented in Table 2.5, indicate that 23.6% of the gold was extracted from the tailings material in 0.138 g/kg NaCN solution, compared to 54.0% in the tests where lead nitrate (0.068 g/kg) was added. Assuming that the gold that reported to the gravity concentrate and middlings was cyanide soluble, it is calculated that the mill leach feed would have contained 92.3% cyanide soluble gold, rather than the 71.1% actually recovered by the mill during April 24-29 timeframe. This calculated gold extraction is in close agreement with the result (91.7%) from the bottle roll test on leach feed material (Table 2.2, series 7).

Table 2.5 Summary of leaching tests on gravity tailings.

Sample	Feed Au, g/kg	Tails Au, mg/kg	Au Ext., %	Acc., %
Table Tails	0.167 ¹	N.A.	N.A.	100.0
Tails w/o Pb(NO ₃) ₂	0.157 ²	0.0035	23.6	94.0
Tails with Pb(NO ₃) ₂	0.184 ³	0.0025	54.0	109.4

¹ Weighted average fire assays.

² Back calculated from test results w/o lead nitrate.

³ Back calculated from test results with lead nitrate.

2.6 ENVIRONMENTAL IMPLICATIONS OF LEAD NITRATE ADDITION

In recent years, significant research efforts have been directed toward gaining a better understanding of the use of lead nitrate in gold cyanidation plants. At present, several companies are using lead nitrate in gold cyanidation circuits in the Canadian Provinces of Quebec, Ontario and Manitoba. None has reported any problem meeting environmental regulations (Deschenes, 2001).

The Eh-pH diagram shown in Figure 2.1 represents the equilibrium conditions for a Pb-S-H₂O system containing 25 ppm S and 50 ppm Pb. Thermodynamically, lead ions (Pb²⁺) are unstable in aqueous systems when the system pH is in excess of 1 and readily precipitate as PbS, PbSO₄, and Pb(OH)₂, depending on the oxidizing potential and pH of the system. The Eh-pH region typical of gold cyanidation, Eh (-0.32 V to 0.07 V) and pH (10.0 to 11.5) is also identified in Figure 2.1. It is likely that the precipitated species would be PbS and Pb(OH)₂. Because lead sulfide is readily oxidized (Kondos *et al.*, 1995), it is expected that the species would be an intermediate product that would be converted to Pb(OH)₂ with a minor increase in the oxidizing condition of the cyanide leach circuit and the final precipitated product would likely be lead hydroxide.

The Pb(OH)₂ will be exposed to lower pH ranges and stronger oxidizing environments during post cyanidation (processing through the cyanide destruction plant and ultimate long term exposure in the placed tailings). However, the lead should be insoluble under all oxidizing conditions and pH ranges expected within the Fort Knox tailing facility. The Eh-pH diagram also indicates that the predominant lead species would likely be PbSO₄, if the pH of the system drops below 6.

For reference, the region generally considered to be strongly oxidizing (McClelland, 2000) and the region of natural water environments have also been identified in Figure 2.1. Natural waters rarely exceed the pH range of 4-10 and aerated waters will generally have an Eh range of 0.295V-0.472V (Manahan, 1994).

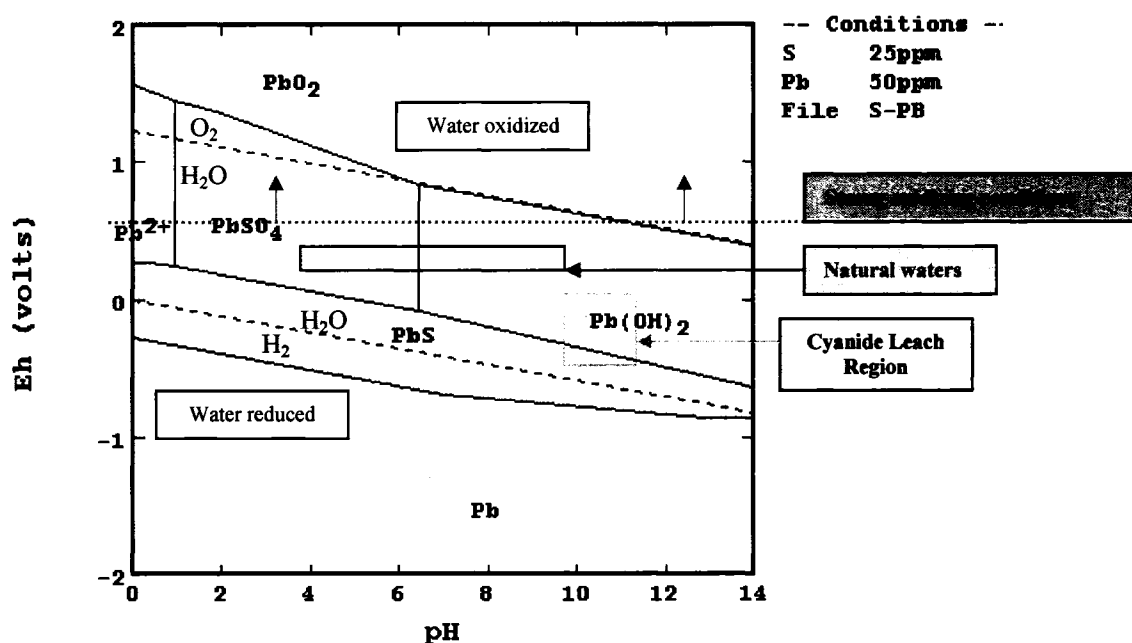


Figure 2.1 Eh-pH equilibrium diagram for the Pb-S-H₂O system at 25°C – STABCAL (1994)

Table 2.6 Lead distribution in cyanidation tests without lead nitrate addition.

	As	Sb	Fe	S	Cu	Pb
Feed solid ¹ , ppm	2,724	>2,000	46,900	900	76	38
Added to Test, ppm						0
Solid Residue ¹ , ppm	2,777	1,927	48,000	700	76	44
Leach Soln. ² , ppm	0.726	5.83	0.82	n.a.	5.83	<0.002
Extraction, %	0.02	0.28	0.0016	n.a.	6.6	<0.0042
Accountability, %	102.0	n.a.	102.3	n.a.	107.1	115.8

¹ Bondar-Clegg analytical results

² IML analytical results

To substantiate the thermodynamic conditions predicted by the STABCAL program, a bottle-roll test program was developed to determine the partitioning and mobility of the lead added to gold cyanidation circuits. Both solid and solution samples from bottle roll-tests, with and without lead nitrate, were analyzed for lead and other elements. Tables 2.6 and 2.7 present the elemental distribution from these cyanidation

tests. The results show that lead in the ore sample, or added as lead nitrate, is stable and remains in solid forms during cyanidation tests. Because the resulting solutions from the cyanidation tests contain less lead than the detection limit, 0.002 ppm, the solution will not cause environmental problems, associated with lead, when it is discharged to the tailing dam.

Table 2.7 Lead distribution in cyanidation tests with lead nitrate addition.

	As	Sb	Fe	S	Cu	Pb
Feed solid ¹ , ppm	2,724	>2,000	46,900	900	76	38
Added to Test, ppm						42
Solid Residue ¹ , ppm	2,844	1,784	48,500	600	77	81
Leach Soln. ² , ppm	0.671	8.95	0.25	n.a.	6.72	<0.002
Extraction, %	0.02	0.43	0.0004	n.a.	7.0	<0.0021
Accountability, %	104.4	n.a.	103.4	n.a.	108.9	101.3

¹ Bondar-Clegg analytical results

² IML analytical results

To determine the stability of the metals contained in the solid residues, composite samples of the solid residue from the cyanidation tests were sent to Intermountain Laboratory to be tested by the meteoric water mobility procedure (MWMP). This procedure is designed to simulate the long-term extraction expected from solids placed in a tailing impoundment. Tables 2.8 and 2.9 show the results of MWMP tests. The results indicate that the lead species in the solid residues are very stable and do not dissolve into solutions in the MWMP tests. The lead concentration in the MWMP leach solution is less than 0.002 ppm. Thus the discharge of the cyanidation solid residues, with or without lead nitrate added in the cyanidation circuits, should not cause environmental concerns associated with lead.

Table 2.8 MWMP test of True North composite cyanidation residue
without lead nitrate addition.

	As	Sb	Fe	S	Cu	Pb
Feed solid ¹ , ppm	2,777	1,927	48,000	700	76	44
Solid Residue ² , ppm	2,570	800	35,800	n.a.	65	40
Leach Soln. ² , ppm	0.853	3.8	0.05	n.a.	<0.01	<0.002
Extraction, %	0.026	0.47	0.0001	n.a.	<0.0154	<0.005
Accountability, %	92.6	42.0	74.6	n.a.	85.3	90.9

¹ Bondar-Clegg analytical results

² IML analytical results

Table 2.9 MWMP test of True North composite cyanidation residue
with lead nitrate addition.

	As	Sb	Fe	S	Cu	Pb
Feed solid ¹ , ppm	2,844	1,784	48,500	600	77	81
Solid Residue ² , ppm	2,700	780	36,700	n.a.	66.6	70
Leach Soln. ¹ , ppm	0.853	6.23	0.06	n.a.	<0.01	<0.002
Extraction, %	0.03	0.78	0.0002	n.a.	<0.015	<0.003
Accountability, %	95.0	44.5	75.7	n.a.	86.5	86.4

¹ Bondar-Clegg analytical results

² IML analytical results

2.7 CONCLUSIONS

Test results indicate that the poor gold recovery experienced at the Fort Knox mill during late April, 2001, is the result of a surface chemistry problem affecting gold particles, and not encapsulation, or depletion of oxygen and cyanide during leaching. The likely cause of the low gold extraction is the formation of a passivating film on free gold particles originating from Fort Knox ore. This film is caused by chemical species resulting from sulfide mineral dissolution, mainly stibnite, contained in True North ore.

The retarding effect of the passivating film was substantially reduced through the addition of lead nitrate and elevated cyanide concentrations in leach.

The results of 24-hour bottle-roll tests for straight True North ore indicate that a higher gold extraction could be realized through the addition of lead nitrate at all cyanide concentrations. However, the improvement in recovery was not as pronounced as for that measured in the tests of blended mill feed material processed during late April at the Fort Knox mill. This is thought to be the result of differences in the particle size distribution of gold between the two ore deposits (Fort Knox having a coarser particle size distribution than True North) and variability in the mineralogy of the True North deposit.

If lead nitrate is added to the leach circuit, it should not negatively impact water quality either during the active mine life or during reclamation and closure, because the lead is likely to precipitate out as stable hydroxide or sulfate species. This has been substantiated through a laboratory simulation test program and is consistent with thermodynamic stability evaluations. In addition, plant operating results from a Canadian mine currently utilizing lead nitrate in a gold cyanidation circuit indicate that process water quality is not significantly affected by lead nitrate addition.

REFERENCES

- Avraamides, J., Dork, K., Durack, G., and Ritchie, I.M., 2000, *Effect of antimony (III) on gold leaching in aerated cyanide solutions: A rotating electrochemical quartz crystal microbalance study*, In Minor Elements 2000: Processing and Environmental Aspects of As, Sb, Se, Te, and Bi, Editor Young C., Society for Mining, Metallurgy, and Exploration, Inc. (SME), 2000, pp. 171-178.
- Barsky, G., Swainson, S.J., and Hedley, H., 1934, *Dissolution of gold and silver in cyanide solutions*, Transactions of the American Institute of Mining & Metallurgical Engineering, Vol. 112, pp. 660-677.
- Cathro, K.J. and Koch, D.F.A., 1964, *The anodic dissolution of gold in cyanide solutions*, Journal of the Electrochemical Society, pp. 1416-1420.

- Chimenos, J.M., Segarra, M., Guzman, L., Karagueorgieva, A. and Espiell, F., 1997, *Kinetics of the reaction of gold cyanidation in the presence of a thallium(I) salt*, Hydrometallurgy, Vol. 44, pp. 269-286.
- Cornejo, L.M. and Spottiswood, D.J., 1984, *Fundamental aspects of the gold cyanidation process: A review*, Mineral and Energy Resources, Vol. 27 No. 2, Colorado School of Mines.
- Crudwell, F.K. and Godorr, S.A., 1996, *A mathematical model of the leaching of gold in cyanide solutions*, Hydrometallurgy, Vol. 44, pp. 147-162.
- Deschenes, G., Wallingford, G., 1995, *Technical note: Effect of oxygen and lead nitrate on the cyanidation of sulphide bearing gold ore*, Minerals Engineering, Vol. 8, No. 8, pp. 923-931.
- Deschenes, G., Rousseau, M., Tardif, J., and Prud'homme, P.J.H., 1998, *Effect of the composition of some sulphide minerals on cyanidation and use of lead nitrate and oxygen to alleviate their impact*, Hydrometallurgy, Vol. 50, pp. 205-221.
- Deschenes, G., Lastra, R., Brown, J.R., Jin, S., May, O. and Ghali, E., 2000, *Effect of lead nitrate on cyanidation of gold ores: progress on the study of the mechanisms*, Minerals Engineering, Vol. 13, No. 12, pp. 1263-1279.
- Deschenes, G., Fulton, M., Jean, P. and Healey, S., 1999a, *Improvement of cyanidation at New Britannia Mine*, Randol Gold and Silver Forum '99, Denver Co.
- Deschenes, G., Fulton, M. and Lofontaine, M., (1999b), *Assessment and control of the gold leaching parameters at Kiena Mines*, 38th Annual Conference of Metallurgists of CIM, Quebec, Canada.
- Deschenes, G., Pratt, Riveros, P., and Fulton, M., 2002, *Reaction of gold and sulfide minerals in cyanide media*, proceedings of SME Annual Conference, Phoenix, Arizona, preprint 02-133.
- Deschenes, G., CANMET, 2001, Personal Communication.

- Fink, C.G. and Putnam, G.L., 1950, *The action of sulphide ion and of metal salts on the dissolution of gold in cyanide solutions*, Transactions AIME, Vol. 187, pp. 952-955.
- Habashi, F., 1967, *Kinetic and mechanism of gold and silver dissolution in cyanide solution*, Bulletin 59, State of Montana Bureau of Mines and Geology.
- Hedley, N. and Howard, T., 1958, *Chemistry of cyanidation*, Mineral Dressing Notes Number 23, American Cyanamid Company, Wayne, N.J.
- Huang, H.H., 1994, Stability Calculation for Aqueous Systems (STABCAL - version 1.5), Montana Tech.
- Jeffrey, M.I., Ritchie, I.M., LaBrooy, S.R. and Parker, A.J., 1996, *The effect of lead on the electrochemistry of gold: Myth or magic*, Proceedings of the Fourth International Symposium on Electrochemistry in Mineral and Metal Processing, pp. 284-295.
- Jeffrey, M.I. and Breuer, P.L., 2000, *The cyanide leaching of gold in solutions containing sulfide*, Minerals Engineering, Vol. 13, No. 10-11, pp. 1097-1106.
- Kameda, M., 1949, *Fundamental studies on dissolution of gold in cyanide solutions. III. Effects of alkalis, lead acetate, and some impurities contained in foul cyanide solutions*, Science Reports of the Research Institute, Tohoku University, Vol. 1, No.4, pp. 435-444.
- Kondos, P.D., Deschenes, G., and Morrison, R.M., 1995, *Process optimization studies in gold cyanidation*, Hydrometallurgy Vol. 39 pp. 235-250.
- Kudryk, V. and Kellogg, H.H., 1954, *Mechanism and rate-controlling factors in the dissolution of gold in cyanide solution*, Journal of Metals, Vol. 6, pp. 541-548.
- Lin, H. K. and Chen, X., 2001, *Electrochemical study of gold dissolution in cyanide solution*, Minerals and Metallurgical Processing, Vol. 18, No. 3, pp. 147-153.
- Liu, G.Q. and Yen, W.T., 1995, *Effects of sulphide minerals and dissolved oxygen on the gold and silver dissolution in cyanide solution*, Minerals Engineering, Vol. 8, No. 1-2, pp. 111-123.

- Lorenzen, L. and van Deventer, J.S.J., 1992a, *The mechanism of leaching of gold from refractory ores*, *Minerals Engineering*, Vol. 5, No. 10-12, pp. 1377-1387.
- Lorenzen, L. and van Deventer, J.S.J., 1992b, *Electrochemical interactions between gold and its associated minerals during cyanidation*, *Hydrometallurgy*, Vol. 30, pp. 177-194.
- Manahan, S.E., 1994, Environmental Chemistry, 6th edition, Lewis Publishers CRC Press, Boca Raton, Florida.
- Marsden, J. and House, I., 1992, The Chemistry of Gold Extraction, Ellis Horwood, New York, pp. 275
- Nicol, M.J., Fleming, C.A. and Paul, R.L., 1987, *The chemistry of the extraction of gold*, In: Stanley G.G.(Editor), The Extractive Metallurgy of Gold in South Africa, The Chamber of Mines of South Africa, The South African Institute of Mining and Metallurgy, Kelvin House, Johannesburg 2001, pp. 860-862.
- Nicol, M.J., 1980, *The anodic behaviour of gold: Part II – Oxidation in alkaline solutions*, *Gold Bulletin*, Vol. 13, No.3, pp. 105-111.
- Thurgood, C.P., Kirk, D.W., Foulkes, F.R., and Grayson, W.F., 1981, Activation energies of anodic gold reactions in aqueous alkaline cyanide, *Journal of the Electrochemical Society*, Vol. 128, No. 8, pp. 1680-1685.
- Tshilombo, A.F. and Sandenbergh, R.F., 2001, *An electrochemical study of the effect of lead and sulphide ions on the dissolution rate of gold in alkaline cyanide solutions*, *Hydrometallurgy*, Vol. 60, pp. 55-67.
- Weichselbaum, J., Tumilty, J.A., and Schmidt, C.G., 1989, *The effect of sulphide and lead on the rate of gold cyanidation*, Aust. IMM Annul. Conference, Perth-Kalgoorlie, pp. 221-224.
- Yannopoulos, J.C., 1991, The Extractive Metallurgy of Gold, Van Nostrand Reinhold, New York, pp. 156-163.

CHAPTER 3
OPTIMIZING CYANIDATION PARAMETERS FOR PROCESSING OF
BLENDED FORT KNOX AND TRUE NORTH ORES
AT THE FORT KNOX MINE¹

3.1 ABSTRACT

The Fort Knox Mine is an open-pit operation, located in Alaska, which started commercial production in March 1997. A conventional mill processes 38,000 tpd of a low grade (1.0 g/t Au) free milling gold ore with a low sulfide component (below 1%). Gold production (11% from gravity and 89% from cyanidation) exceeds 400,000 ounces per year. Short retention time (20 h), low temperature (7°C) and low-grade make high leaching kinetics critical for the performance of the process. In April 2001, the treatment of True North ore, which represented 14.4% of the mill throughput and contained more sulphide in the form of pyrite, arsenopyrite and stibnite, resulted in a substantial drop in the average gold extraction from 87% to 72.6%. Laboratory investigations indicated that the addition of lead nitrate increased gold extraction to 91.7%. Further investigations were initiated to determine the leaching parameters and the nature of the problem. Subsequently, a lead nitrate addition scheme was implemented at the Fort Knox mill that resulted in 2002 gold production being in excess of 49,000 ounces higher than that estimated for the non-lead nitrate reagent scheme, during the 18 months evaluated. This paper presents the results of laboratory investigations to determine the nature of the problem, the new leaching conditions, modifications in plant operating practices and plant production data.

¹ Hollow, J.T., Hill, E.M., Deschenes, G., Guo, and H., Fulton, M., (2003), Hydrometallurgy 2003 – Fifth International Conference in Honor of Professor Ian Ritchie, Vol. 1: Leaching and Solution Purification, pp. 21-34.

3.2 INTRODUCTION

The Fort Knox and True North Mines, owned by Kinross Gold Corporation, are located approximately 40 kilometers northeast of Fairbanks, Alaska. The mines are operated by Fairbanks Gold Mining, Inc. (FGMI), a 100% owned subsidiary of Kinross Gold. The Fort Knox Mine, a 91.3 million metric ton resource (grade of ~0.8 g/t Au) is a free milling ore, with low sulfide and is processed at a relatively coarse grind (65%-100 mesh). The gravity recoverable gold (GRG) content is variable, but ranges from 30-65% of total gold in the mill feed. The True North Mine is located 15 kilometers northeast of the Fort Knox processing facility and contains an estimated 6.4 million metric tons (grade of ~1.5 g/t Au). Gold mineralization is more variable in the True North reserve, with a GRG content less than 4%, and can be associated with sulfides. Ore from the True North mine is trucked to the Fort Knox facility where it is blended with Fort Knox ore for processing. The True North ore represents approximately 25% of the annual material processed through the mill facility at an average rate of 38,000 tpd.

The ore is blended at the primary gyratory crusher located at the edge of the Fort Knox Mine, where the material is reduced to -8 inch prior to being conveyed to the coarse ore stockpile at the mill. Reclaimed ore is processed through a conventional SABC circuit (Magnuson *et al.*, 2001) to produce a final product averaging 65% -100 mesh.

A split of the grinding circuit circulating load is processed through a gravity plant, where approximately 30% of the GRG is recovered. The remaining gold is recovered from the ground slurry through a conventional leach/CIP circuit. The CIP tailings discharge to a tailings thickener, where approximately 60% of the spent leach solution is recycled prior to processing in the cyanide destruction circuit and subsequent placement in the tailings impoundment. A simplified process flowsheet is presented in Figure 3.1.

The Fort Knox mill began processing a blend of True North ore in April of 2001. Within two weeks the plant recovery dropped by approximately 20% and numerous processing approaches were attempted in order to remedy the poor gold recovery.

Ultimately the True North ore was campaigned through the mill for the majority of second and third quarters of 2001, while a better understanding of the circuit metallurgy was developed.

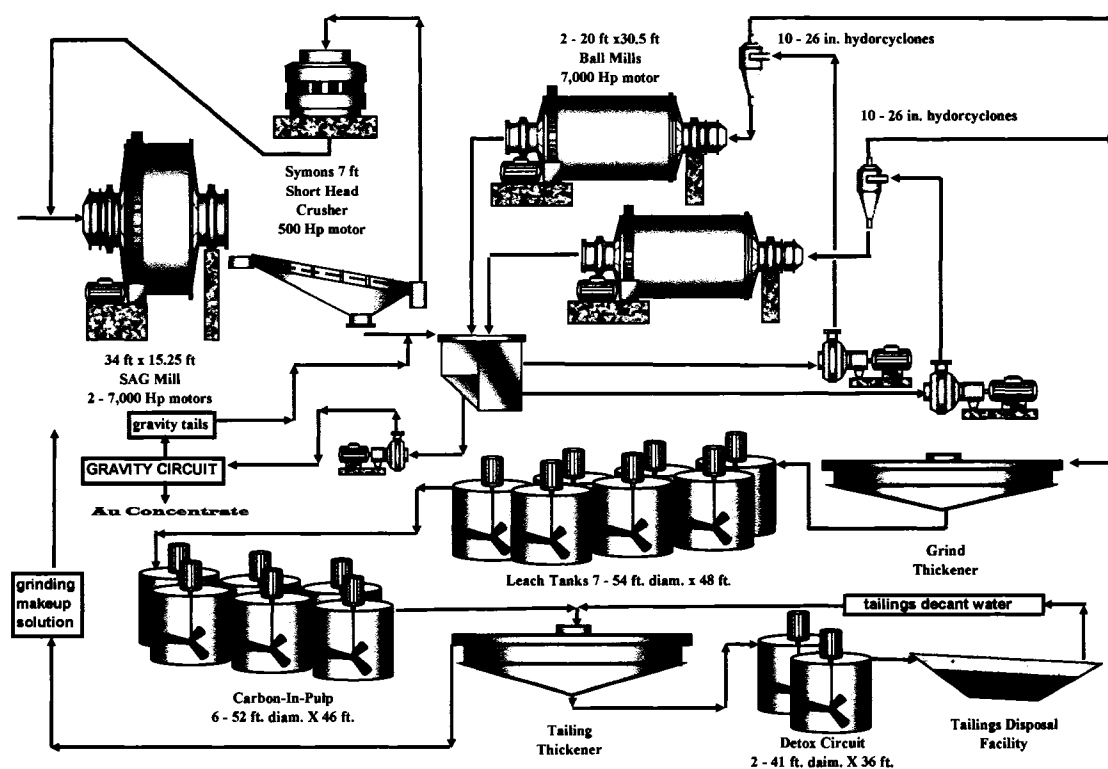


Figure 3.1 Fort Knox mill process flowsheet.

At that time, a detailed evaluation of the cyanidation plant tailings was conducted in association with the Mineral Industry Research Laboratory at the University of Alaska Fairbanks. Laboratory results representing this evaluation were previously presented (Hollow *et al.*, 2003) and described the reduction in gold extraction resulting from processing blended True North and Fort Knox ores. Also presented was laboratory evidence, that lead nitrate addition substantially improved the gold extraction results and had no significant environmental impact on tailings pond chemistry during operations or at closure. Government agency approvals were received and a lead nitrate addition scheme was implemented in December 2001.

In addition, FGMI entered into an agreement with the Mining and Mineral Sciences Laboratories, Natural Resources Canada, CANMET, to perform additional laboratory investigations in the 3rd quarter of 2001. The initial focus of the work was to determine the impact lead nitrate addition would have on gold extraction in the remaining True North reserve, that produced poor results under standard cyanidation conditions and typically contain higher sulfide mineralization. This material was ultimately found to be refractory and gold extraction was not significantly improved by any of the cyanidation variables (cyanide concentration, lead nitrate addition, oxygen addition, pH, CIL, particle size and temperature) evaluated (Deschenes *et al.*, 2002a). The results were consistent with those produced by the FGMI metallurgical laboratory, where it was also determined that blending of this material with a composite of Fort Knox ore did not have the adverse effects being seen in the plant. A second True North ore composite, representing material being actively mined and processed at Fort Knox, was sent to CANMET for the remainder of the work.

A composite of blasthole reject material from both the True North and Fort Knox mines is built each month and represents the ore shipped to the Fort Knox mill. The Fort Knox sample and the second True North sample, sent to CANMET, were splits of the February 2002 composite from each mine. The FGMI laboratory has developed procedures that allow for successful simulation of the Fort Knox leach circuit performance. The laboratory equipment at the mine does not, however, allow for maintaining the controlled conditions required to test a number of the variables known to impact gold leach kinetics and overall extraction. Therefore, the composites were sent to CANMET for a controlled cyanidation study to develop a better understanding of the leach parameters and more specifically, the nature of the reduced gold extraction, when the two ores are blended. Results from laboratory test work on the second True North ore sample, the Fort Knox ore sample, and a blend of the two samples, are presented in this paper. Also included is a comparison between the CANMET results, the FGMI laboratory results for February, and 18 months of actual plant gold extraction data beginning January 2002.

3.3 CANMET LABORATORY INVESTIGATION

A blend sample of 20 kg was produced by mixing the Fort Knox ore and the True North ore sample, 3:1 ratio, in a drum tumbler under nitrogen atmosphere for 6 hours. The samples of the two ores were half splits of a larger sample prepared at Fort Knox, where size reduction and GRG gold removal was performed. The other half split was retained at the Fort Knox laboratory for confirmation testing.

Table 3.1 Mineralogical and chemical analysis of the blend sample, % except for Au and Ag

(Fort Knox Sample: True North Sample = 3:1)

Au	0.71 g/t	Major phases 99.01%
Ag	0.22 g/t	quartz, albite,
Si	31.06	chlinochlore, orthoclase,
Al	6.64	montmorillonite,
Fe	2.65	muscovite, and calcite
Ca	1.95	Minor phases 0.59%
Mg	0.78	goethite, rutile and
C _{total}	0.76	ilmenite
S	0.03	Trace phases
As	0.069	arsenopyrite 0.14%
Zn	0.02	pyrite 0.11%
Sb	0.009	pyrrhotite 0.04%
Pb	0.003	arseniosiderite 0.01%
Cu	0.002	stibnite 0.01%
Ni	0.002	chalcopryrite 0.01%
Co	0.002	monazite 0.01%
Hg	0.0004	pentlandite 0.003%
Bi	0.0007	cervantite 0.003%
Te	<0.0008	galena 0.004%

The samples were splits of the February 2002 composite from each mine. The blend was divided into 1000 g lots using a rotary splitter. Representative samples were taken for chemical, mineralogical and screen analyses. The blend sample had a size distribution of 65% -100 mesh. Table 3.1 shows the results of chemical and mineralogical analysis.

The gold content, obtained by fire assay, was 0.71 g/t (duplicate). The mineralogy was determined by quantitative backscattered electron image analysis. As shown in Table 3.1, 99% of the sample consisted of gangue minerals: quartz, albite, chlinochlore, orthoclase, montmorillonite, muscovite, and calcite. Small amounts (0.6%) of iron oxides (geothite, hematite, ilmenite and sphene) and trace amounts of sulfides (0.09%) including pyrite, arsenopyrite, pyrrhotite, arseniosiderite, stibnite, chalcopyrite, pentlandite, cervantite and monazite were found in the sample. There were antimony minerals at 0.01%, (stibnite and cervantite) in the sample (Deschênes *et al.*, 2002b).

The lime, sodium cyanide, lead nitrate, compressed air and oxygen were all certified reagent grade chemicals. All of the cyanidation tests were conducted in jacketed glass cells, which allowed accurate control of the pulp temperature. The cap of the test cell has four openings which allowed mechanical agitation of the pulp, injection of air/oxygen, and monitoring of the pulp pH and dissolved oxygen. Lime, sodium cyanide and a mixture of air and oxygen were added to the pulp to maintain the preset target values. The experimental details used for cyanidation were described in a previous paper (Deschênes and Fulton, 1998).

3.3.1 Leachable Gold Content

In order to test the leachability of the gold in the blend sample, tests were conducted in duplicate at 98% - 400 mesh, pH: 10.2, DO: 12 ppm, 200 ppm NaCN, duration of cyanidation: 48 hours, temperature: 21°C, and with the addition of 100 g/t lead nitrate. The results are shown in Figure 3.2.

The results indicate that 95.8% of the gold in the blend sample could be leached out within 48 hours (average residue at 0.03 g/t Au), which indicates that the second True

North ore sample was easier to leach than the first True North ore sample. Fine grinding accelerated the leaching rate over the initial cyanidation period, and an extraction of 91% could be achieved within 6 hours, which is the time required to reach a steady state. Additional liberation of gold enhanced the extraction. The cyanide consumption for the leachable gold tests was increased significantly. The additional liberation of sulfide minerals also enhanced the reaction with cyanide. An average of 0.20 kg/t NaCN was consumed in the 48-hour cyanidation, while only 0.04 kg/t NaCN was consumed for the baseline test as shown in Figure 3.3.

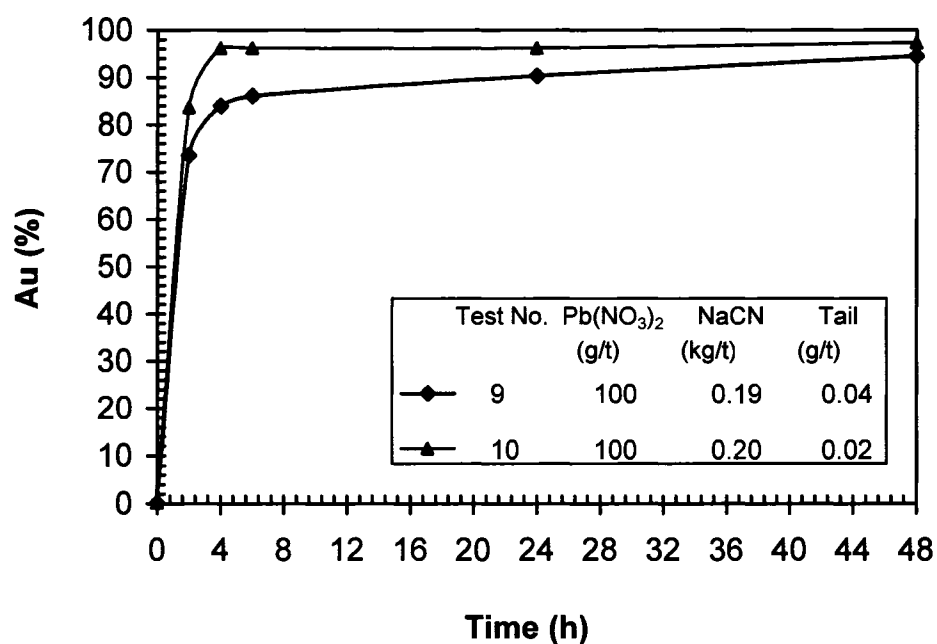


Figure 3.2 Leachable gold of the blend sample from Fort Knox; NaCN in legend represents addition, Tail is gold concentration.

3.3.2 Effect of Pre-treatment

The effect of pre-treatment, a six-hour slurry conditioning period after pH adjustment and prior to cyanide addition, was then tested, both with and without the addition of lead nitrate. The pre-treatment was done while maintaining the remaining variables constant: pH: 10.2; DO: 12 ppm; NaCN: 75 ppm; Temperature: 10°C; time: 20 hours. The results from the pre-treatment test are shown in Table 3.2 and Figure 3.3.

The results indicate that a 6-hour pre-treatment without lead nitrate had no effect on gold leaching kinetics and overall gold extraction, the overall gold extraction for 20-hour cyanidation was the same as the baseline test (tailings at 0.16 g/t Au). Pre-treatment with lead nitrate and direct addition of lead nitrate during a straight cyanidation achieved the same gold extraction. The overall gold extraction increased by 7.0% and the gold content in the tailing was reduced from 0.16 g/t Au to 0.11 g/t Au. A pre-treatment did not have an effect on the cyanide consumption. Also, the system is far away from an steady state, with significant extraction occurring in the 5 to 20 hour portion of the test.

Table 3.2 Effect of pretreatment on the cyanidation of the blend sample.

Test No.	Variables		Results		
	Pretreatment	Pb(NO ₃) ₂	Au Extraction	Au in Tailings	NaCN Consumption
		(g/t)			
1	NO	0	77.5	0.16	0.04
4	NO	100	84.5	0.11	0.04
2	YES	0	77.5	0.16	0.05
3	YES	100	84.5	0.11	0.04

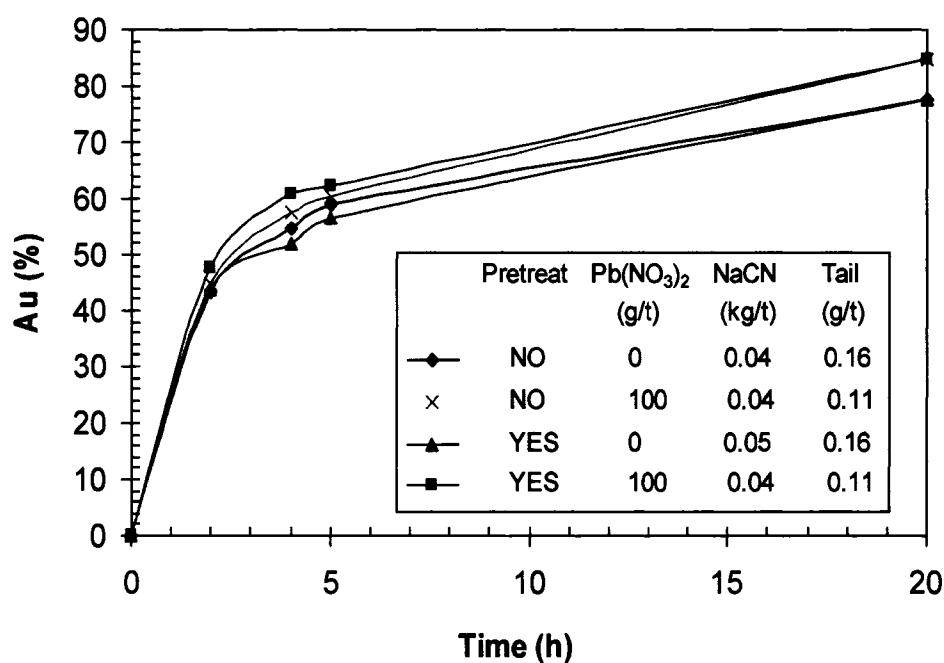


Figure 3.3 Effect of pre-treatment, with and without lead nitrate, on the cyanidation of the blend sample from Fort Knox; NaCN and Pb(NO₃)₂ in legend represents addition, tail is gold concentration.

3.3.3 Effect of Lead Nitrate Addition

The effect of lead nitrate on cyanidation, without pre-treatment was tested at levels of 50 g/t, 100 g/t, 125 g/t and 200 g/t, while maintaining the remaining variables constant: pH: 10.2; DO: 12 ppm; NaCN: 75 ppm; Temperature: 10°C; time: 20 hours. The results are shown in Figure 3.4.

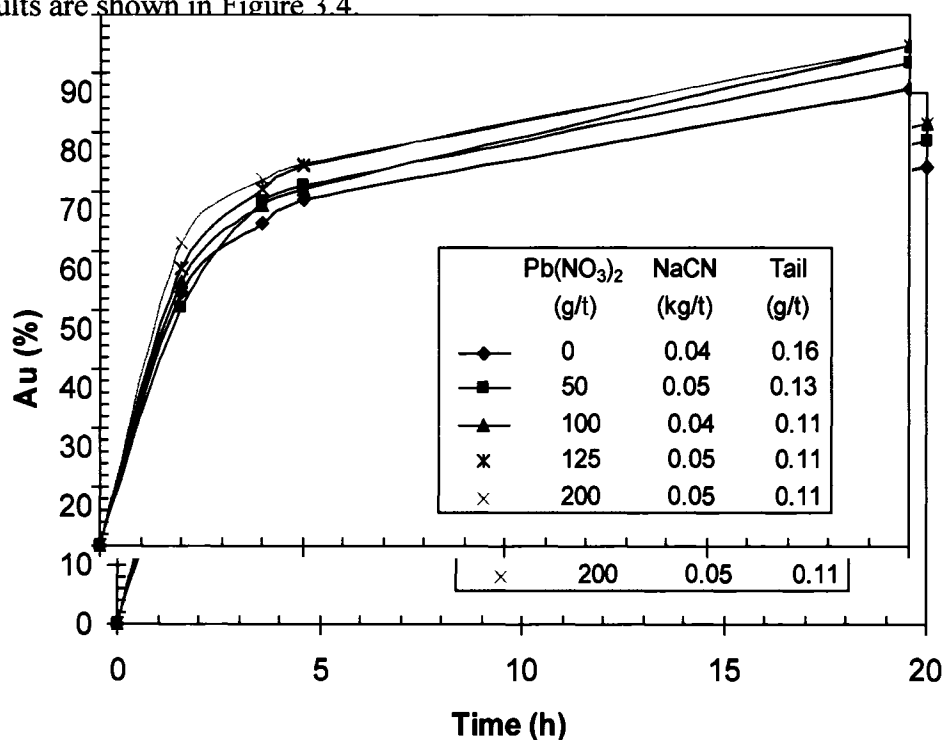


Figure 3.4 Effect of lead nitrate addition on cyanidation, without pretreatment, of the blend sample from Fort Knox; NaCN and Pb(NO₃)₂ in legend represents addition, tail is gold concentration.

The addition of lead nitrate showed a remarkable benefit on gold leaching kinetics and over all gold extraction. Gold extractions were increased by 4.2% and 7.0% when 50 g/t and 100 g/t Pb(NO₃)₂ were used, respectively. The gold content in the tailings was reduced from 0.16 g/t to 0.13 g/t and 0.11 g/t. No further benefit was observed, if the amount of lead nitrate was increased to 125 g/t and 200 g/t. The addition of lead nitrate did not have remarkable effect on the cyanide consumption; the cyanide consumption being already very low.

The improvement of the gold leaching rate was not effective enough to bring the system to a steady state within 20 hours as significant extraction occurred in the 5 to 20 hour portion of the test. Improvement of the leaching rate will be addressed later with other parameters in this investigation.

3.3.4 Effect of Cyanide Concentration

Three cyanide concentrations, 75 ppm, 100 ppm and 150 ppm, were tested to determine the effect of free cyanide concentration on the leaching kinetics and the overall gold extraction of the sample. 100 g/t lead nitrate was added in these tests. In order to obtain more details on the gold dissolution before the end, an extra liquid sample was taken at 16 hours in the first two tests. The third test, with a NaCN concentration of 150 ppm, had a duration time of 24 hours and a liquid sample was taken at 20 hours. The test results are shown in Figure 3.5.

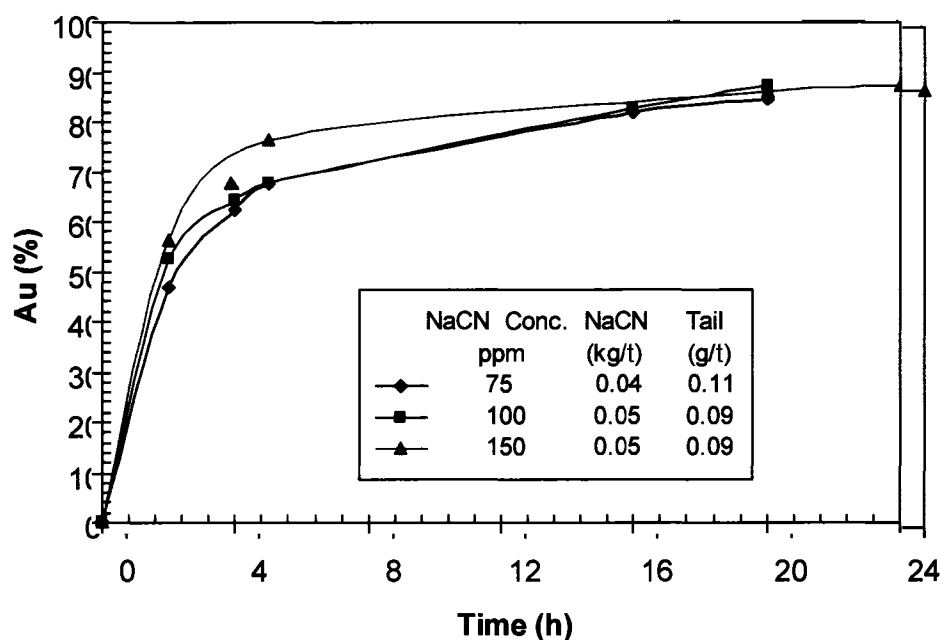


Figure 3.5 Effect of NaCN concentration on leaching of the blend sample from Fort Knox; NaCN in legend represents addition, tail is gold concentration.

The increase of sodium cyanide concentration from 75 ppm to 100 and 150 ppm resulted in higher gold leaching kinetics during the initial leaching period, and did not apparently affect the cyanide consumption. There was a faster gold dissolution with 150 ppm NaCN and the system reached a steady state in 20 hours leaching. The gold extraction remained basically unchanged with a slight increase of 1.2%. Because the cyanidation with 150 ppm NaCN appeared to reach a steady state within the retention time of the plant, it is recommended to consider using a higher free cyanide concentration in the plant.

3.3.5 Effect of Dissolved Oxygen Concentration

The effect of using a higher dissolved oxygen level on cyanidation, with and without lead nitrate, was tested by increasing the D.O. level to 18 ppm, while maintaining the remaining variables constant: pH: 10.2; DO: 12 ppm; NaCN: 75 ppm; Temperature: 10°C; time: 20 hours. Figure 3.6 illustrates the effect of using a higher dissolved oxygen level on the gold leaching kinetics, with and without lead nitrate addition.

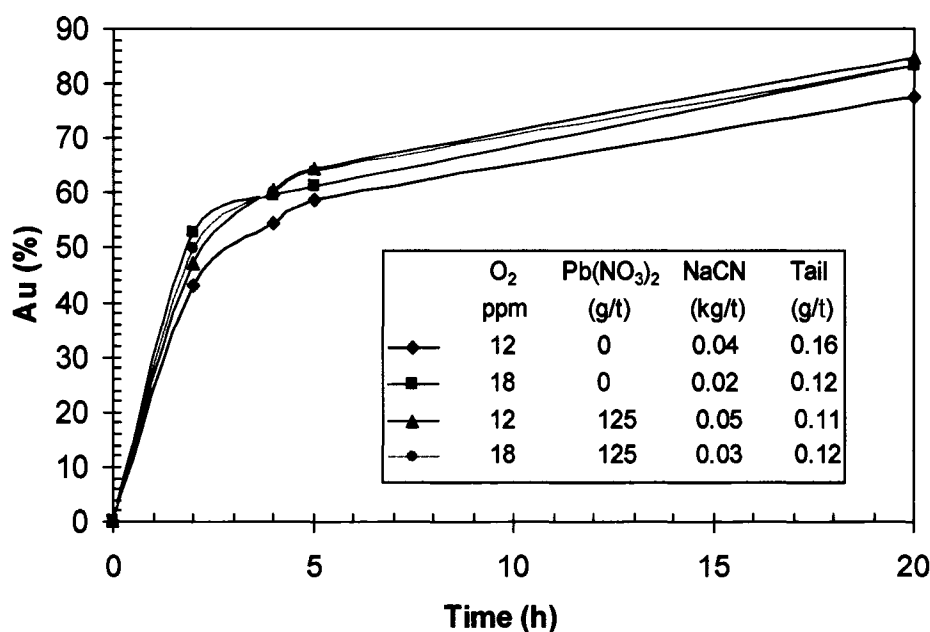


Figure 3.6 Effect of dissolved oxygen concentration on leaching of the blend sample from Fort Knox, with and without lead nitrate addition; NaCN and Pb(NO₃)₂ in legend represents addition, tail is gold concentration.

In the absence of lead nitrate, increasing the dissolved oxygen level of the pulp, from 12 ppm to 18 ppm, improved the leaching kinetics, and the overall gold extraction was increased from 77.5% to 83.1%. The gold content of the tailings decreased from 0.16 g/t to 0.12 g/t. The addition of 125 g/t lead nitrate slurry did not further increase the overall gold extraction. The cyanide consumption appeared to be slightly affected by the dissolved oxygen level of the pulp. The dissolved oxygen did not improve the leaching rate enough to bring the system to an equilibrium state as significant extraction occurred in the 5 to 20 hour portion of the test.

3.3.6 Effect of Slurry pH

Trace amount of antimony minerals (stibnite, cervantite) was detected in the second True North ore sample. When cyanidation occurs at high pH, antimony could form an insoluble compound (aurostibnite) on the gold surface and retard the gold leaching process. The effect of using a lower slurry pH on cyanidation, with and without lead nitrate, was tested by reducing the pH level to 9.8, while maintaining the remaining variables constant. The results are shown in Figure 3.7.

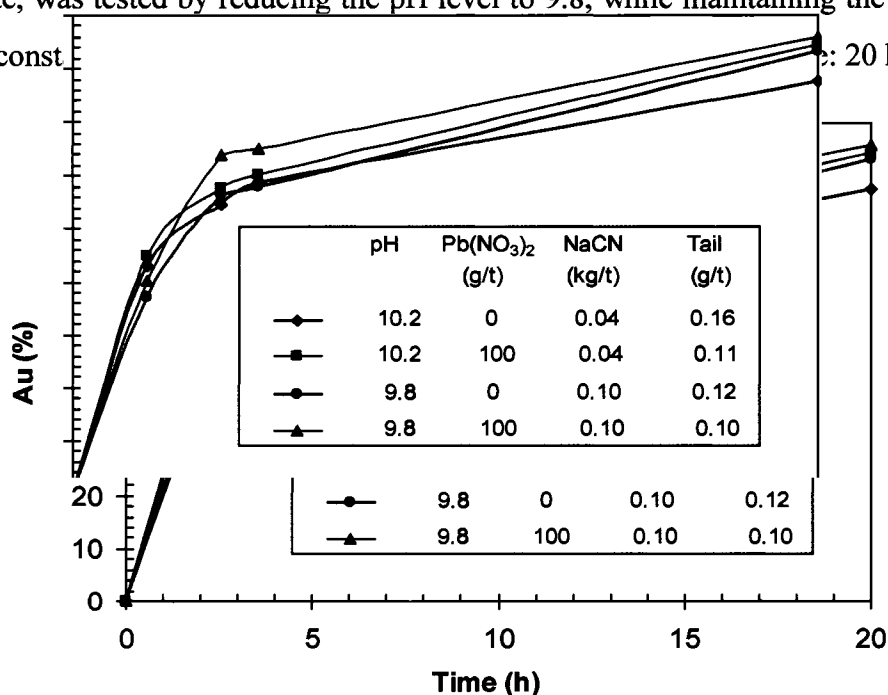


Figure 3.7 Effect of slurry pH on cyanidation of the blend sample from Fort Knox; NaCN and Pb(NO₃)₂ in legend represents addition, tail is gold concentration.

The results of Figure 3.7 indicate that a higher extraction was achieved at a lower pH. Without lead nitrate addition, the gold extraction increased from 77.5% to 83.1% when the pH was reduced from 10.2 to 9.8. The gold content in the tailings was reduced by 0.04 g/t Au. The tests were performed in duplicate to confirm this trend. With 100 g/t lead nitrate addition, the gold extraction rate was almost the same, with an increase of 1.4%, when the pH was reduced from 10.2 to 9.8.

The cyanide consumption was increased at low pH. The test results for the effect of pH indicate that antimony may have some negative effect on leaching of the gold in the blend sample and addition of lead nitrate at pH 10.2 could alleviate its negative effect. The decrease in pH or the addition of lead nitrate did not improve the leaching rate enough to bring the system to an equilibrium state as significant extraction occurred in the 5 to 20 hour portion of the test.

3.3.7 Effect of Antimony on Gold Extraction

The True North ore contains sulfide minerals that are known to impact gold leach kinetics and overall recovery. Stibnite (antimony sulfide), arsenopyrite, orpiment and realgar (arsenic sulfides) are examples of these minerals (Hedley and Howard, 1958; Habashi, 1967; Nicol et al., 1987; Yannopoulos, 1991; Marsden and House, 1992). Under laboratory conditions, it was found that the addition of 1,000 ppm stibnite completely stopped gold dissolution from a rotating gold disc (Liu and Yen, 1995). The retarding effect of the stibnite was attributed to neither cyanide nor oxygen depletion, but to the formation of a dark-brown colored film on the gold disc surface. The passivating effect of SbO^+ , generated during the oxidation of stibnite, on gold leaching has also been confirmed (Avraamides *et al.*, 2000).

As part of the Fort Knox fundamental test program at CANMET, a mixture of quartz, gold powder and stibnite was used to quantify the retarding effect of stibnite concentration on gold dissolution (Figure 3.8). A very strong retarding effect on gold leaching kinetics was obtained at a concentration as low as 0.002%. The gold extraction

over 4 hours was only 38.0% with 0.002% stibnite compared to 90% without stibnite. Gold extraction fell to 24.9% and 12.6% at stibnite concentrations of 0.01% and 0.3%.

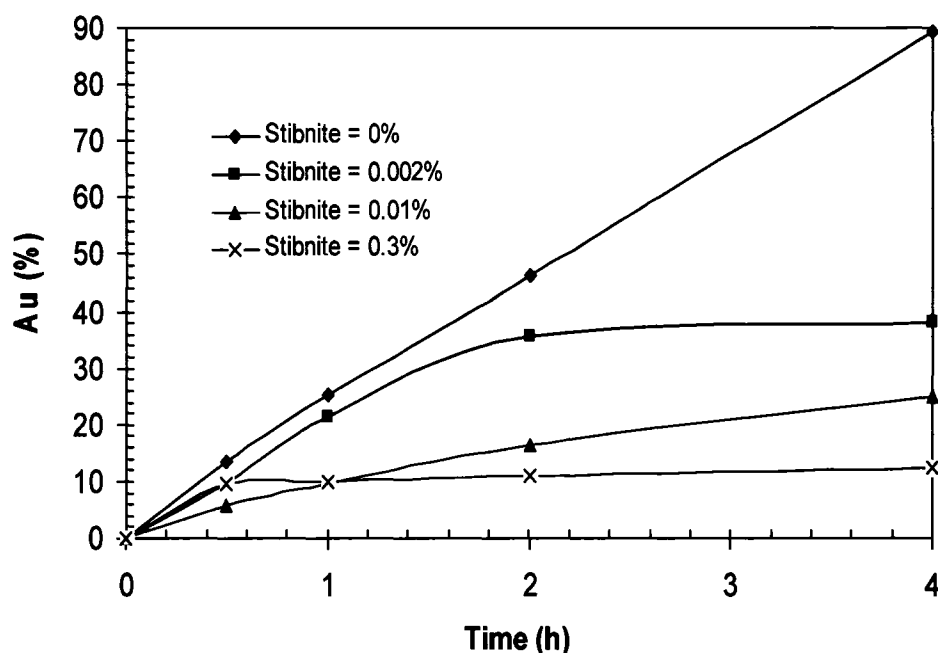


Figure 3.8 Effect of stibnite concentration on gold recovery by cyanidation in the synthetic ore.

3.4 FORT KNOX LABORATORY RESULTS

As part of FGMI's routine monthly metallurgical testing, a composite of True North and Fort Knox ores is built from blasthole reject material and represents the ore mined from each pit and shipped to the Fort Knox mill. These composites were then subject to a bottle roll test program that was developed to simulate actual gold extraction, when the ore is processed through the Fort Knox mill. The simulation testing, that was originally developed by Hazen Research and modified by FGMI, produces results that correlate strongly with the actual mill gold extraction.

Initial testing is performed on each monthly ore composite separately and then on a blended sample, under conditions that simulate actual average monthly mill conditions for leach NaCN concentration, slurry pH and leach circuit retention time.

3.4.1 Effect of Lead Nitrate Addition on Leaching Fort Knox Ore

Results of tests performed at the FGMI laboratory, from January 2002 to June 2003, indicated no significant benefit from the addition of lead nitrate on leaching of Fort Knox ore composites, with the average gold extraction being 85.4% and 85.7% for the tests performed with and without lead nitrate, respectively. The individual test results were, however, more variable due to the lower gold content and coarser size distribution of gold in the samples. Since the gravity circuit at the Fort Knox mill processes less than 25% of the grinding circuit circulating load, the circuit recovers approximately 40 – 60% of the GRG value in the mill feed. However, under normal cyanidation conditions, the remaining gravity recoverable gold can be extracted within the retention time of the circuit. The results of the laboratory tests on Fort Knox ore, with and without lead nitrate addition, are shown in Figure 3.9.

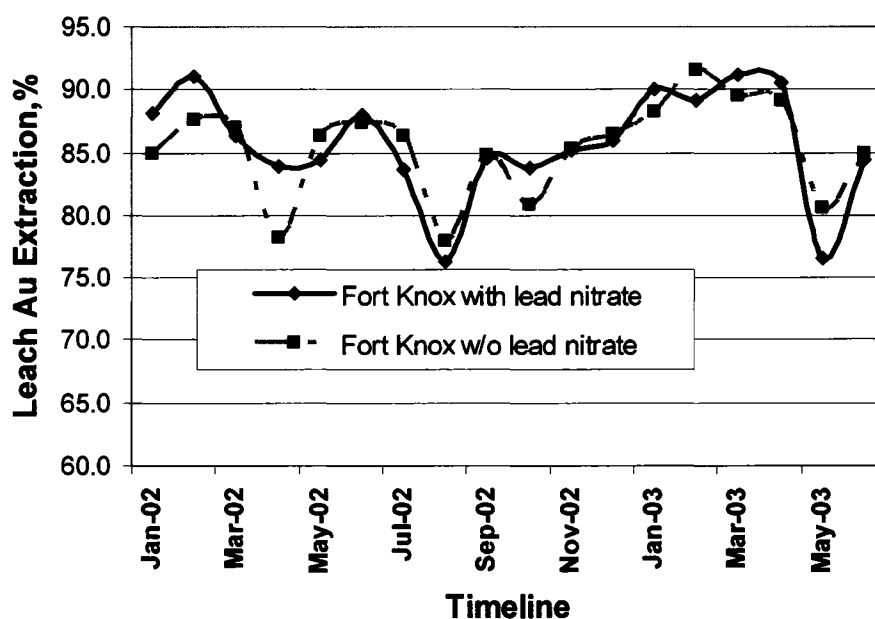


Figure 3.9 Comparison of the extraction of gold from Fort Knox ore composites, with and without lead nitrate.

3.4.2 Effect of Lead Nitrate Addition on Leaching True North Ore

Similar to the performance of the Fort Knox ore, results of tests performed at the FGMI laboratory, from January 2002 to June 2003, indicated only minimal benefit from the addition of lead nitrate on leaching True North ore composites (1.0% increase in leach Au extraction). The average gold extraction was 78.3% and 79.3% for the tests performed, with and without lead nitrate, respectively. The results of the laboratory tests of True North ore, with and without lead nitrate addition, are shown in Figure 3.10.

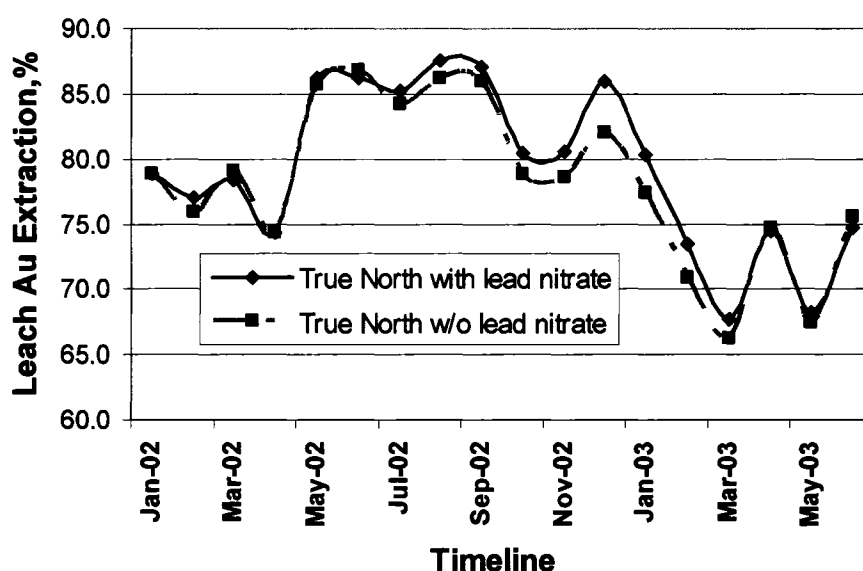


Figure 3.10 Comparison of the extraction of gold from True North ore composites, with and without lead nitrate.

3.4.3 Effect of Lead Nitrate Addition on a Blend of True North and Fort Knox Ores

The leaching of blended True North/Fort Knox ore samples averaged 76.5% during the first 18 months beginning January 2002, in the absence of lead nitrate. This value is substantially less than the average calculated value of 83.9%. The laboratory leaching of the blended samples processed with lead nitrate averaged 84.3%. The gold extraction is in excellent agreement with the expected average value (84.3%) calculated based on a weighted average of the results from the testing of the ores independently and

was in good agreement with the actual average Fort Knox mill extraction of 84.6%.

The simulations were initially performed on a standard 3:1 ratio of Fort Knox to True North in 20 hour cyanidation tests. The procedure was modified during the year and improved the correlation in the results from the simulations with lead and the actual leach plant performance. The primary changes included adjusting the duration of the simulation test time to represent the average circuit retention time each month and developing the blended sample based on the actual average blend ratio processed for the month.

Table 3.3 contains the expected leach extraction based on the weighted average calculation from the individual monthly ore samples and the actual results for the monthly simulations with and without lead. Also included in Table 3.3 are the actual monthly leach circuit gold extractions. The summary of the monthly results are also illustrated in Figure 3.11.

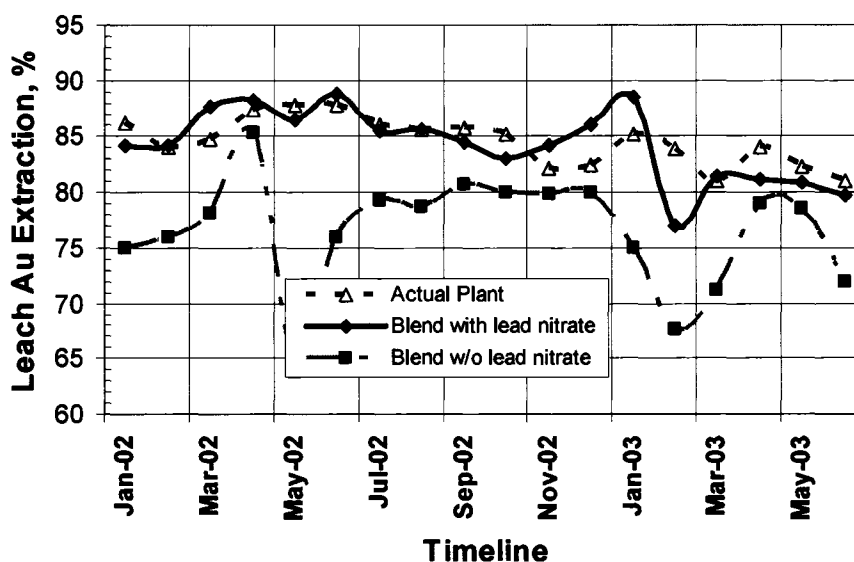


Figure 3.11 Comparison of plant performance and FGMI laboratory testing on a blend sample of True North and Fort Knox ores, with and without lead nitrate.

Table 3.3 Actual plant and bottle roll test results on blended sample.

Year	Calculated w/o lead nitrate Leach Au Extraction %	Calculated With lead nitrate Leach Au Extraction %	FK/TN Blend w/o lead nitrate Leach Au Extraction %	FK/TN Blend with lead nitrate Leach Au Extraction %	Change Leach Au Extraction %	Actual Plant Leach Au Extraction %
Jan 02	83.4	85.8	75.0	84.2	9.2	86.2
Feb 02	84.7	87.5	76.0	84.2	8.2	84.1
Mar 02	85.0	84.3	78.1	87.7	9.6	84.8
Apr 02	77.4	82.0	85.3	88.3	3.0	87.4
May 02	86.3	84.7	63.8	86.5	22.7	87.8
Jun 02	87.3	87.6	76.0	88.8	12.8	87.8
Jul 02	85.8	84.1	79.3	85.5	6.2	86.1
Aug 02	80.1	79.1	78.7	85.6	6.9	85.7
Sep 02	85.1	85.2	80.7	84.5	3.8	85.8
Oct 02	80.5	83.1	80.0	83.1	3.1	85.2
Nov 02	83.9	84.2	79.9	84.2	4.3	82.2
Dec 02	85.6	86.0	80.0	86.0	6.0	82.4
Jan 03	86.5	88.6	75.0	88.6	13.6	85.2
Feb 03	86.7	85.4	67.7	77.0	9.3	83.9
Mar 03	85.2	86.8	71.2	81.5	10.3	81.1
Apr 03	86.1	87.1	79.0	81.2	2.2	84.0
May 03	77.3	74.5	78.6	80.9	2.3	82.3
Jun 03	82.7	82.1	72.0	79.8	7.8	81.1
Average	83.9	84.3	76.5	84.3	7.8	84.6

3.4.4 Effect of Antimony and Lead Nitrate Addition

The negative effect of antimony on gold leaching is illustrated in Figure 3.12. The gold extractions strongly correlated with the antimony content of the feed sample with

leach extraction decreasing as the antimony content of the feed material increased in the blended ore samples. This relationship was virtually eliminated, when lead nitrate was added to cyanidation tests. Consequently, the negative effect of antimony can be compensated for through a lead nitrate addition. However, it was found that antimony is not an issue when True North ore is leached individually. This suggests that additional mechanisms are also influencing the gold extraction.

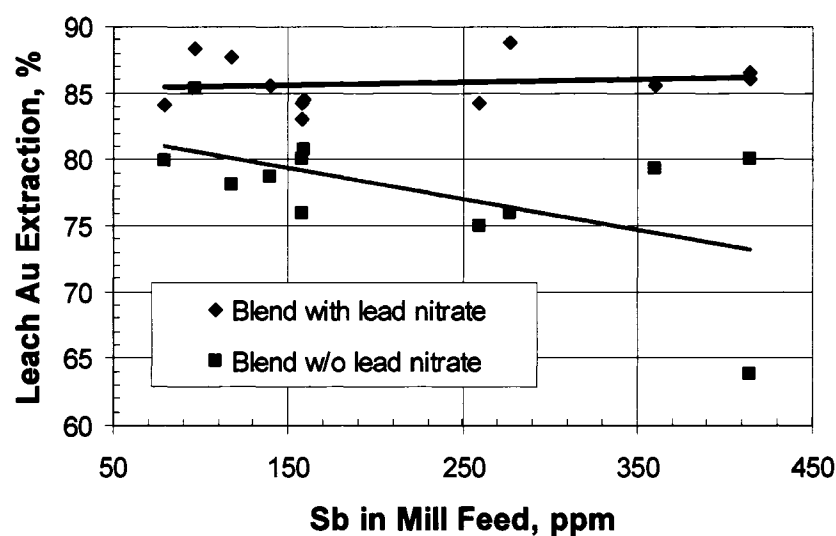


Figure 3.12 Effect of antimony concentration in the feed.

These results further substantiate the conclusion reached in 2001, when a detailed evaluation of actual plant tails indicated that low gold extraction was caused by the formation of a passivating film on free gold particles originating from Fort Knox ore. The film was thought to be caused by chemical species resulting from sulfide mineral dissolution, mainly stibnite, contained in True North ore, with the primary difference being in the particle size distribution of gold between the two ore deposits (Fort Knox having a coarser particle size distribution than True North) (Hollow *et al.*, 2003).

3.5 COMPARISON FORT KNOX AND CANMET RESULTS

Results of the CANMET cyanidation study on the February Fort Knox ore sample were consistent with results from the FGMI leach circuit simulation work done under similar conditions. Although the February True North composite was not tested independently at CANMET, it was used to produce the blended sample that was analyzed in the cyanidation study. This allowed for direct comparison of the CANMET findings to the FGMI laboratory results that have been correlated to actual mill performance.

Table 3.4 contains the results of the CANMET and FGMI testing of both the Fort Knox ore sample and the Fort Knox/True North blend. Results from both labs on the blended material, with lead added to cyanidation, were consistent with actual mill performance in February.

Table 3.4 FGMI, CANMET laboratory results and actual plant performance

	FGMI Lab blend w/o lead	CANMET blend w/o lead	FGMI Lab blend with lead	CANMET blend with lead	Fort Knox actual plant With lead
Leach time, hrs	20	20	20	20	18.5
NaCN, ppm	184	76	184	76	90.5
D.O., ppm	8.4	12	8.4	12	12
Temp., °C	19.2	10	19.2	10	9.8
PH	11.35	10.2	11.35	10.2	10.1
Pb(NO ₃) ₂ , g/t	0	0	75	100	70.5
Grind, % -100 mesh	64.9	65.0	64.9	65.0	84.9
Head grade, g/t	0.71	0.72	0.71	0.72	0.75
Au extraction, %	76.0	77.5	84.1	84.5	84.1

The FGMI laboratory simulation work is performed at room temperature, where the maximum dissolved oxygen that can be maintained in the bottle roll test is 6-9 ppm. And is likely the reason that it requires approximately 2 times the cyanide concentration to produce results similar to plant performance.

The impact of lead nitrate addition was also apparent in the leach kinetics curves. The lab procedures at the FGMI lab incorporate sampling at the 1, 2, 16, 18 and 20-hour points to allow for better definition of the extraction rate in the later hours of the test. This approach allows for better prediction of the gold losses expected when increased mill throughput rates reduce circuit retention time. Figure 3.13 contains the kinetics data from both labs in comparison to the actual mill performance in February.

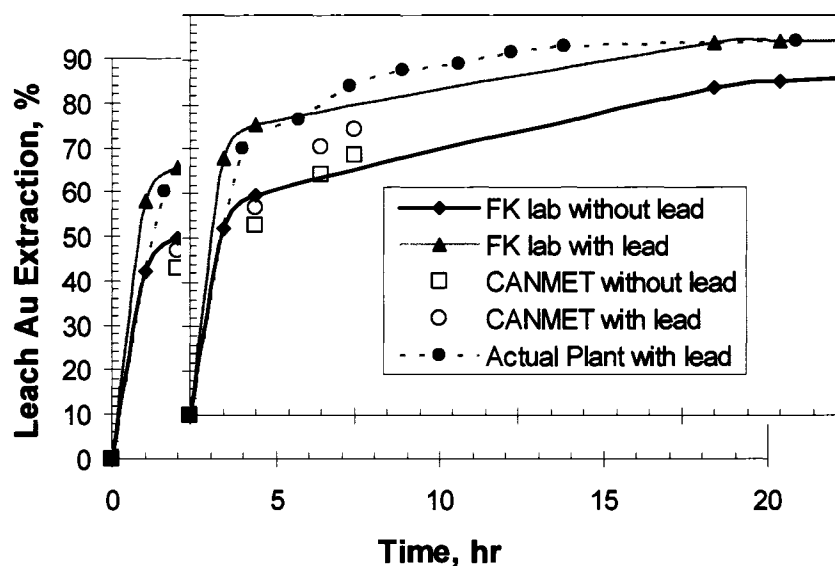


Figure 3.13 Effect of lead nitrate - comparison between laboratory and plant results for February 2002.

With good correlation between the CANMET test results and the FGMI laboratory simulation test results on the February samples, it is expected that any conclusions reached in the detailed CANMET study can be applied to the remainder of the 2002 FGMI test data. Process simulations tests are also performed on a blend of the True North and Fort Knox ores on a monthly basis at the FGMI metallurgical laboratory. The gold extraction results from the monthly simulation testing of the blended samples take into account the interactions of the individual ore types and are a good indication of actual plant performance.

Lead nitrate has been added to the Fort Knox leach circuit on a continuous basis, since late December 2001. Therefore, no direct comparison between processing with lead and without lead can be provided for the plant. However, due to the strong correlation between the results of the lab simulation tests with lead addition and the actual plant performance, it is assumed that the results of the FGMI laboratory data simulate adequately the difference of using lead addition to predict plant performance. It is estimated that gold production from the Fort Knox mill was increased by 49,600 ounces between January 2002 and June 2003 due to the addition of lead nitrate. With a total lead nitrate cost of \$1,600,000 during the same period, the cost per incremental ounce produced was approximately \$US32.

The FGMI laboratory simulation procedure was developed for metal accounting and recovery calculations and was not intended for predicting reagent consumptions. Although the average consumptions were consistent (0.065 kg/t plant, 0.067 kg/t lab), the correlation between the monthly data is poor. Additional work is required to explain the variation in the monthly cyanide consumption data measured in the FGMI laboratory.

3.6 DISCUSSION

The laboratory results from FGMI correlated strongly with the CANMET laboratory results. The laboratory results of cyanidation without lead under typical circuit conditions (65% -100 mesh grind, D.O. of 12 ppm, free cyanide concentration of 75 ppm NaCN and pH 10.2) were found to be approximately 77%. The extraction could be increased to approximately 84% by reducing pH to 9.8, increasing D.O. concentrations to 18 ppm or through the addition of 100 ppm lead nitrate. The 84% laboratory extraction was consistent with plant extraction and the best leaching parameters were found to be identical to the base line parameters currently used in the plant. The system however did not reach a steady state in 20 hours and pretreatment did not show any significant advantage over straight cyanidation.

The concentration of antimony is similar to the feed processed at Williams Mine of Hemlo (Deschenes *et al.*, 1999), where cyanidation at a pH below 10 is used to

minimize the negative effect of antimony on gold extraction. Although reduction of the pulp pH proved to be efficient in laboratory tests, it is not an option in the Fort Knox mill, where operating the circuit at a reduced pH results in above threshold level HCN concentrations in the tank enclosures. The enclosures are required to allow the circuit to be operated and maintained in a sub-Arctic environment.

At a free cyanide concentration of 150 ppm, the gold leaching kinetics were significantly improved and the system reached a steady state, however, the overall extraction was not significantly improved. The higher cyanide concentrations were not detrimental on cyanide consumption in the CANMET laboratory test. However in plant practice, only 60% of the barren leach solution is recycled and the remainder requires cyanide destruction. Consequently, using higher cyanide concentrations in leach circuit not only increases reagent costs for cyanide but also increases the detox circuit reagent costs and close consideration of the incremental cost per ounce produced is required when setting the optimum NaCN concentration for the plant.

3.7 CONCLUSIONS

- The blend sample studied contained 0.71 g/t Au, with small amounts (below 1%) of pyrite, arsenopyrite and pyrrhotite and trace amounts of stibnite, cervantite, arseniosiderite, scorodite and chalcopyrite.
- A total of 96% of the gold was leachable.
- The presence of antimony is responsible for retarding gold leaching.
- The gold particle size has a significant impact on the final gold content of leach residue.
- The addition of lead nitrate was found to be the most practical and cost effective way to alleviate the negative effects of antimony.
- The use of low pH is not a practical alternative for Fort Knox Mine, because of the generation of a high HCN concentration in the tank enclosures required in a sub-

Arctic environment. Increasing the D. O. level of the leaching slurry requires extra equipment.

- The laboratory results at CANMET correlate strongly with the results at FGMI and the results from both labs correlate well with the performance of the plant which indicates that the approach used in the labs is reliable.
- During the 18 month period beginning in January 2002, the new scheme increased the gold extraction by 7-9% and resulted in gold production being in excess of 49,000 ounces higher than that estimated for the non-lead nitrate reagent scheme.

3.8 ACKNOWLEDGEMENTS

The authors wish to thank Jean Cloutier for his work on fire assay, Dr. Rolando Lastra for the mineralogical analysis and FGMI and CANMET for the authorization to publish this paper.

REFERENCES

- Avraamides, J., Dork, K., Durack, G., and Ritchie, I.M., 2000, *Effect of antimony (III) on gold leaching in aerated cyanide solutions: A rotating electrochemical quartz crystal microbalance study*, In Minor Elements 2000: Processing and Environmental Aspects of As, Sb, Se, Te, and Bi, Editor Young C., Society for Mining, Metallurgy, and Exploration, Inc. (SME), 2000, pp. 171-178.
- Deschênes, G. and Fulton, M., (1998) "*Improving cyanidation of a sulphide orebody using an efficient pre-leaching*", Proceedings of Int. Symp. Recovery of Gold, Montreal, CIM Annual General Meeting, 1998, pp. 63-69.
- Deschênes, G., Putz, A., and Riveros, P., 1999, "*The third survey of gold cyanidation plants*", MMSL Report 99-010 (CR).
- Deschênes, G., Fulton, M., and Atkin, A., 2002a, "*Cyanidation study of a gold ore from Fort Knox Mine*", CANMET MMSL Report 02-035(CR).

- Deschênes, G., Guo, H., Fulton, M., and Swist, E., 2002b, "*Cyanidation of a Fort Knox ore sample from Fort Knox Mine*", CANMET MMSL Report 02-053(CR).
- Habashi, F., 1967, *Kinetic and mechanism of gold and silver dissolution in cyanide solution*, Bulletin 59, State of Montana Bureau of Mines and Geology.
- Hedley, N. and Howard, T., 1958, *Chemistry of cyanidation*, Mineral Dressing Notes Number 23, American Cyanamid Company, Wayne, N.J.
- Hollow, J.T., Hill, E.M., Lin, H.K. and Walsh, D.E., 2003, *The effect of $Pb(NO_3)_2$ addition on the processing of blended Fort Knox and True North ores at the Fort Knox Mine*, Minerals and Metallurgical Processing, Vol. 20, No. 4, pp. 185-190.
- Liu, G.Q. and Yen, W.T., 1995, *Effects of sulphide minerals and dissolved oxygen on the gold and silver dissolution in cyanide solution*, Minerals Engineering, Vol. 8, No. 1-2, pp. 111-123.
- Magnuson, R., Hollow, J.T., Mosher, J., and Major, K., "*The Fort Knox Mill: design, commissioning and operations*", International Autogenously and Semiautogenous Grinding Technology 2001, Editors: D.J. Barratt, M.J. Allan, and A.L. Mular, (2001), Vol. 1, pp. 159-173.
- Marsden, J. and House, I., 1992, The Chemistry of Gold Extraction, Ellis Horwood, New York, pp. 275
- Nicol, M.J., Fleming, C.A. and Paul, R.L. 1987, *The chemistry of the extraction of gold*, In: Stanley G.G.(Editor), The Extractive Metallurgy of Gold in South Africa, The Chamber of Mines of South Africa, The South African Institute of Mining and Metallurgy, Kelvin House, Johannesburg 2001, pp. 860-862.
- Yannopoulos, J.C., 1991, The Extractive Metallurgy of Gold, Van Nostrand Reinhold, New York, pp. 156-163.

CHAPTER 4

MODELING THE INFLUENCE OF SLURRY TEMPERATURE ON GOLD LEACH AND ADSORPTION KINETICS AT THE FORT KNOX MINE, FAIRBANKS, ALASKA¹

4.1 ABSTRACT

The Fort Knox Mine is located in Alaska's interior where the average ambient air temperatures range from -24°C (-11°F) in January to 16°C (61°F) in July. The mill processes a free-milling gold ore utilizing a gravity recovery circuit and conventional cyanide leach/carbon-in-pulp circuits. Plant slurry temperature cycles seasonally and allows for a unique opportunity to measure the impact that temperature has on gold leach kinetics, carbon adsorption efficiency and cyanide destruction reactions. Mathematical models were developed to accurately predict actual mill performance. This paper describes the development of the models and presents data, which allow for a better understanding of the impact of circuit operating temperature on process efficiencies.

4.2 INTRODUCTION

The Fort Knox Mine, which is located in the Fairbanks Mining District, 40 km (25 miles) by road northeast of Fairbanks, Alaska, began commercial gold production in the first quarter of 1997. The average annual temperature at the site is -3.6°C (26°F) with daily temperatures averaging -23.8°C (-10.9°F) in January and 15.8°C (60.4°F) in July. The mine receives an average of 0.43 m (17 in.) of annual precipitation, with most of the precipitation falling in the summer and early fall. The average snow pack is 1.65 m (65 in.) and snow remains on the ground from early October until early April. The mine is accessible all year from Fairbanks via the Steese Highway and 9.7 km (6 miles) of well-

¹ Hollow, J.T., Hill, E.M., Lin, H.K., and Walsh, D.E., (2006), *Minerals and Metallurgical Processing*, Vol. 23, No. 3, pp. 151-159.

maintained gravel road. The Fort Knox gold deposit is hosted within a multiphase granitic body with an elongated surface exposure. Gold is contained in milky-white quartz stockwork veins and veinlets, as well as along shears and fractures within the granite. The quartz filled shears contain evenly distributed gold, generally less than 100 microns in size, while the gold in the milky-white stockwork veins and veinlets is similar in size, but has a more erratic occurrence.

The Fort Knox mill feed rate averaged 37,467 tpd (41,300 stpd) in 2003. The run-of-mine ore is crushed to minus 13 cm (5 in.) in a 1.9 m x 2.7 m (74 in x 105 in) primary gyratory crusher located near the pit, before being conveyed 0.8 km to the coarse ore stockpile at the mill site. The coarse ore is reclaimed from the stockpile and conveyed to a 10 m (34 ft) diameter by 4.5 m (15 ft) long SAG mill, which operates in close circuit with a 3.0 m x 7.3 m (10 ft x 24 ft) double deck vibrating screen. Screen undersize is processed through two Svedala 6 m (20 ft) diameter by 9 m (30 ft) long ball mills operated in closed circuit with twenty, 66 cm (26 in.) diameter cyclones. The SAG mill is driven by two 5,200 kw (7,000 hp), synchronous, electric motors controlled by LCI drives to provide variable speed control. Each ball mill is powered by a fixed speed, 5,200 kw (7,000 hp), synchronous electric motor. The final product from the grinding circuit was designed to be 80% passing 149 microns (100 mesh).

Pinched sluices, located in each of the ball mill discharge launders, are used to produce approximately 436 tph (480 stph) material that is processed through two Knelson concentrators, where approximately 15 percent of the total gold production is recovered by gravity concentration. Gravity tailings are returned to the grinding circuit for further comminution. The grinding circuit product is processed through a high capacity thickener, which produces a 50-54% (w/w) solids underflow that is pumped to the seven-stage cyanide leach circuit. The slurry discharging from the leach circuit is processed through a conventional, six-stage, carbon-in-pulp (CIP) circuit, where the dissolved gold is adsorbed onto granular activated carbon. At present, the plant is operating at 25% above the design throughput rate and therefore, a significant portion of the leaching occurs in the CIP circuit. In the original plant design, the CIP tailings pass directly to an

The Fort Knox mill processed blended ore from both ore deposits from April 2001 through March 2004. The focus of this investigation is to evaluate leach and carbon adsorption kinetics for Fort Knox ore. Therefore, the data evaluated will be from time periods when the mill was processing straight Fort Knox ore.

As operating history was generated at the Fort Knox mill, seasonal fluctuations in leach circuit slurry temperature were observed. The slurry temperatures ranged from lows of less than 10°C (50°F) in the winter months to maximum temperatures in excess of 25°C (77°F) during the summer. In general, the leach temperature cycles with changes in the ambient air temperature. Figure 4.2 shows this relationship.

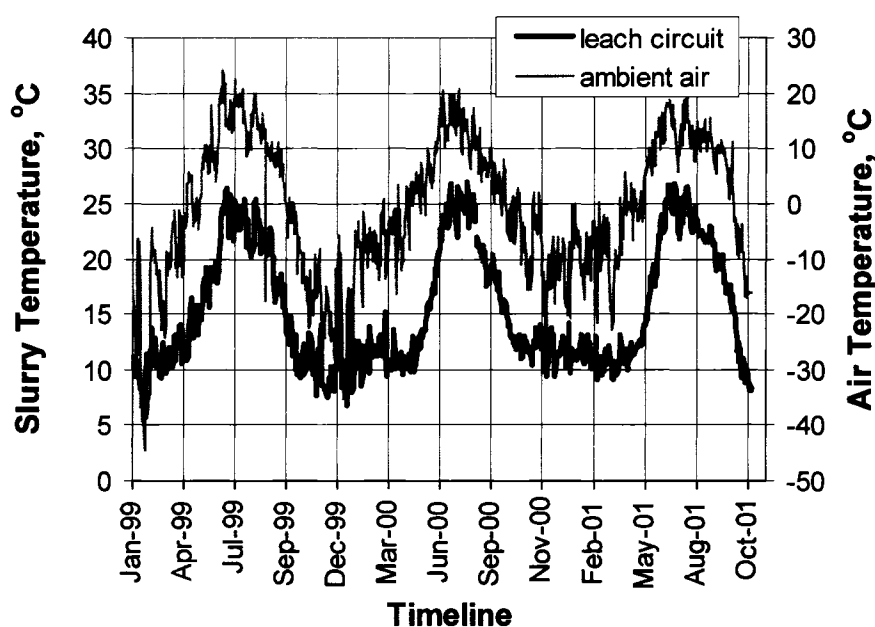


Figure 4.2 Leach slurry and ambient air temperatures, °C (1999-2001).

In addition, it became apparent that variations in leach circuit gold extraction were correlated to leach circuit slurry temperature. Figure 4.3 contains a simple regression of leach gold recovery and circuit operating temperature during the initial years of operation at the Fort Knox mill. The results suggested that although a significant relationship existed between leach temperature and gold extraction, a more sophisticated model was needed to further explain the variability in the actual plant results

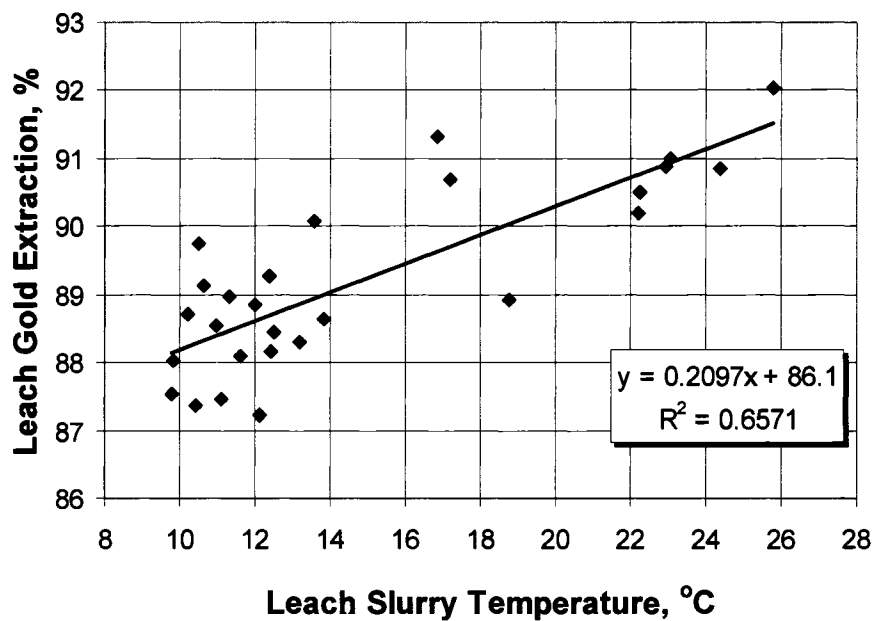


Figure 4.3 Regression - Leach gold recovery vs. slurry temperature (1998-2001).

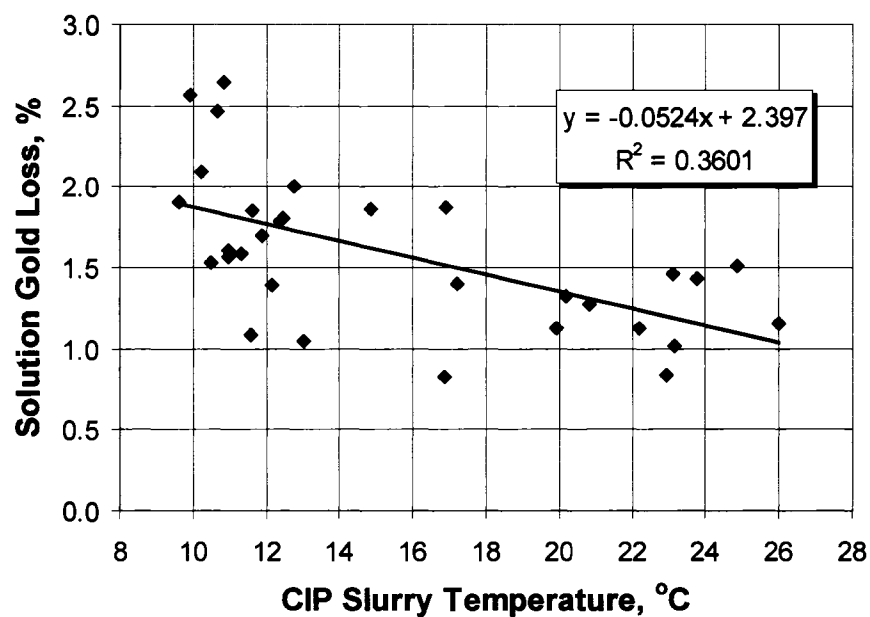


Figure 4.4 Regression - CIP solution gold loss vs. slurry temperature (1998-2001).

Variations in mill solution gold losses have also trended seasonally (Figure 4.4) and can be partially explained by a simple linear relationship with solution gold losses (expressed as a percent of leach feed ounces) being dependent on leach/CIP circuit slurry

temperature. Development of the detailed model describing leach and carbon adsorption kinetics is included in this paper.

The relationship between circuit slurry temperature and fluctuations in reagent addition rates were also observed during the initial years of operation at the Fort Knox mill. Figure 4.5 contains the relationship between the lime addition rate and circuit operating temperature. Additional variation in the lime addition rate can be explained by variations in circuit pH as a second dependent variable.

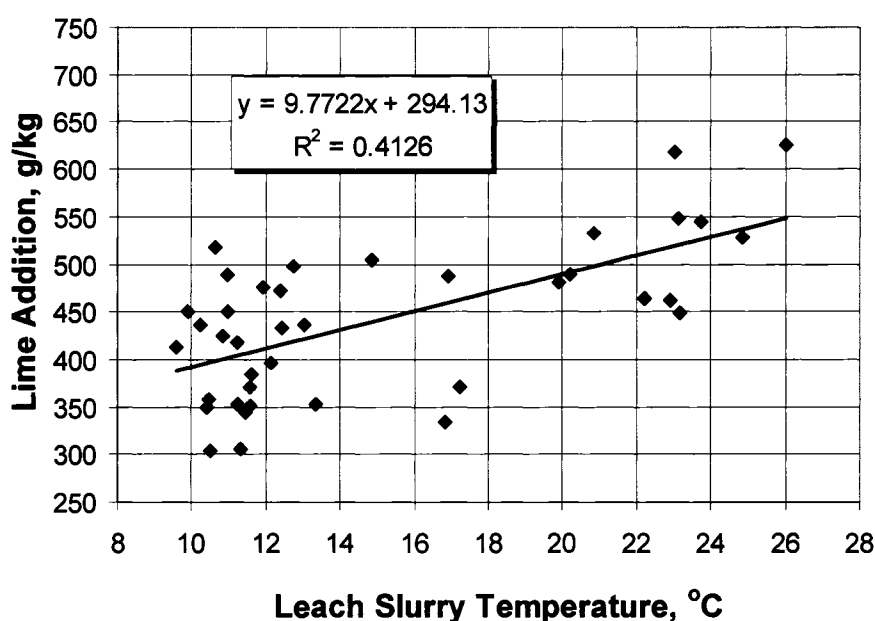


Figure 4.5 Regression - Leach circuit lime addition vs. slurry temperature (1998-2001).

The SO_2 /air cyanide destruction circuit is another area where reagent addition is correlated with circuit operating temperature. Figure 4.6 contains the simple regression model representing this relationship.

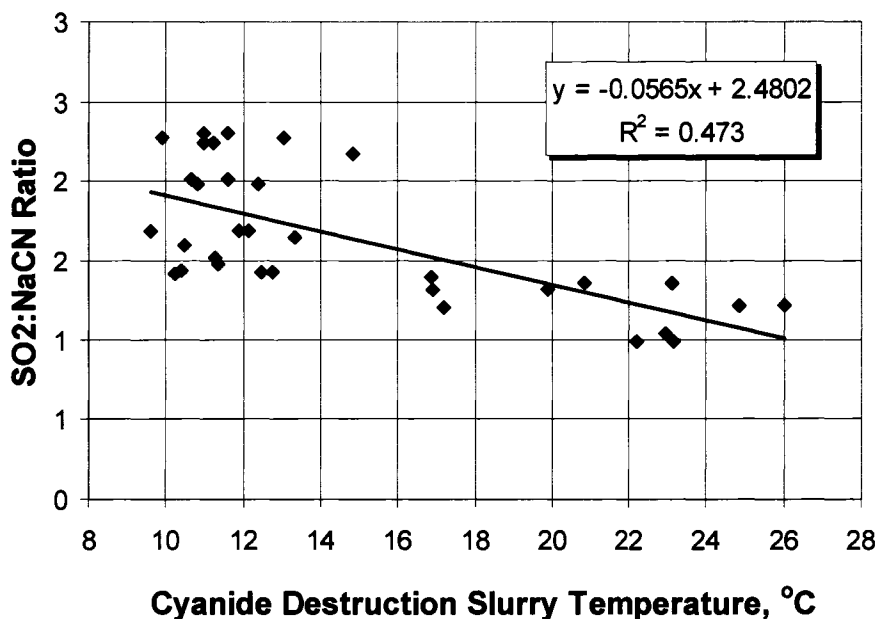
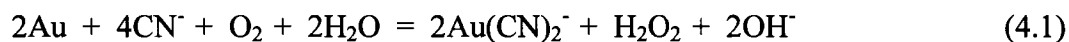


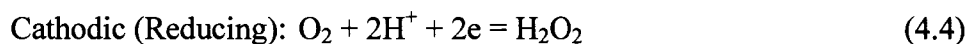
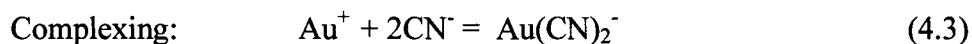
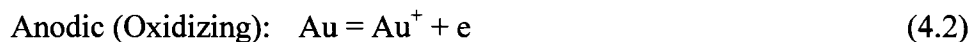
Figure 4.6 Regression – Ratio of SO₂:NaCN vs. slurry temperature (1998-2001).

4.3 MODEL DEVELOPMENT

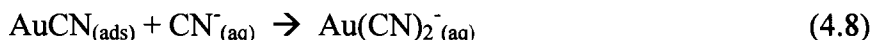
4.3.1 Gold Dissolution in Cyanide Solution

The mechanism for gold dissolution using cyanide as the complexing agent has been studied extensively, and there is a general consensus that the reaction is electrochemical in nature (Christy, 1896; Boonstra, 1943; Thompson, 1947; Kirk *et al.*, 1978; Lin and Chen, 2001). Additional gold cyanidation evaluations have also been conducted (Kudryk and Kellogg, 1954; Habashi, 1967; Wadsworth, 1991) with emphasis placed on reaction kinetics. The role of the primary reactants (O₂ and CN⁻) can be described by evaluating the individual anodic and cathodic half-reaction equations. Equation (4.1) represents the overall reaction (Elsner's equation), while equations (4.2) and (4.3) express the anodic reaction and complexing reaction, respectively. Equations (4.4) and (4.5) represent the cathodic reactions.





The anodic and complexing reactions (gold oxidation) have been further defined as follows (Cathro and Koch, 1964; MacArther, 1972; Thurgood *et al.*, 1981; Wadsworth, 1991; Lin and Chen, 2001):



where the subscript (ads) refers to surface adsorbed species and (aq) refers to the aqueous species.

Kudryk and Kellogg (1954) concluded that the kinetics of gold cyanidation were directly related to the concentration of the complexing agent (cyanide) under one regime, while the kinetics are controlled by the concentration of the oxidant (oxygen) in another.

Based on the anodic and cathodic reactions listed above, they concluded that 2 moles of cyanide ion were required to dissolve one mole of gold and release one mole of electrons in the anodic reaction. It was also concluded that one mole of oxygen (when reduced to hydroxyl ions) would consume 4 moles of electrons, that the reaction was essentially 100 % efficient in discharging oxygen, and that the intermediate formation of hydrogen peroxide did not occur in significant amounts. This resulted in the theoretical cyanide to oxygen molar ratio, 8:1.

Deitz and Halpern (1953) evaluated the kinetics of the dissolution of silver in sodium cyanide solution and concluded that the reducing reaction described by equation 4 did not appear to participate to any extent. The conclusion was based on results of tests, where H_2O_2 was added to the solution and did not affect the gold dissolution rate. Additionally their test results indicated that the transition from the region, where the rate is controlled by the transport of CN^- to the region of control by the transport of O_2 , occurs at a ratio of concentration $[\text{NaCN}]:[\text{O}_2]$ of 4.4.

Habashi (1967), upon review of previously published works (including Kudyk and Kellogg, 1954), concluded that the intermediate formation of the H_2O_2 and hydroxyl ion expressed by equation (4) was the final step in the cyanidation reaction and that only two electrons would be required to reduce the oxygen. Habashi proposed that the ratio of the molar concentrations of cyanide to oxygen, at which the rate controlling concentration changes from cyanide to oxygen, was 6:1 (9.1 ppm NaCN:1 ppm O_2) and ranged from 4.6:1 to 7.4:1. This value also represents the rate at which the diffusion of both reactants should be at their maximum.

Wadsworth (1991) presented data indicating that the reduction of hydrogen peroxide begins at different potentials for various metals. He concluded that the rate at which peroxide diffuses away from the metal surface may also influence the effective use of oxygen and it is likely that both the 4-electron and 2-electron processes are occurring simultaneously and that the number of electrons transferred varies with potential.

Ling *et al.* (1996) presented data from cyanidation experiments on a particular gold ore, where the objective was to decouple the effects of free cyanide $[\text{CN}^-]$ and dissolved oxygen $[\text{O}_2]$ concentration. They found the leach rate reached a plateau when $[\text{CN}^-]$ was higher than 100 ppm on tests performed with $[\text{O}_2]$ at 8.5 ppm, and an oxygen to free cyanide ratio of 11.8:1.

Heath and Rumball (1998) suggested a method for determining whether gold leaching in CIP/CIL circuits is limited by the lack of either oxygen or cyanide concentration. They presented data generated using a gold (96%)/silver (4%) alloy disc

electrode placed in leaching pulp, with its corrosion potential measured against a reference electrode. The results suggested the optimum cyanide:oxygen ratio was approximately 10.5 ppm NaCN to 1 ppm O₂ (6.9:1 molar ratio). Their conclusions were supported by Wadsworth's (2000) findings that silver surface reactions used the four-electron process while oxygen reduction on the gold surface used the two-electron processes. They suggested that the difference between the 6:1 molar ratio proposed by Habashi and their finding of 6.9:1 was the result of using an alloy electrode in pulp rather than a pure gold electrode evaluated in clear solution. They also noted that previous measurements were voltametric, with the gold electrode forced to either be an anode or a cathode, rather than both simultaneously occurring as in actual plant conditions.

Heath and Rumball (1998) repeated the procedure on a variety of Western Australian CIP/CIL slurries and determined that the cyanide to oxygen ratio was essentially unchanged by the pulp type and consistent with the results on pure solution. They suggested that the actual diffusion rate of oxygen and cyanide to the gold particle surface under plant conditions will be significantly different from that measured in the laboratory. However, the diffusion rate of both the oxygen and cyanide can be expected to be impacted by the same amount and the optimum cyanide to oxygen ratio should remain unchanged.

4.3.2 Effect of Temperature on Leach Slurry Rheology

Rheology studies of Fort Knox leach feed materials were completed to provide data for the engineering and design phases of the project (Link, 1993). Six slurry runs were completed in an extrusion rheometer at temperatures ranging from 18°C to 26°C (64°F to 78°F) and slurry densities ranging from 41.9% solids to 61.4% solids (w/w).

The results indicate that the slurries are Bingham plastics in all expected operating conditions. Results also indicated that slurry viscosities would be significantly affected by both the density (percent solids, w/w) and the temperature of the slurry. Slurry viscosity increased slowly up to a value of approximately 50% solids (w/w), at which point the rate of increase then accelerated up to a value of approximately 56% solids

(w/w). Additionally, as slurry temperatures decreased from 21°C (70°F) to 8°C (46°F), the dynamic viscosities increased by as much as 67% and the Reynolds number of mixing dropped from 50,552 to 33,220.

Although no laboratory work was done with the same slurry at different temperatures other than 18° to 26°C, the effects of temperature on slurry viscosity are similar to those for other fluids and can be predicted by a simple power law relationship over usefully large temperature ranges (Link, 1993). The results of the six tests were used to compute rheologic constants that were then used to calculate the effect of density and temperature on slurry dynamic viscosity. Figure 4.7 contains these results, which indicate that variations in leach-circuit slurry densities typical for the Fort Knox mill (48% to 51% solids w/w) will have significantly less impact on viscosity than the effects due to variations in leach-circuit slurry temperature.

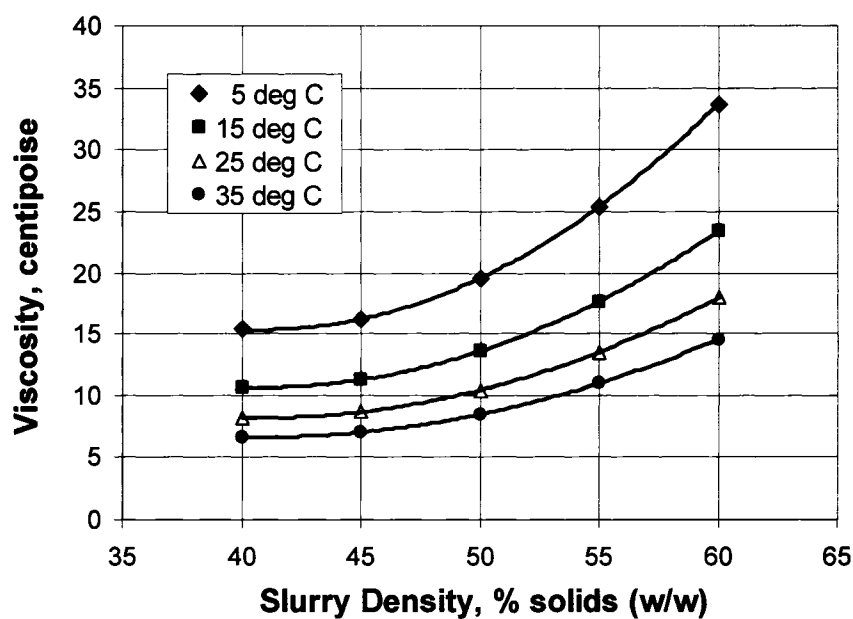


Figure 4.7 Summary of 1993 rheology studies on Fort Knox leach sample.

It is proposed that these variations in slurry rheology result in measurable impacts to reactions controlled by diffusion within the Fort Knox mill's leaching/CIP circuits.

These impacts can be predicted using temperature as the independent variable, since a direct measurement of slurry viscosity is not available in the plant.

4.3.3 Effect of Temperature on Leach Oxygen Concentration

Habashi (1970) described the cyanidation process as a heterogeneous reaction taking place between three phases; gold (solid), aqueous NaCN (liquid), and oxygen (gas). Since the rate at which oxygen is transferred from the gaseous phase to the liquid phase is much faster than the other reactions taking place, the process is reduced to a solid-liquid reaction. The gold dissolution rate increases with temperature, as a result of increased surface reaction and diffusion rates of reactants and products, up to a maximum of 85°C (Marsden and House, 1992). Deitz and Halpern (1953) evaluated the rate of silver dissolution in NaCN solutions at temperatures ranging from 24°C to 110°C. They generated an Arrhenius plot and determined the reaction rate was linear over the entire temperature range tested, with a slope that indicated the activation energy was low and the rate was controlled by a diffusion process.

Ling *et al.* (1996) presented data that showed the oxygen level maintained during the 48 hour laboratory leach tests was mainly affected by variations in temperature rather than the rate of oxygen consuming reactions, the rate of oxygen mass transfer, or the ionic strength.

At the Fort Knox mill, the seven 16.5 m (54 ft) in diameter, 14.6 m (48 ft) tall leach tanks are constructed of carbon steel and are sealed with an insulated cover that allows for a slight partial pressure to be maintained over the slurry. The tanks are located outdoors with no insulation other than the covers. The oxygen is added as atmospheric air injected into the tanks via spargers located near the bottom of the tanks. Data for the leach circuit's dissolved oxygen concentration $[O_2]$, are presented in Figure 4.8. The data suggest that $[O_2]$ can be expressed as a function of slurry temperature.

The reaction rate has been shown to be a function of the circuit oxygen concentration (Habashi, 1967; Ling *et al.*, 1996; Rubisov *et al.*, 1996; Fang *et al.*, 1998). However, in the Fort Knox leach circuit, since the dissolved oxygen concentration is

primarily dependent on circuit operating temperature, any expression of the rate constant as a function of temperature will also account for variations in oxygen concentration

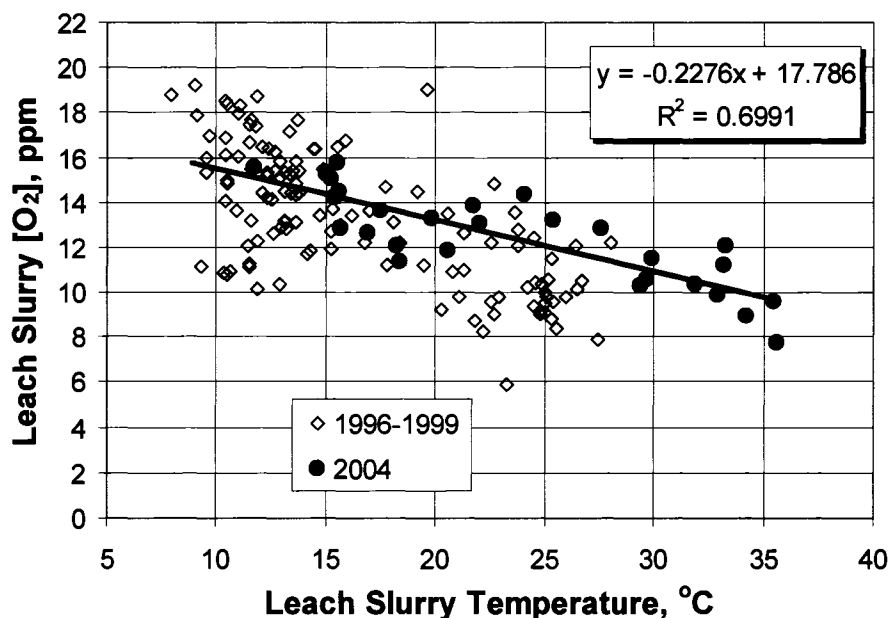


Figure 4.8 Historical Fort Knox leach slurry [O₂] vs. slurry temperature.

Assuming that the optimum [NaCN]:[O₂] ratio at Fort Knox is 11 ppm NaCN to 1 ppm O₂ or 5.8 ppm CN⁻ to 1 ppm O₂, the rate limiting conditions can be expressed as a function of leach slurry temperature. Figure 4.9 contains this relationship for the Fort Knox leach circuit.

Also included in Figure 4.9 are the average monthly leach circuit NaCN concentrations maintained in the Fort Knox leach circuit in recent years. The data suggest under all normal operating conditions, gold cyanidation is being controlled by cyanide diffusion, and the reaction rate will be a function of the cyanide concentration. In many laboratory tests and plant operations, gold cyanidation has been considered controlled by the diffusion of oxygen. However, at the Fort Knox Mine, gold cyanidation is controlled by diffusion of cyanide due to the very low cyanide concentrations and relatively high oxygen concentrations applied in the mill's leach circuit, as shown in Figure 4.8.

In general, the leach circuit has been operated at NaCN concentrations ranging from 70 ppm to 80 ppm (37 to 42 ppm CN^-) during periods when the mill is processing straight Fort Knox ore. Periods where the concentration was higher than 80 ppm are primarily associated with processing blends of Fort Knox and True North ores. All new cyanide is added at leach tank #1, where the pH is maintained between 10.2 and 10.4 through dry lime addition to the grinding circuit.

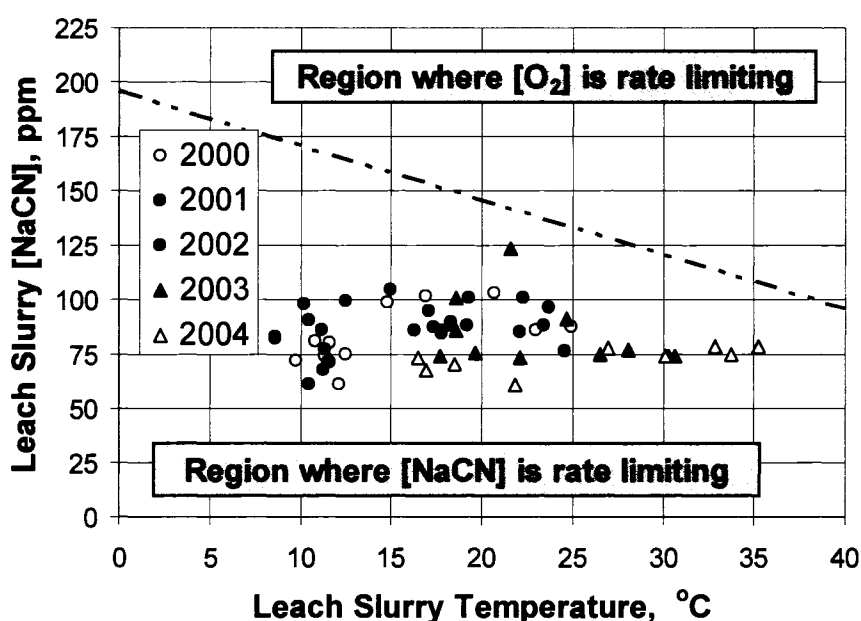


Figure 4.9 Theoretical rate controlling regions vs. slurry temperature.

Figure 4.10 contains a timeline of the historic leach concentrations and indicates that only a minimal reduction in $[\text{NaCN}]$ is observed in the leach circuit (5% to 10%) when processing straight Fort Knox ore. The majority of the cyanide loss is occurring in the CIP circuit. This is consistent with the findings of Adams (1990), who evaluated the kinetics of cyanide loss in a typical leach/CIP process. He observed only minor loss in the absence of activated carbon with fairly high losses when carbon was present. The losses were due to adsorption onto activated carbon, to some extent, and to a carbon-catalyzed oxidation of cyanide to cyanate. For periods when True North ore was blended with Fort

Knox ore (April 2001 – March 2004), more dramatic cyanide losses were observed. This loss is the result of cyanide-consuming sulfide minerals (Adams, 1990) in the True North ore.

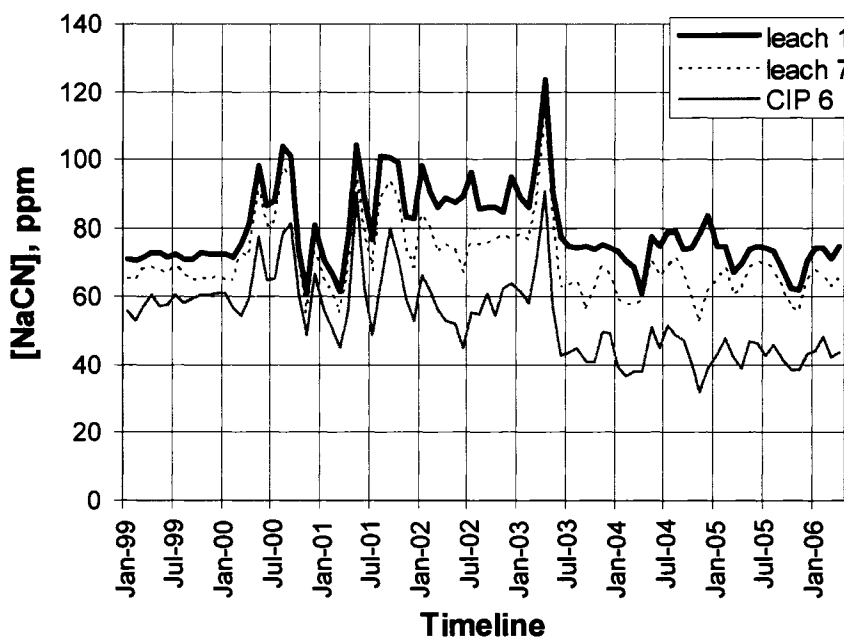


Figure 4.10 Historic Fort Knox leach/CIP circuit [NaCN] (2000–2006)

4.3.4 Effect of Temperature on Gold Leach Rate

Plant tailings are sampled and analyzed at room temperature on a daily basis at the Fort Knox mill. In one analysis, bottle-roll tests are performed on tailings slurry samples to determine the remaining cyanide soluble gold content. The average monthly results, presented in Figure 4.11, indicate the seasonal variations became more pronounced after mill throughput rates increased during 1998 and further substantiates the proposed relationship between leach kinetics and circuit operating temperature.

The model form chosen to estimate leach gold extraction at the Fort Knox mill is given in Equation 4.9 under conditions of constant temperature, cyanide concentration and mill head grade. The equation is the form of the Mintek expression described by Nicol *et al.* (1984).

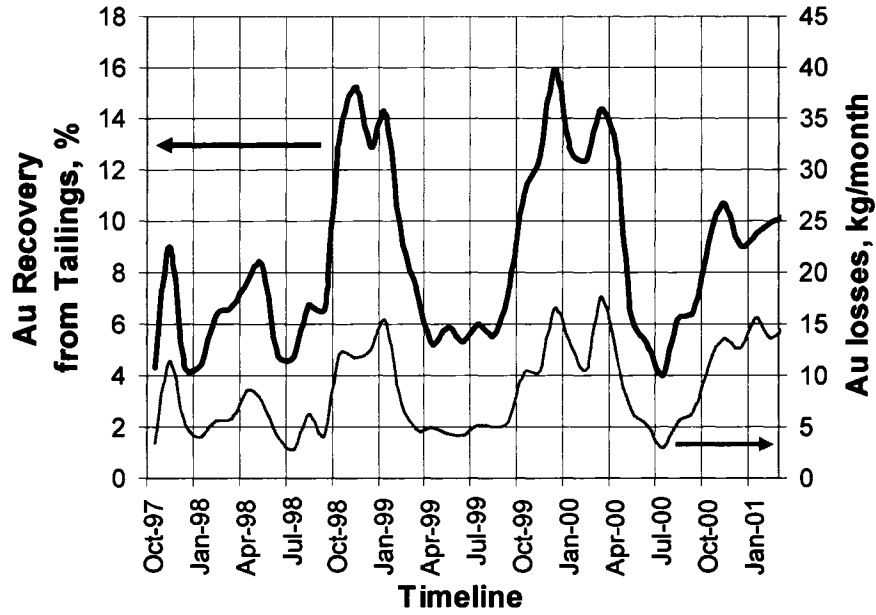


Figure 4.11 Monthly cyanide soluble gold in solid tailings; (1997–2001).

$$\frac{d[Au]}{dt} = -k_{leach} ([Au]_t - [Au]_{\omega})^n \quad (4.9)$$

where $[Au]_t$ and $[Au]_{\omega}$ are the solid gold concentration at time (t) and unleachable gold concentration, respectively.

Integration of equation (4.9) with the initial condition of $[Au]_t = [Au]_o$ at $t = 0$ yields the following general relationship, when the reaction order is not equal to 1:

$$k_{leach} = \frac{1}{(n-1)t} \{ ([Au]_t - [Au]_{\omega})^{(1-n)} - ([Au]_o - [Au]_{\omega})^{(1-n)} \} \quad (4.10)$$

By rearranging equation (4.10), a general expression for calculating $[Au]_t$ takes the following form:

$$[Au]_t = \left[(n-1)k_{leach}t + \frac{1}{([Au]_o - [Au]_{\omega})^{(n-1)}} \right]^{-1/(n-1)} + [Au]_{\omega} \quad (4.11)$$

Finally, the gold extraction (X) is calculated using Equation (4.12):

$$X = \frac{([Au]_o - [Au]_t)}{[Au]_o} \quad (4.12)$$

The model indicates that the reaction rate is a function of the difference between the gold grade $[Au]_i$ at time (t) and the unleachable gold concentration $[Au]_{\infty}$. Ling *et al.* (1996) found the unleachable gold concentration at infinite leach time $[Au]_{\infty}$ was dependent only on the particle size distribution of the ore tested. The unleachable gold concentration in the proposed Fort Knox model has been determined to be a function of the ore particle size represented by the ore P_{80} (microns) and mill feed grade $[Au]_{HG}$ (mg/kg). Although variability exists in the data ($R^2 = .39$), the multiple linear relationship presented in equation (4.13) provides the baseline required to account for a known dependent variable in the leach circuit performance model.

$$[Au]_{\infty} = 0.00033(P_{80}) + 0.0312[Au]_{HG} - 0.0267 \quad (4.13)$$

The order of the rate function (n) has been described by various authors. Rees and Van Deventer (2001) found $n = 1.28$ for the relatively simple oxide ore analyzed under controlled laboratory conditions. McLaughlin and Agar (1991) used the first order form of the equation to accurately model the rate of gold extraction by cyanidation on four distinct ore samples. Ling *et al.* (1996) presented data from cyanidation experiments on a particular gold ore, where the objective of the experiment was to decouple the effects of free cyanide and dissolved oxygen concentrations, and suggested a version of the model where $n = 1.5$. Nicol *et al.* (1984) indicated the reaction was actually second order.

Laboratory bottle-roll test procedures were developed to simulate actual plant gold extraction by taking into account plant operating conditions with respect to ore particle size, cyanide concentration, slurry density (w/w) and gravity recovery efficiency. The duration of the test is calculated based on actual plant throughput rates and were intended to predict total gold extraction. However, the tests are performed at room temperature (20°C) and do not provide data to evaluate the effect of temperature on the cyanidation rate.

Figure 4.12 contains the laboratory data and the results estimated from the three rate orders evaluated. The results indicate that in laboratory bottle-roll tests, the order of

the rate function, that best fits the actual gold extraction from Fort Knox ore, is 1.5 which is consistent with the work of Ling *et al.* (1996).

A detailed leach/CIP sampling program is performed at the Fort Knox mill on a weekly basis and used to monitor actual plant performance. Each profile represents a snap shot of the cyanide leach circuit for that given time and alone does not supply sufficient data to do kinetics calculations. However, an average of numerous profiles allows sufficient data to develop a baseline model. The value for the rate constant k was calculated for each of the 13 sample points, representing the seven leach and six CIP tank discharges. The average rate constant from the 13 calculations was used for the remaining model calibration.

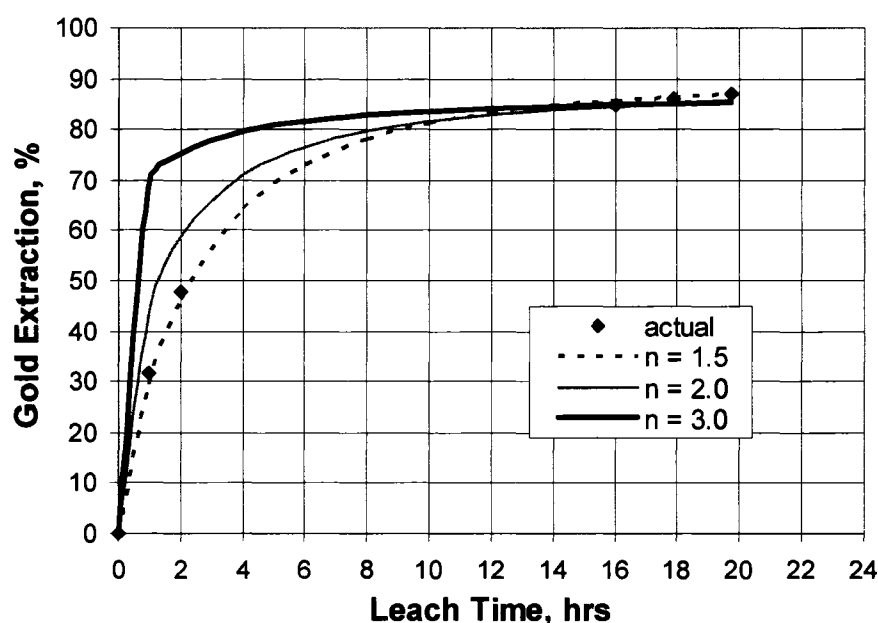


Figure 4.12 Comparison of 2004 laboratory results and order (n) of the rate equation

The value for n could then be determined by minimizing the error term when the model estimated value for $[\text{Au}]_t$ was regressed against the actual values determined from the weekly profile data. Figure 4.13 contains results obtained, when the relationships described by Equations 4.9 through 4.12 were used to fit the actual plant data collected between 1997 and 1999, and the plant slurry temperatures averaged 12°C and ranged from 8°C to 15°C .

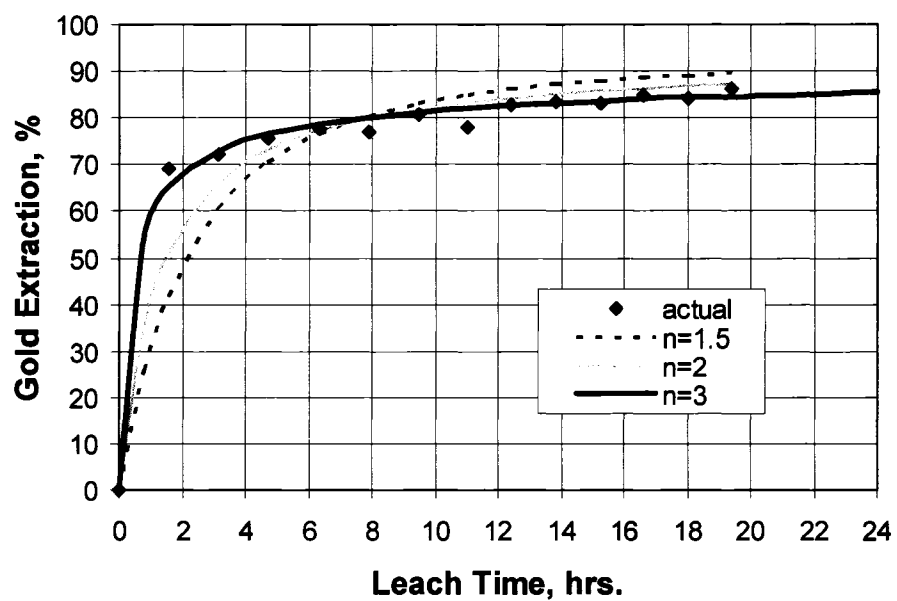


Figure 4.13 Comparison of plant data and order (n) of rate equation; (1997-1999).

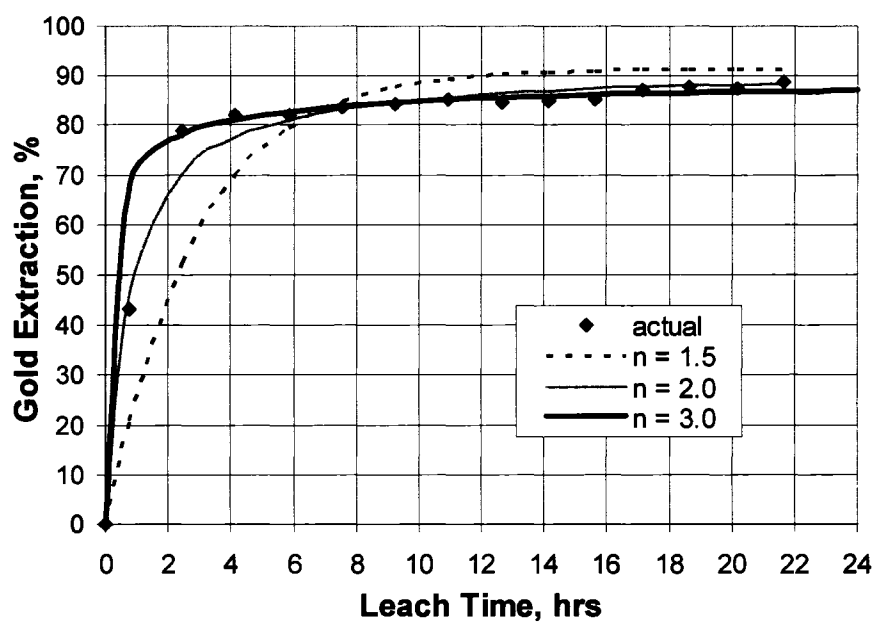


Figure 4.14 Comparison of plant data and order (n) of the rate equation; (2004).

Figure 4.14 contains similar data for the periods during 2004, when the mill was processing straight Fort Knox ore and slurry temperatures averaged 31°C, and ranged from 29°C to 34°C.

The results suggest that a third order rate equation ($n = 3.0$) provides the best fit for both data sets with the coefficient of correlation (R^2) = 0.996 and 0.999, respectively. This value is significantly different from that calculated from the laboratory bottle-roll results (Figure 4.12) and indicates that the order of rate equation is a function of plant conditions and not the mineralogy of the ore being processed. The bottle-roll tests were conducted at room temperature with a NaCN concentration of approximately 200 ppm. Thus, the gold-leach kinetics was controlled by oxygen diffusion (Figure 4.5) and the reaction order was similar to the results reported by other researchers (Nicol et al., 1984; Ling et al., 1996). However, in the leach circuit at the Fort Knox Mine, the kinetics is controlled by cyanide diffusion, due to very low NaCN concentrations (70 to 80 ppm). Therefore, the baseline form of the gold leaching model that best estimates actual Fort Knox plant performance is a 3rd order equation that can be expressed as follows:

$$\frac{d[Au]}{dt} = -k_{leach} ([Au] - [Au]_w)^{3.0} \quad (4.14)$$

Integration of equation 4.14, with the initial condition of $[Au]_t = [Au]_o$ at $t = 0$, yields the following:

$$k_{leach} = \frac{0.5}{t} \{ ([Au]_t - [Au]_w)^{-2.0} - ([Au]_o - [Au]_w)^{-2.0} \} \quad (4.15)$$

By rearranging equation (4.15), $[Au]_t$ can be calculated for the Fort Knox circuit as follows:

$$[Au]_t = \left[2.0 k_{leach} t + \frac{1}{([Au]_o - [Au]_w)^{2.0}} \right]^{-0.50} + [Au]_w \quad (4.16)$$

where: $[Au]$ is expressed in mg/kg and (t) is expressed in hours.

Historic daily operating data, as well as laboratory results, indicate that gold extraction at Fort Knox is a function of leach NaCN concentration and temperature, in

addition to mill head grade. By plotting the logarithm of the rate constant against $1/T$ (Arrhenius plot), the relationship between the rate constant and temperature (Figure 4.15) can be established.

An expression for the rate constant was then developed using the Arrhenius equation, adjusted to account for variations in the leach cyanide concentration. The rate constant k_{leach} is calculated using Equation 4.17.

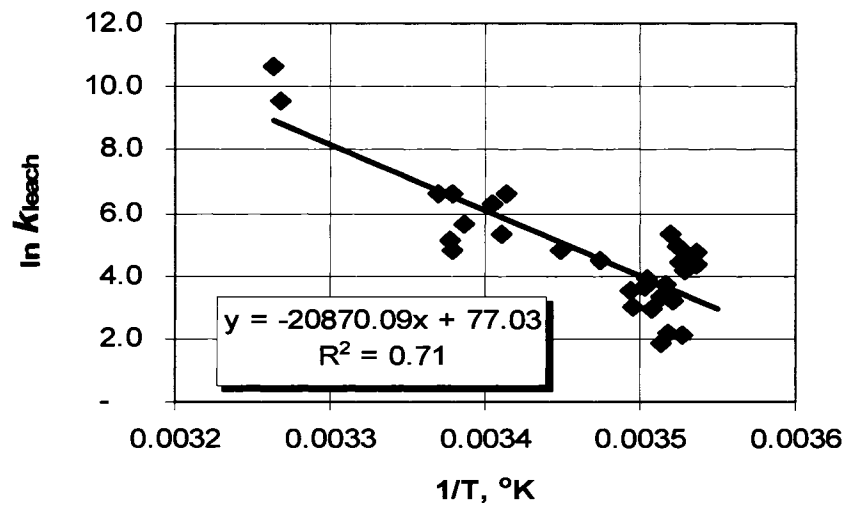


Figure 4.15 Arrhenius plot - effect of slurry temperature on leach rate constant.

$$k_{\text{leach}} = \left\{ \frac{[\text{NaCN}]_{\text{actual}}}{[\text{NaCN}]_{\text{ave}}} \right\} 2.84 \times 10^{33} e^{-20,870(1/T)} \quad (4.17)$$

where: $[\text{NaCN}]_{\text{actual}}$ = actual cyanide concentration, ppm

$[\text{NaCN}]_{\text{ave}}$ = average cyanide concentration, ppm

T = temperature, °K

The rate constant calculated from Equation 4.17 was then used in Equation 4.16, in order to estimate the mill's final solid tailings loss, $[\text{Au}]_t$. Although the rate constant is proportional to NaCN concentration range shown in Figure 4.10, reagent and detoxification costs are also factors for selecting the proper cyanide concentrations in the plant operation.

4.3.5 Effect of Temperature on CIP Circuit Efficiency

Nicol *et al.* (1984) indicated that the rate at which gold disappears from solution can be described in terms of an apparent first-order process over short time periods (less than 12 hours). At the Fort Knox mill, CIP retention time varies from 6 to 10 hours, depending on variations in mill processing rates, and falls well within the criteria described by Nicol. Leach/CIP circuit profiles have been performed on a weekly basis since the Fort Knox mill began commercial operation in 1997. The CIP solution gold concentration can be estimated using the following equation:

$$\frac{d[Au]}{dt} = -k_{CIP} [Au]_t \quad (4.18)$$

Integration of equation 4.18, with the initial condition of $[Au]_t = [Au]_{L7}$ at $t = 0$, yields the following equation:

$$\ln \frac{[Au]_t}{[Au]_{L7}} = -k_{CIP} t \quad (4.19)$$

where: $[Au]_t$ = gold concentration in solution at time t

$[Au]_{L7}$ = initial gold concentration in solution

t = contact time (min)

By rearranging equation (4.19), the solution gold concentration $[Au]_t$ can be calculated for the discharge of each CIP tank in the Fort Knox circuit.

$$[Au]_t = [Au]_{L7} e^{-k_{CIP} t} \quad (4.20)$$

Each of the leach profiles described above were viewed as a snapshot of a steady-state operating condition and provides a measurement of the gold concentration remaining in the solution at the discharge of each of the six stages in the CIP circuit. The time used at each point was based on the tank volume and average circuit conditions with respect to slurry feed rate and slurry density measured during the profile. A typical solution profile is contained in the Figure 4.16.

By plotting the gold concentration with respect to time and using a nonlinear regression analysis, a relationship was determined that estimated the solution gold concentration at the discharge of each CIP tank. Although the approach provided a good fit to the weekly data, variability was found to exist in the regression slope calculated from month to month. The high variability suggested the actual slope was dependent on additional variables. Fleming and Nicol (1984) evaluated the influence that a number of variables had on the rate of gold cyanide loading onto activated carbon. They concluded that mixing efficiency and slurry rheology were the most important parameters governing the adsorption rate. Because the Fort Knox mill has operated under consistent mixing conditions since startup, the variance in the CIP tailings solution gold concentrations is likely due to changes in slurry rheology that have been shown to be a function of slurry temperature.

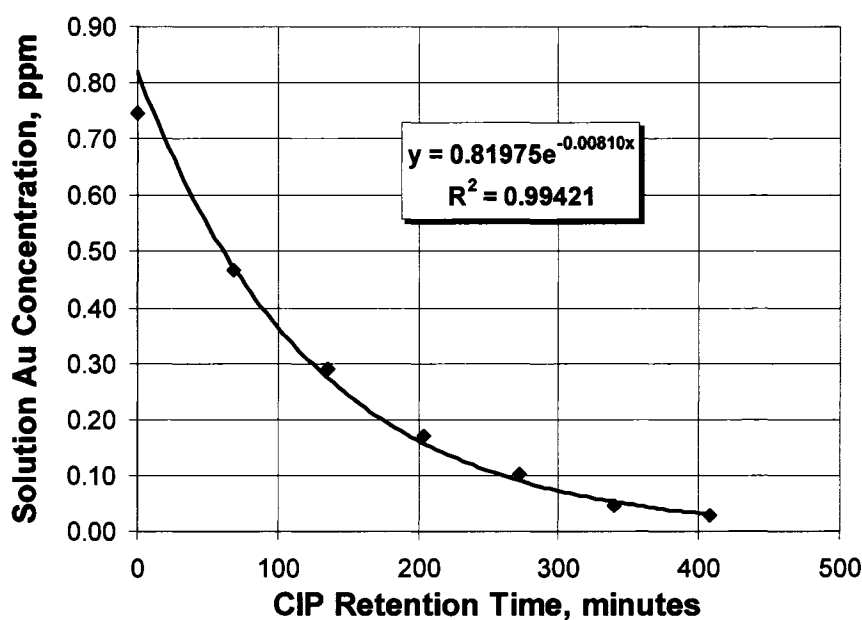


Figure 4.16 Typical first-order rate relationship CIP profile.

The initial variable evaluated to explain the variance in k_{CIP} was circuit operating temperature. By plotting the logarithm of the rate constant against $1/T$ (Arrhenius plot), the relationship can be established. The results suggested that the explained variance,

(60%), may be due to variations in the slurry rheology as predicted by changes in the slurry temperature. The results of the Arrhenius plot of the plant data are shown in Figure 4.17.

The relationship between the slope and the circuit temperature was then incorporated into the original model and provided a significantly better approach for estimating final solution gold concentrations in the Fort Knox CIP tailings. The new relationship was again used to recalculate the monthly data. The remaining variance was reevaluated with the most significant relationship existing between the variance and the average carbon advance rate used during the individual months. This relationship is shown in Figure 4.18. The rate constant, estimated using the Arrhenius equation, was then adjusted to account for variations in the CIP carbon advance rate. The rate constant, k_{CIP} , was calculated using Equation 4.21.

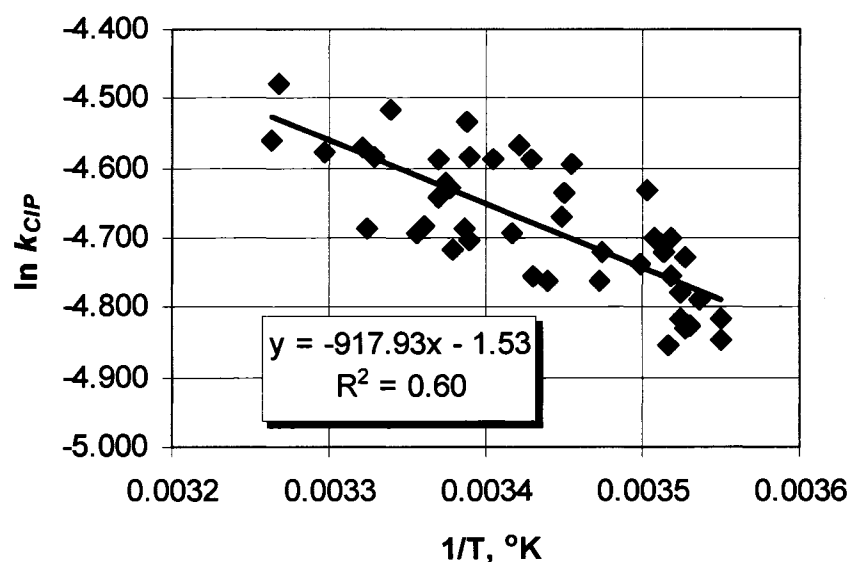


Figure 4.17 Arrhenius plot - effect of slurry temperature on CIP model rate constant.

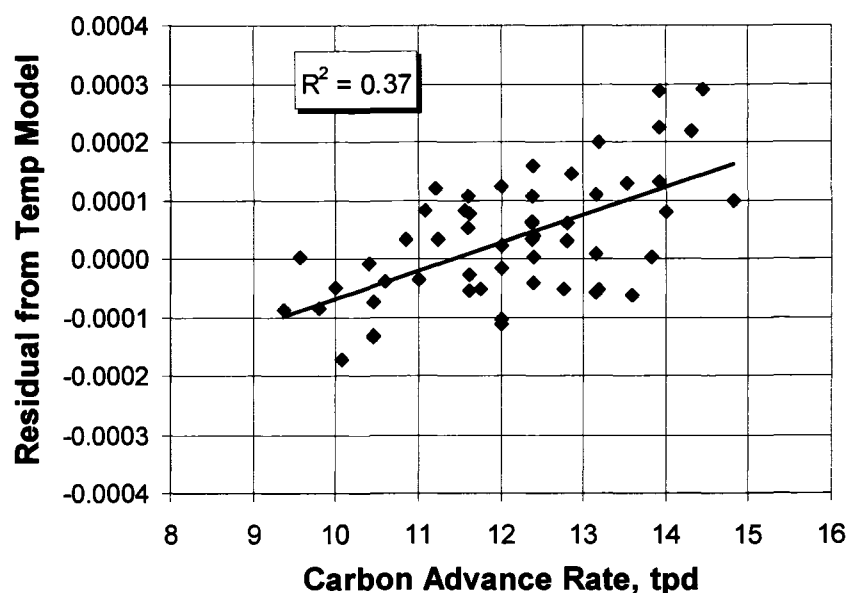


Figure 4.18 Model error term vs. carbon advance rate.

$$k_{\text{CIP}} = \left\{ \frac{\text{AR}_{\text{actual}}}{\text{AR}_{\text{ave}}} \right\} 0.22 e^{-918 (1/T)} \quad (4.21)$$

where: $\text{AR}_{\text{actual}}$ = actual CIP carbon advance rate, tpd

AR_{ave} = average CIP carbon advance rate, tpd

T = temperature, °K

The rate constant calculated from Equation 4.21 was then used in Equation 4.20, in order to estimate the final CIP solution gold loss.

4.4 MODEL PREDICTIONS AND DISCUSSION

The third-order rate model (Equation 4.16) developed for the Fort Knox leach circuit gold dissolution kinetics was used to estimate the gold grade of the solid tailings between 1998 and 2004. The comparison of actual vs. predicted solid tailings grade (Equation 4.16) is displayed in Figure 4.19. The predicted values provide a reasonable fit to actual plant results. Areas of high variability are likely due to a poor estimate of $[\text{Au}]_0$ and not associated with the form of the model. This is most apparent in the 2001 through

2003 data, when the mill processed True North ore that is more variable with respect to sulfide mineral and refractory gold content (Hollow *et al.*, 2003a, 2003b).

It is also likely that the rate constant (k_{leach}) is significantly different, when the mill is processing a blend of Fort Knox and True North ores, because blended ore has been shown to be sensitive to leach cyanide concentration, [NaCN] (Hollow *et al.*, 2003a, 2003b). Because the model developed here was based on relationships established while the mill was processing straight Fort Knox ore, additional work will be required to account for variations in ore mineralogy.

The first-order rate model (Equation 4.20) for the CIP circuit performance was used to estimate solution tailings gold concentrations between 1999 and 2004 and provided a reasonable fit to actual plant solution tailings gold concentrations. This comparison is displayed in Figure 4.20.

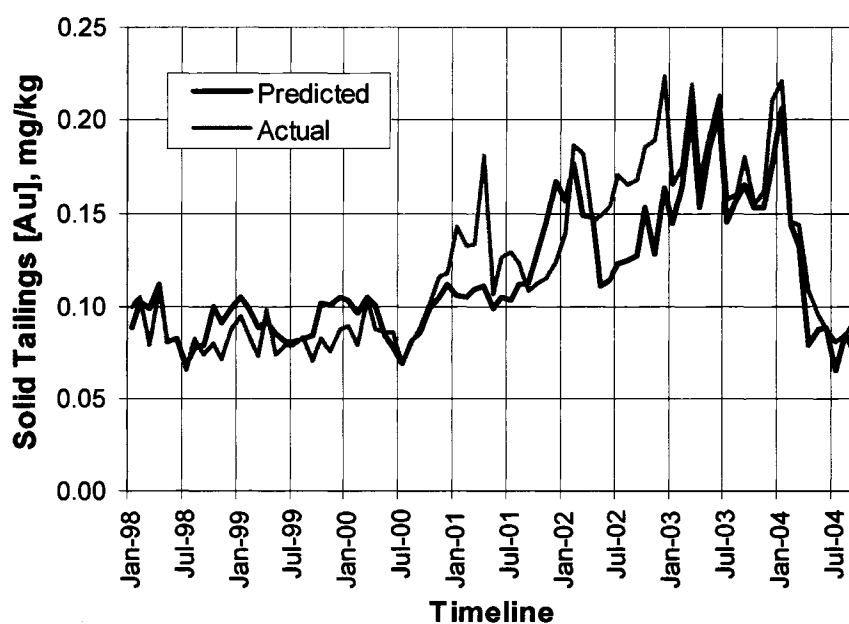


Figure 4.19 Comparison of plant solid tailings [Au] and predicted values.

The proposed CIP model, which accounts for variations in circuit operating temperature and carbon advance rates, provides a reasonable estimate of actual plant performance and provides a good tool for evaluating upset conditions. In general, the remaining variance in the model can be attributed to the error in the prediction of the CIP feed solution concentration, $[Au]_o$, estimated from the leach model. The primary source of this error is in the estimate of the unleachable solid gold concentration, $[Au]_{\infty}$. When the data in Figure 4.20 is compared to that of Figure 4.19, it can be seen that when the actual solid tailings gold concentration is significantly understated by the leach model, the CIP solution model will predict higher than actual final solution tailings gold concentrations. Additionally, variations in CIP circuit carbon concentration (g/L) and carbon activity likely add to the error in the model and warrant further investigations.

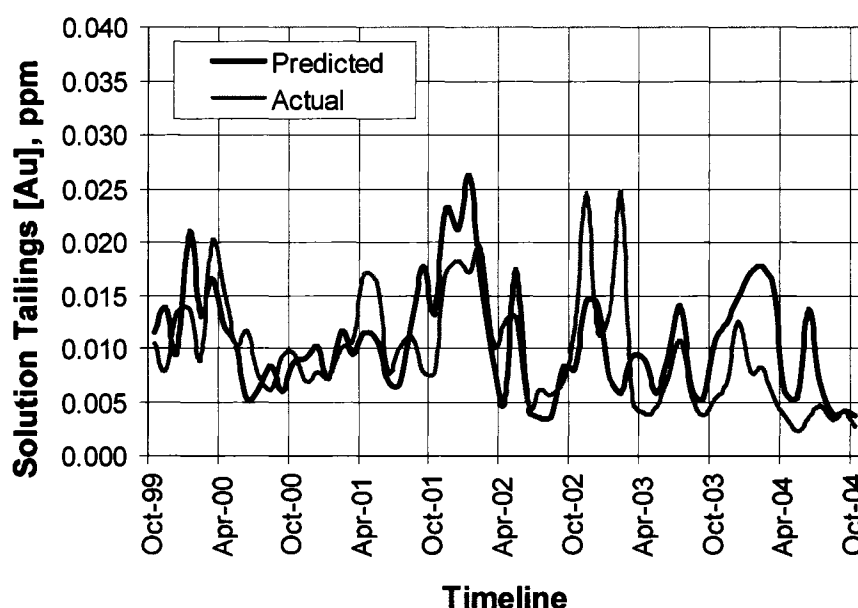


Figure 4.20 Comparison of plant solution tailings [Au] and predicted values.

The rate constants calculated with Equations 4.17 and 4.21 were used in Equations 4.16 and 4.20 to predict the effect of temperature on overall Fort Knox mill

recovery under average conditions. Table 4.1 contains a summary of the mill parameters used in the evaluation, and Table 4.2 contains the models' outputs.

Table 4.1 Mill conditions evaluated.

Parameter	
mill feed rate, tpd	37,467
mill feed grade, mg/kg	0.96
gravity gold recovery, %	16.0
leach particle size P ₈₀ , microns	201
leach density, % solids (w/w)	52
leach [NaCN], ppm	75
carbon advance rate, tpd	12

The results contained in Table 4.2 indicate that the leach gold extraction increases from 86.5% to 89.4% when the plant slurry temperature increases from the 10.0°C (typical of winter operation) to 26.7°C (typical of summer operation). This represents a difference in daily leach gold production of approximately 1.02 kg.

Table 4.2 Predicted mill grades and losses.

Parameter	10.0°C	26.7°C	37.8°C
leach feed grade, mg/kg	0.81	0.81	0.81
leach solid tailings, mg/kg	0.11	0.08	0.07
CIP solid tailings, mg/kg	0.10	0.08	0.07
unleachable gold grade, mg/kg	0.07	0.07	0.07
CIP solution tailings, ppm	0.011	0.007	0.003
solid tailings gold loss ¹ , %	12.0	9.8	8.8
solution tailings gold loss ¹ , %	1.5	0.9	0.4
total gold recovery, %	86.5	89.4	90.8
solid tailings gold loss, kg/day	4.32	3.51	3.17
solution tailings gold loss, kg/day	0.53	0.32	0.13
total gold loss, kg/day	4.85	3.83	3.30

¹ losses are percent of leach feed gold content

4.5 CONCLUSIONS

- Presented was an evaluation of the primary rate determining factors affecting gold recovery in the Fort Knox mill's leach/CIP circuit.
- It is proposed that variations in slurry rheology result in measurable impacts to reactions controlled by diffusion within the Fort Knox mill's leach/CIP circuits, and that these impacts can be predicted using temperature as the independent variable.
- Historically, the leach cyanide concentration, [NaCN], has been maintained at levels where the [NaCN] is rate limiting; the oxygen concentration, [O₂], is not rate limiting.
- The following third-order rate model provides an estimate of solid tailings gold concentration [Au]_t that best fits the actual plant data:

$$[Au]_t = \left[2.0k_{\text{leach}} t + \frac{1}{([Au]_o - [Au]_{\omega})^{2.0}} \right]^{-0.50} + [Au]_{\omega}$$

- The model uses the leach particle size (P₈₀) and mill feed grade [Au]_{HG} to determine the unleachable gold content [Au]_ω.
- The retention time (*t*) is a function of mill throughput rates (t/d) and slurry density (percent solids, w/w).
- The leach rate constant (*k*_{leach}) is a function of leach circuit operating temperature and leach cyanide concentration [NaCN].

$$k_{\text{leach}} = \left\{ \frac{[NaCN]_{\text{actual}}}{[NaCN]_{\text{ave}}} \right\} 2.84 \times 10^{33} e^{-20,870(1/T)}$$

- The CIP circuit solution tailings gold concentration is best estimated by the following first-order rate equation, where [Au]_{L7} is the gold concentration in the CIP feed solution.

$$[Au]_t = [Au]_{L7} e^{-k_{\text{CIP}} t}$$

- The CIP rate constant (*k*_{CIP}) is a function of CIP circuit slurry temperature (T) and the carbon advance rate (AR) as follows:

$$k_{\text{CIP}} = \left\{ \frac{AR_{\text{actual}}}{AR_{\text{ave}}} \right\} 0.22 e^{-918 (1/T)}$$

- The periodic processing of straight Fort Knox ore in 2004 allowed for validation of the gold leach and adsorption models that were developed primarily on pre-2001 data. Modeling the effect of processing True North ore can now be completed using the Fort Knox ore processing model as a baseline to isolate variances associated with ore types.
- A second paper in this series will focus on modeling the impact of slurry temperature on the cyanide destruction circuit at the Fort Knox mill.

REFERENCES

- Adams, M.D., 1990, *The chemical behaviour of cyanide in the extraction of gold. 2. Mechanisms of cyanide loss in the carbon-in-pulp process*, J.S. Afr. Inst. Min. Metall., Vol. 90, No.3, pp. 67-73.
- Boonstra, B., 1943, *Über die losungsgeschwindigkeit von gold in kaliumcyanid lösungen*, Korros Metallschutz, Vol. 19, pp. 146-406.
- Cathro, K.J. and Koch, D.F.A., 1964, *The anodic dissolution of gold in cyanide solutions*, Journal of the Electrochemical Society, Vol. 111, pp. 1416-1420.
- Christy, S.B., 1896, *The solution and precipitation of the cyanide of gold*, Transactions of the American Institute of Mining Engineers, Vol. 26, pp. 735-772.
- Deitz, G.A. and Halpern, J., 1953, *Reaction of silver with solutions of cyanide and oxygen*, Journal of Metals, pp. 1109-1116.
- Fang, Z., Meloun, M. and Muhammed, M., 1998, *Modeling and optimization of cyanidation process. A chemometric approach by regression analysis*, Analytica Chimica Acta, pp. 123-133.
- Fleming, C.A. and Nicol, M.J., 1984, *The adsorption of gold cyanide onto activated carbon. III. Factors influencing the rate of loading and the equilibrium capacity*, J.S. Afr. Inst. Min. Metal., Vol. 84, No.4, pp. 85-93.

- Habashi, F., 1967, *Kinetics and mechanisms of gold and silver dissolution in cyanide solution*, Montana College of Mineral Science and Technology, Bulletin 59, Bureau of Mines and Geology, Butte, Montana, pp. 29-34.
- Habashi, F., 1970, Principles of Extractive Metallurgy, Vol.2: Hydrometallurgy, Gordon and Breach, NY, pp. 18-19.
- Heath, A.R. and Rumball, J.A., 1998, *Optimizing cyanide:oxygen ratios in gold CIP/CIL circuits*, Minerals Engineering, Vol. 11, No. 11, pp. 999-1010.
- Hollow, J.T., Hill, E.M., Lin, H.K., and Walsh, D.E., 2003a, *The effect of $Pb(NO_3)_2$ addition on the processing of blended Fort Knox and True North ores at the Fort Knox Mine*, Minerals and Metallurgical Processing, Vol. 20, No. 4, pp. 185-190.
- Hollow, J., Deschenes, G., Guo, H. and Hill, E., 2003b, *Optimizing cyanidation parameters for processing of blended Fort Knox and True North ores at the Fort Knox Mine*, Hydrometallurgy 2003 – Fifth International Conference in Honor of Professor Ian Ritchie, Vol. 1: Leaching and Solution Purification, pp. 21-34.
- Kirk, D.W., Foulkes, F.R. and Graydon, W.F., 1978, *A study of anodic dissolution of gold in aqueous alkaline cyanide*, Journal of the Electrochemical Society, Vol. 125, pp. 1436-1443.
- Kudryk, V. and Kellogg, H.H., 1954, *The mechanism and rate controlling factors in the dissolution of gold in cyanide solution*, Journal of Metals, Vol. 6, pp. 541-548.
- Lin, H. K. and Chen, X., 2001, *Electrochemical study of gold dissolution in cyanide solution*, Minerals and Metallurgical Processing, Vol. 18, No. 3, pp. 147-153.
- Ling, P., Papangelakis, V.G., Argyropoulos, S.A. and Kondos, P.D., 1996, *An improved rate equation for cyanidation of a gold ore*, Canadian Metallurgical Quarterly, Vol. 35, No. 3, pp. 225-234.
- Link, J. M., 1993, *Rheology studies with Fort Knox leach feed slurries*, Report Prepared for: AMAX Gold, inc.

- MacArther, D.M., 1972, *A study of the anodic dissolution of gold in concentrated KCN solutions*, Journal of the Electrochemical Society, Vol. 119, pp. 672-677.
- Marsden, J. and House, I., 1992, *The Chemistry of Gold Extraction*, Ellis Horwood Limited, England, pp. 266-270.
- McLaughlin J. and Agar, G.E., 1991, *Development and application of a first order rate equation for modeling the dissolution of gold in cyanide solution*, Minerals Engineering, Vol. 4, No. 12, pp. 1305-1314.
- Nicol, M.J., 1980, *The anodic behaviour of gold: Part II – Oxidation in alkaline solutions*, Gold Bulletin, Vol. 13, No.3, pp. 105-111.
- Nicol, M.J., Fleming, C.A. and Cromberge, G., 1984, *The adsorption of gold cyanide onto activated carbon. I. The kinetics of absorption from pulps*, J.S. Afr. Inst. Min. Metal., Vol. 84, No.2, pp. 50-54.
- Rees, K.L. and Van Deventer, J.S.J, 2001, *Gold process modeling. I. Batch modeling of the processes of leaching, preg-robbing and adsorption onto activated carbon*, Minerals Engineering, Vol. 14, No. 7, pp. 753-773.
- Rubisov, D.H., Papangelakis, V.G. and Kondos, P.D., 1996, *Fundamental kinetics models for gold ore cyanide leaching*, Canadian Metallurgical Quarterly, Vol. 35, No. 4, pp. 353-361.
- Thompson, P.F., 1947, *The dissolution of gold in cyanide solution*, Transactions of the Electrochemical Society, Vol. 91, pp. 41-71.
- Thurgood, C.P., Kirk, D.W., Foulkes, F.R. and Graydon, W.F., 1981, *Activation energies of anodic gold reactions in aqueous alkaline cyanide*, Journal of the Electrochemical Society, Vol. 128, pp. 1680-1685.
- Wadsworth, M.E., 1991, *Rate processes in the leaching of gold and other metals forming stable complexes*, H.H. Kellogg International Symposium Quantitative Description of Metal Extraction Processes, Edited by N.J. Themelis and P.F.Duby, The Minerals, Metals and Materials Society, pp. 197-216.

Wadsworth, M.E., 2000, *Surface processes in silver and gold cyanidation*, Int. J. Miner. Process., Vol. 58, pp. 351-368.

CHAPTER 5
MODELING THE INFLUENCE OF SLURRY TEMPERATURE ON THE
CYANIDE DESTRUCTION PLANT AT THE FORT KNOX MINE,
FAIRBANKS, ALASKA¹

5.1 ABSTRACT

The Fort Knox Mine is located in Alaska's interior where the average ambient air temperatures range from -24°C in January to 16°C in July. The mill processes a free milling gold ore utilizing both a gravity recovery circuit and conventional cyanide leach/carbon-in-pulp circuits. Plant tailings are further processed in a cyanide destruction circuit, utilizing the patented INCO SO₂/air process to reduce the weak acid dissociable cyanide concentration to below permit stipulated concentrations, prior to deposition in the tailings storage facility. Slurry temperature cycles seasonally and allows for a unique opportunity to measure the impact of temperature on cyanide destruction reactions. Statistical models were developed to accurately predict actual mill performance. This paper describes the development of the models and presents data, that allow for a better understanding of the impact of slurry temperature on cyanide destruction circuit efficiencies and reagent usage.

5.2 INTRODUCTION

The Fort Knox Mine, located in the Fairbanks Mining District, 40 km (25 miles) northeast of Fairbanks, Alaska, began commercial gold production in the first quarter of 1997. The Fort Knox gold deposit and gold recovery flowsheet have been described in detail (Lin *et al.*, 2002; Hollow *et al.*, 2005). The final process in the flowsheet utilizes patented technology (INCO process) to oxidize the weak acid dissociable cyanide (CN_{WAD}) and reduce its concentration in the mill tailings to levels stipulated in the mine operating permits, prior to the tailings being discharged to the tailings storage facility (TSF).

¹ Hollow, J.T., (2002), prepared for Fairbanks Gold Mining - Internal Report

The facility is operated in a Sub-Arctic environment. Slurry temperature cycle seasonally, and provides a unique opportunity to evaluate actual process kinetics over a broad temperature range at full scale production rates. Linear regression modeling was used to quantify variability in reaction kinetics and reagent usage in the cyanide destruction circuit at the Fort Knox Mine. A simplified flowsheet of the Fort Knox Mine leach/CIP and cyanide destruction circuits is shown in Figure 5.1

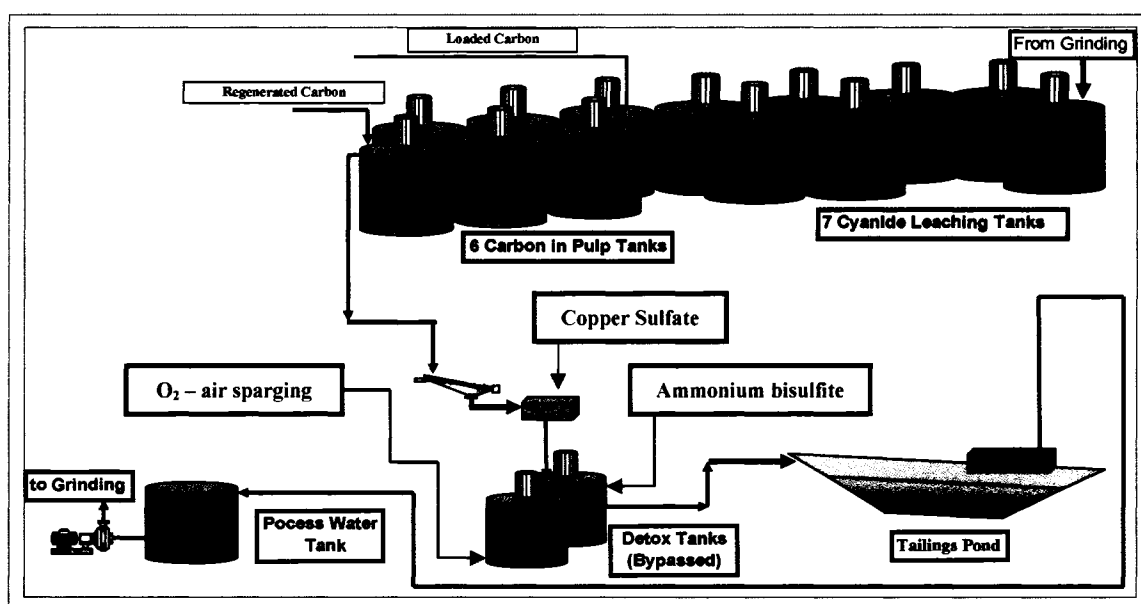


Figure 5.1 Simplified flowsheet of the Fort Knox leach/CIP and cyanide destruction circuits.

5.2.1 Process Description

The INCO SO_2/O_2 cyanide destruction process oxidizes cyanide (CN^-) to cyanate (CNO^-). It uses a mixture of sulfur dioxide (SO_2) and air (O_2) which rapidly oxidizes free cyanide (CN^-) and WAD metal cyanide complexes in aqueous solution. The reaction is catalyzed by the presence of copper ions (Cu^{2+}) and the pH range is controlled (Marsden and House, 1992), (Oleson *et al.*, 2005). A solution of ammonium bisulfite (ABS, NH_4HSO_3) is used as the source of the SO_2 , while copper ions are added to the reactors as concentrated copper sulfate solution (approximately 15% Cu^{2+}). O_2 is added through air

sparging. The pH is controlled by the addition of excess SO_2 to reduce pH, and lime to increase pH (INCO, 1992).

CN_{WAD} , which includes all free cyanide, zinc cyanide, copper cyanide, and nickel cyanide are oxidized to CNO^- . The ions released from the cyanide are precipitated as metal hydroxides. The strong cyanide complexes are precipitated as insoluble ferrocyanide salts. In addition, a minor amount of thiocyanate (SCN^-) and other species ($\text{S}_2\text{O}_3^{2-}$ and $\text{S}_4\text{O}_6^{2-}$) are oxidized (INCO, 1992). The SO_2 added is converted to SO_4^{2-} during the oxidation process. It is precipitated as calcium sulfate ($\text{CaSO}_4 \cdot 2\text{H}_2\text{O}$, commonly called gypsum).

5.2.2 Process Chemistry

The oxidation of free cyanide to cyanate, in the presence of copper, can be described by the following chemical reaction equation:



Based on the above equation, the stoichiometric or theoretical $\text{SO}_2:\text{CN}^-$ molar ratio is 1:1 and weight ratio is 2.46:1. Since the source of SO_2 at Fort Knox Mine is ABS (ABS solution contains 65% ABS by weight of which only 42% is actually SO_2), the theoretical weight ratio of $\text{ABS}:\text{CN}^-$ is 5.88:1

The plant was commissioned in November 1996, at which time the expected $\text{SO}_2:\text{CN}^-$ ratio was determined to be between 4:1 and 6:1 ($\text{ABS}:\text{CN}^-$ ratio of 9.88 to 14.48:1). Additionally, the required operating range for the concentration of copper in the slurry was determined to be 3 to 5 ppm; a minimum dissolved oxygen concentration of 2 ppm was required (INCO, 1996).

The best pH range for the Inco Process is 8.0 to 9.0, and is normally controlled by lime addition. However, when excess undissolved lime is present, extra SO_2 is required to reduce the pH. At Fort Knox Mine, the feed slurry pH ranges from 9.5 to 10.5; no lime addition is required.

The sulfuric acid (H₂SO₄) generated during the oxidation of cyanide (and other oxidation reactions) is neutralized with lime to form calcium sulfate, commonly known as gypsum.



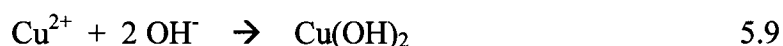
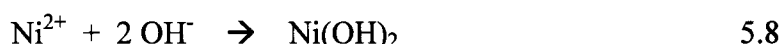
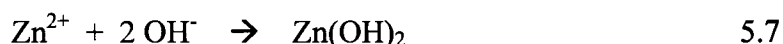
The cyanide destruction feed contains weak metallo-cyanide complexes, M(CN)_4^{2-} , that are decomposed as follow:



Copper, as the cuprous ion, is oxidized to the cupric ion form with the INCO process before it precipitates as copper hydroxide. If the cuprous to cupric reaction is incomplete, thiocyanate (SCN⁻) will maintain the copper in solution as Cu(SCN)_4^{2-} (INCO, 1992).



The liberated metal ions are then precipitated as metal hydroxides.

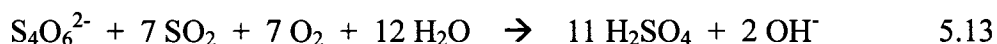


Iron cyanide complexes are not decomposed in the INCO process. Ferricyanide is reduced to ferrocyanide with SO₂, then the ferrocyanide forms a metallo-ferrocyanide complex, which precipitates with available metal ions, $\text{M}^{2+} = \{\text{Zn}^{2+}, \text{Ni}^{2+} \text{ or } \text{Cu}^{2+}\}$. When excess iron is present, $[\text{Fe}] > 2.3 \times [\text{Cu}]$, additional copper sulfate may be added in order to remove the iron cyanide (INCO, 1992).

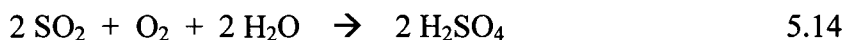


Other strong cyanide complexes such as gold cyanide, $\text{Au}(\text{CN})_2^-$, silver cyanide, $\text{Ag}(\text{CN})_2^-$, and mercury cyanide, $\text{Hg}(\text{CN})_4^{2-}$ are not destroyed by the INCO process. Laboratory work indicates that none of the gold cyanide is destroyed.

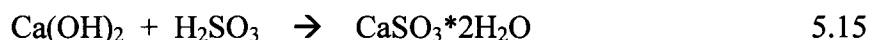
Sulfur compound are partially oxidized by the SO_2 /Air process only when there is very little cyanide present and excess SO_2 is being added.



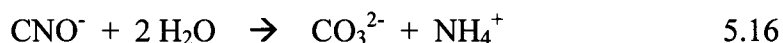
If the SO_2 finds nothing to oxidize and there is plenty of oxygen present, the SO_2 reacts according to the reaction, equation 5.14.



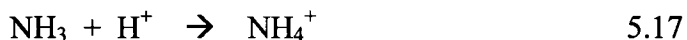
However, if there is no oxygen available, the SO_2 will precipitate as calcium sulfite. The calcium sulfite will dissolve in the tailings storage facility and react with any residual cyanide present there.



The cyanate ion, CNO^- , is not stable and will hydrolyse to carbonate and the ammonium ion. The reaction below is greatly accelerated at low pH.



The carbonate ion, which is essentially dissolved CO_2 , will precipitate as calcium carbonate. The ammonium is in equilibrium with ammonia and, at high pH, most of the ammonium ion has been converted to ammonia. The ammonia will exit the water system as ammonia gas in the grinding circuit and leach tanks where the pH is high. The equilibrium is given in equation 5.17.



The treated effluent and reclaim water will be saturated in sulfates. The sulfates will precipitate with calcium when the pH increased. Reclaim water should only be

added where the precipitating calcium sulfate can deposit on the solids rather than on the walls of the tank and inside pumps.

5.2.3 Cyanide Analytical Techniques

Free cyanide (CN^-) is a measure of the unreacted cyanide in the slurry and is determined by the silver nitrate titration procedure. To accurately determine the free cyanide concentration, a normalized silver nitrate solution is dosed to a process solution sample, with a manual or automatic burette. The silver ions complex the free cyanide ions in the solution sample. When all free cyanide is consumed to form silver cyanide complex, the excess silver ions indicate the endpoint of the titration. An indicator (rhodanine) is used for the endpoint determination, which changes color with the appearance of free silver ions. The analytical equipment used for the titration is rather simple.

The determination of weak acid dissociable cyanide (CN_{WAD}) by the picric acid technique has a detection limit of 0.26 ppm CN_{WAD} , (INCO, 1992). In the picric acid technique, free and weak acid dissociable cyanide react with the picric acid reagent to produce an orange color, which can be measured colorimetrically at 520 nm. The reacted sample is then compared against prepared standards for determination of cyanide concentration.

In the picric acid technique, the dissolved alkali metal picrate is converted by cyanide into the colored salt of isopurpuric acid and its concentration measured. The presence of nickel in the analyzed solutions has a positive effect on the overall performance of the method, but is not absolutely necessary. The reduction of picric acid is affected by free cyanide only. Therefore, diethylenetriaminepentaacetic acid (DTPA) is also added as part of the picric acid buffer solution. The DTPA is required to liberate the cyanide tied up in copper, nickel, zinc or cadmium complexes

Thiocyanate, cyanate, and thiosulfate ions have no adverse effects and can be tolerated at levels normally occurring in gold mill effluents. The method also requires close control of pH, since it affects the color intensity produced by the cyanide-picric

acid reaction. The most intense coloration results at pH 9.0-9.5, therefore, the picric acid reagent solution is buffered by a mixture of sodium tetraborate and carbonate as well as the DTPA itself. The picric acid technique is the preferred field method for use by the circuit operator to monitor plant performance, as it is relatively simple, with procedural errors resulting in a high assay bias (INCO, 1992).

The CN_{WAD} concentration of a solution can also be determined with a Perstorp Analytical Cyanide analyzer, which is the accepted procedure for permit compliance. The Perstorp analyzer utilizes a ligand-exchange/flow injection amperometric method for determination of cyanide concentration. The sample is first treated with specific ligand-exchange reagents to liberate cyanide from the weak metal-cyano complexes. When the solution is acidified, the free CN^- is converted to HCN and diffuses across a hydrophobic-membrane and is absorbed into a basic acceptor solution. The CN^- is then detected in a flow cell amperometrically, with an Ag working electrode and a Ag-AgCl reference electrode. The current generated is proportional to the cyanide concentration present in the original sample. A schematic diagram of the perstorp WAD cyanide analyzer and a detailed description of its operation has been reported by Oleson *et al.*, 2005.

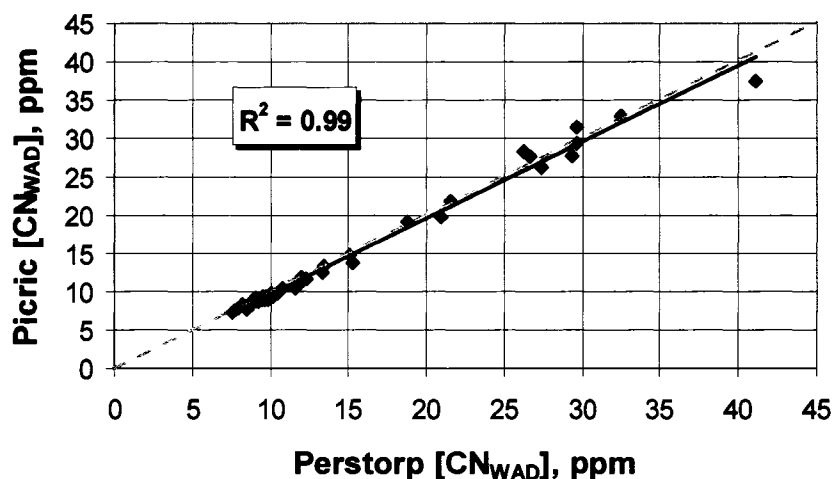


Figure 5.2 Comparison of analytical techniques used to determine weak-acid dissociable cyanide concentration $[CN_{WAD}]$ in the cyanide detoxification circuit.

Figure 5.2 is a comparison of picric acid determinations and Perstorp analyzer results produced from the same circuit shift composite samples. The results indicate that the picric acid determination is a strong indicator of the Perstorp value approved by the EPA and specified in the Fort Knox Mine operating permits.

Fort Knox ore is relatively clean and contains only trace amounts of metals that react to form weak metal-cyano complexes. Consequently, the simple silver nitrate titration for free cyanide produced an acceptable indication of the CN_{WAD} concentration in the detox feed slurry. Figure 5.3 contains the relationship between the two cyanide concentrations in the Fort Knox CIP discharge slurry and supports the assumption that the majority of the cyanide in the detox feed slurry is present as free cyanide.

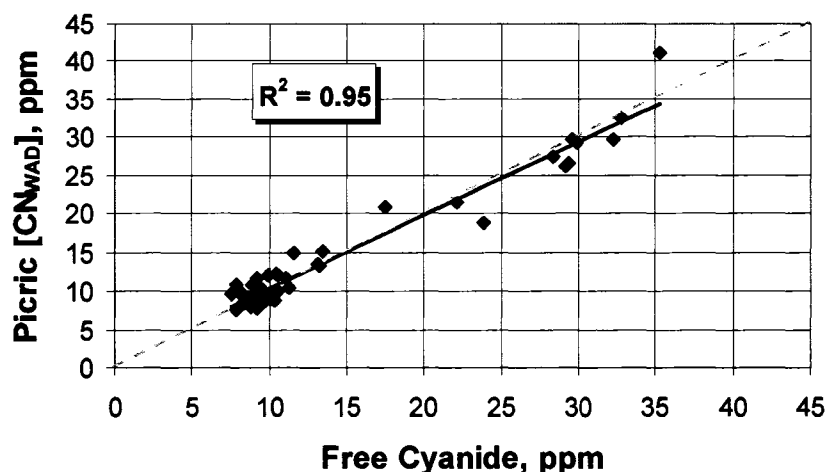


Figure 5.3 Comparison of detox feed slurry free cyanide concentration $[CN]$ and weak acid dissociable cyanide concentration $[CN_{WAD}]$ determined by picric acid technique.

5.2.4 Plant Performance

The actual plant ABS and copper sulfate consumption, during plant start-up (November 1996 to March 1997), were both excessive and inconsistent. Consequently, plant operating data for this period was excluded from all circuit evaluations. ABS addition was reduced substantially during the subsequent period, as the result of numerous procedural modifications and the natural learning curve associated with operating a new plant.

In addition, a number of significant process variables that affect overall circuit efficiencies were identified. With the increased understanding of the process, numerous improvements were made to produce more accurate and consistent field readings. Tighter QC programs were instituted and more sophisticated process control strategies were implemented. Table 5.1 contains a list of critical dates associated with the improved efficiencies in the detox circuit operations. All have had an impact, to some degree, on the quality of the data utilized in the development of the 2000 Detox Model.

Table 5.1 Critical dates in detox circuit operating history.

Nov 1996	Mill and detox circuit commissioned
Mar 1997	Consistent circuit performance achieved
Jul 1997	Crystal formation in bulk ABS storage tank and reagent delivery piping
Nov 1998	QC program developed for daily ABS quality monitoring
Jan 1998	Flow meters installed on discharge piping for ABS metering pump
Jan 1998	<i>Allowable Reactor CN_{WAD} concentration increased (first time)</i>
Feb 1998	Flow meters installed on discharge piping for Cu metering pumps
Mar 1998	Instrumentation installed to allow for real time flow measurements
Apr 1998	DCS control loops developed to control pump ABS addition
Jul 1998	<i>Increased normal Cu concentration set point from 5ppm to 10 ppm</i>
Oct 1998	Temperature measured on a daily basis
Aug 1998	<i>Allowable Reactor CN_{WAD} concentration increased (second time)</i>
Aug 1999	<i>New vendor for ABS supply - increase in average SO_2 content (6%)</i>
Jan 2000	QC program developed for analytical standards
Feb 2000	<i>Reactor sample determinations delayed</i>

The cyanide load feeding the reactors is a mass flow measurement and is expressed as a rate in lbs. CN_{WAD} /hr. Since the cyanide is contained in the solution portion of the slurry and saturated into the pore spaces of the solids, the mass flow of cyanide is calculated by determining the mass flow of solution and multiplying by the $[CN_{WAD}]$ of the solution. The mass flow of solution is calculated by measuring the volumetric flow rate (gallons per minute) of slurry and the pulp density of the slurry (percent solids, w/w).

Figure 5.4 contains a timeline of the free cyanide concentration $[CN^-]$ in the detox feed slurry, as well as the weak-acid dissociable cyanide concentration $[CN_{WAD}]$ in the discharge slurry, determined by operators (control) and by the assay lab (compliance).

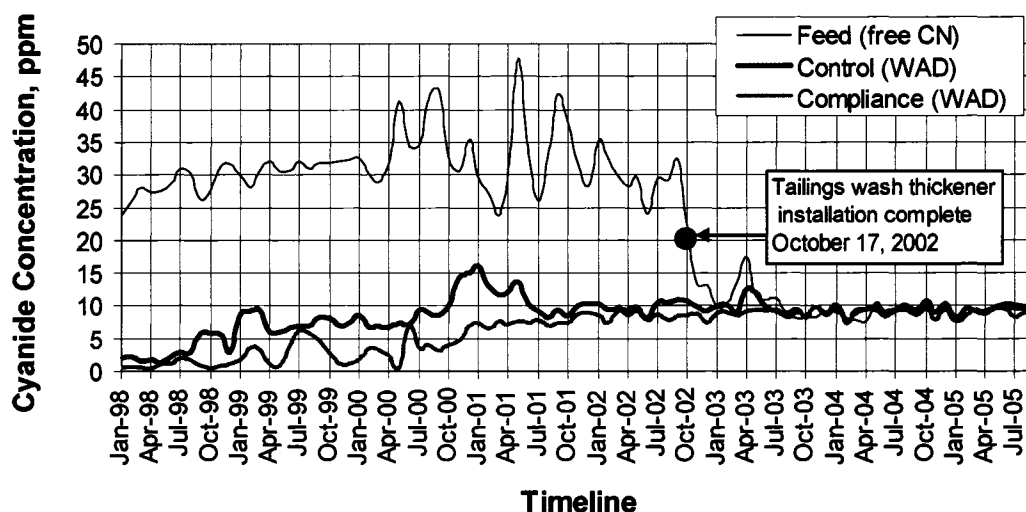


Figure 5.4 Timeline of detox feed, detox control and detox compliance cyanide concentrations, ppm.

A preliminary circuit model was developed in early 1998 and was utilized to identify deviations from normal plant efficiencies (control charts) rather than to predict future plant performance. The model continued to evolve as improvements in field and laboratory measurements were implemented, and through a better understanding of plant operations. The current form of the model was completed in 2000. It is a robust multiple regression model that is used for quality control monitoring, to generate calculated inputs for process control and optimization, and as a predictive tool to evaluate process alternatives by providing accurate operating cost estimates expected over a range of operating conditions.

5.3 DETOX MODEL DEVELOPMENT

The most significant change to the detox circuit performance was made in the 1st quarter of 1998, when the control range of CN_{WAD} concentration was increased from

5ppm to 10ppm. Historically, the operators would adjust the ABS addition, in order to maintain the CN_{WAD} concentration discharging from the reactors at ≤ 5 ppm. When the plant was operated in this manner, the permit compliance samples, which were collected and analyzed in the assay lab, rarely exceeded 1ppm $[CN_{WAD}]$. The discrepancy between the operational values and the compliance values indicated that excess ABS remained in the slurry and the reaction continued after the slurry was discharged from the detox circuit. The control parameters for $[CN_{WAD}]$ were increased periodically throughout 1998 and had a measurable impact on ABS consumption, while maintaining $[CN_{WAD}]$ below permit stipulated discharge concentrations.

New instrumentation was installed during the 1st quarter of 1998. This allowed for continuous measurements of both the ABS and copper solution addition rates. Prior to that period, reagent feed pump speeds were monitored and controlled, with no feedback of actual reagent delivery. With the addition of the new instrumentation, a more sophisticated control strategy was implemented in the plant's distributed control system, which allowed the controller to adjust reagent addition based on live process monitoring.

In the summer of 1998 a better understanding of circuit operating temperatures was developed. Although the circuit operating temperature information was only collected weekly, sufficient data existed to evaluate the seasonal temperature variations and show the significance of the relationship between increased ABS usage and decreasing slurry temperature. Daily temperature measurements were available after October 1998. In March 2000, instrumentation was added to provide continuous temperature monitoring in key process plant locations including the detox feed distributor.

Also in 1998, a substantial change to reagent addition philosophy occurred. During a circuit test on an alternative SO_2 source (sodium metabisulphite) and an alternative ABS supplier, the operators were able to reduce the addition rate of the metabisulfite solution by increasing the addition rate of the copper solution. The relationship was tested numerous times during May and June using ABS and produced consistent results. In July 1998, the standard copper concentration $[Cu^{2+}]$ was increased

from the historic operating range (5ppm to 10ppm) to values as high as 25 ppm. The circuit was subsequently operated at an $[\text{Cu}^{2+}]$ to ABS ratio that minimized overall circuit operating costs. This operating philosophy allowed for a unique opportunity to expand the model to include a $[\text{Cu}^{2+}]$ term.

The influence of copper ion concentration and temperature on the reaction kinetics of the oxidation of cyanide with SO_2 was evaluated under laboratory conditions (Oleson *et al.*, 2005). The authors concluded that the reaction rate was first-order with respect to $[\text{Cu}^{2+}]$, up to 30 ppm and the reaction kinetics are temperature sensitive with the measured activation energy representative of a diffusion controlled reaction.

In the summer of 1999, the understanding of the relationship between elevated $[\text{Cu}^{2+}]$, temperature and reaction kinetics was expanded when the $[\text{Cu}^{2+}]$ was substantially reduced without requiring the ABS addition rate to be increased. This indicated that the copper catalyst required to maintain reaction kinetics is a function of slurry temperature, with the $[\text{Cu}^{2+}]$ being inversely proportional to slurry temperature. Beginning in July 1999, economics were added to the equation and it was determined that at any given operating temperature, there was an optimum ratio of ABS to copper that minimized total reagent costs for the circuit. Since that time, the copper concentration set point has been adjusted based on circuit operating temperature.

From late December 1999 to early January 2000, excessive ABS consumption was again observed. It was determined that poor-quality analytical standards were being used in the determination of the $[\text{CN}_{\text{WAD}}]$ in the detox reactors. This prompted the development of a QC program to ensure that fresh, accurate standards were always available for the operators in the detox plant. At that time, the consistent discrepancy between the operator's field cyanide readings and the analytical labs compliance assays was again evaluated. It was apparent that there was excess SO_2 remaining in the reactor discharge and that the reaction was not complete at the time the operators were making there determinations.

Figure 5.5 contains the historic relationship between the monthly average $[CN_{WAD}]$ (operator determinations) and the $[CN_{WAD}]$ determined in the compliance samples analyzed by the assay lab. This bias is not the result of the difference in analytical procedures, but essentially a reaction time issue. In an attempt to compensate for the discrepancy, in February 2000 the detox standard operating procedure was changed to allow the slurry samples to sit for a period of time prior to performing the cyanide determination. The reagent addition rate was then controlled based on the delayed analysis.

Figure 5.5 also shows that during the summer months, the operator determinations are much closer to the compliance samples, indicating a difference in chemical reaction rates associated with changes in circuit operating temperature. Therefore, in the colder months excess ABS is required to accelerate the reaction kinetics, but is not consumed by the reactions prior to discharge from the reactors (20-60 minutes). By delaying the $[CN_{WAD}]$ determinations on the control samples and adjusting the ABS addition based on these results, excess ABS added to the reactors is minimized.

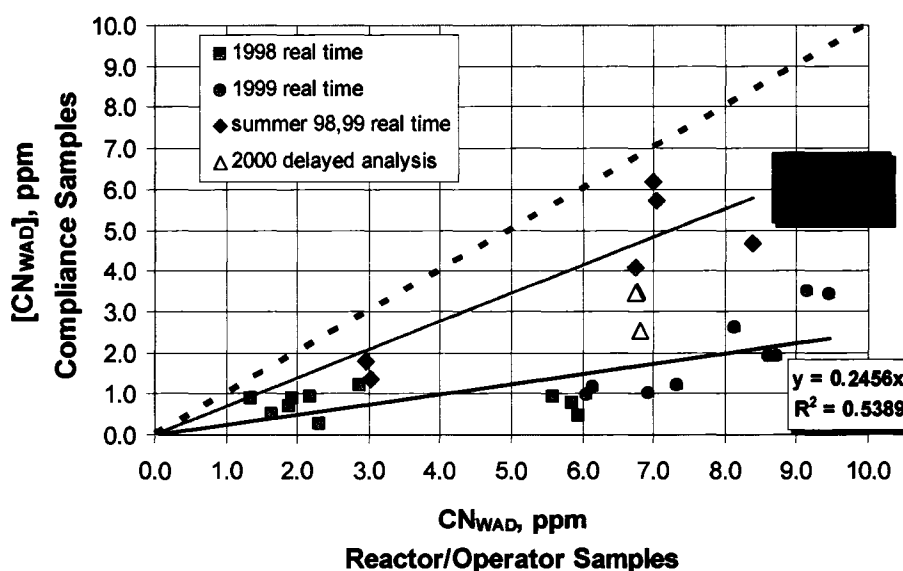


Figure 5.5 Relationship between $[CN_{WAD}]$ measured in compliance and operator samples.

In the initial 2000 detox modeling efforts, the values representing July 1997 through November 1997 were excluded. During this period, numerous ABS delivery and pump plugging problems occurred and the actual ABS usage was not representative of stable plant operation. The preliminary 2000 detox model included the following independent variables:

- 1) detox feed cyanide load, lbs. CN_{WAD} /day
- 2) detox feed slurry pH
- 3) temperature, °F
- 4) copper concentration, ppm
- 5) reactor CN_{WAD} concentration, ppm

Although the literature suggests that slurry pH should be an independent variable in determining the plant ABS addition rate, it has never been a statistically significant independent variable when included in regression analysis. The detox feed slurry pH has historically been within a fairly narrow range (9.5 to 10.5) as shown in Figure 5.6. Therefore, detox feed slurry pH was eliminated in all subsequent modeling efforts.

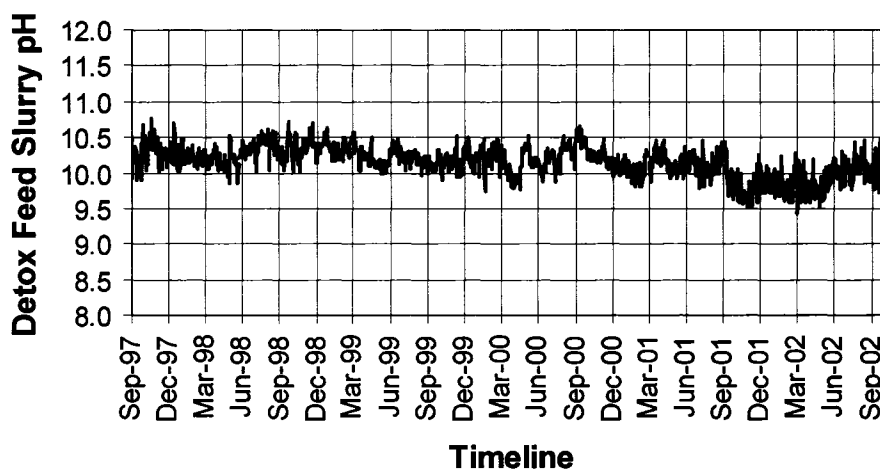


Figure 5.6 Trend line of detox feed slurry pH at the Fort Knox mill.

Table 5.2 contains the regression data analysis output for the 2000 Detox Model. The model utility test (F) indicates that the overall regression model is highly significant.

estimated by the model. In Figure 5.9, the standardized residuals were plotted on a timeline in an attempt to identify any trends that may warrant additional investigation and model modifications.

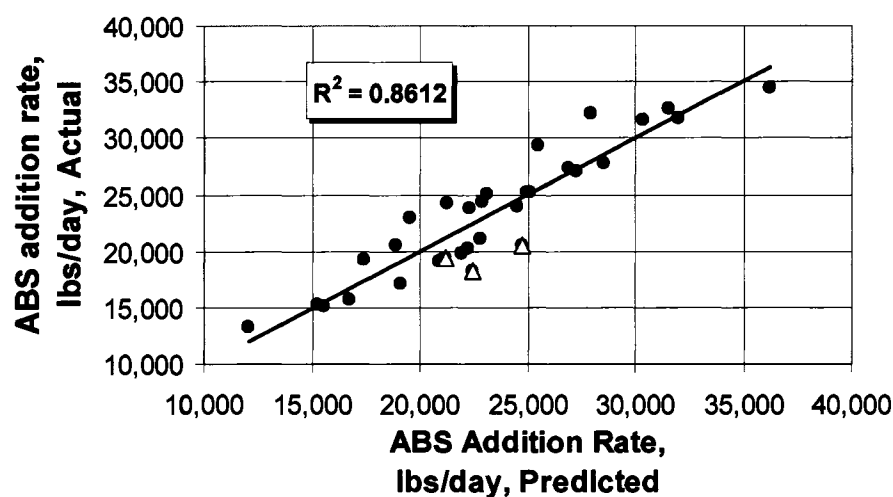


Figure 5.7 Actual ABS addition rate vs. ABS addition rate predicted by Detox Model 2000.

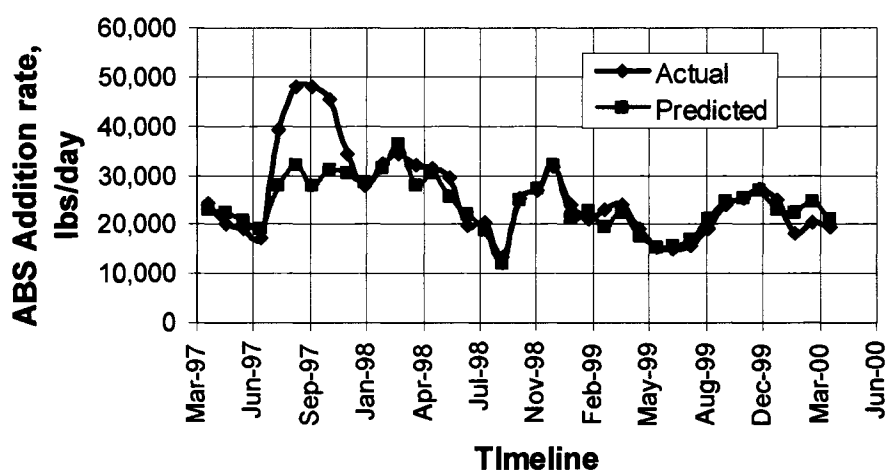


Figure 5.8 Trend line of actual and predicted ABS addition rates, lbs/day, Detox Model 2000.

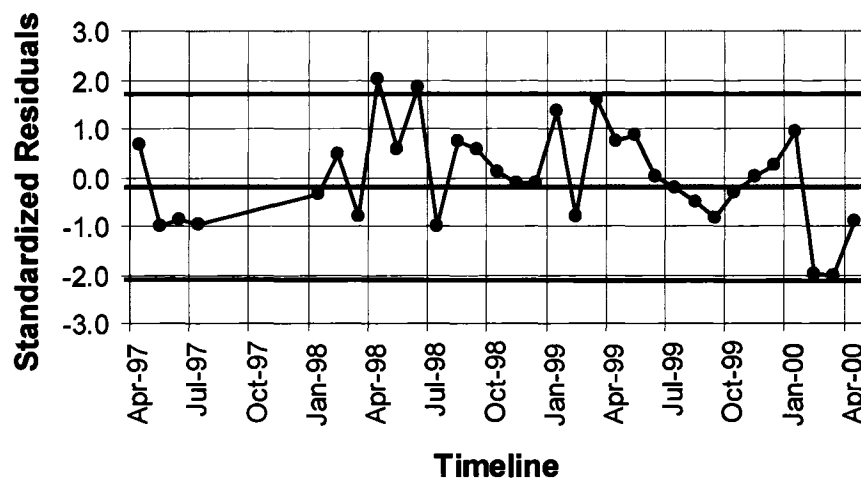


Figure 5.9 Standardized residual timeline, Detox Model 2000.

The most noticeable deviation (other than the deleted 1997 data) in the data is associated with the observations for February through April 2000. The change in standard operating procedures that was responsible for these consistent negative deviations was determined to be the implementation of delayed cyanide control determinations. This is effectively a change to the reaction time for the control of ABS addition and should ultimately be evaluated as a numeric independent variable. Unfortunately, little operational data is available for the circuit operated with the new procedures. It is expected that the addition of a delayed determination independent variable would improve the predictive power of the model.

Due to the limited data available, a dummy or indicator variable was added to the regression and represented the categorical data associated with the change in standard operating procedure: 1 for delayed readings, 0 for real time readings. This technique allowed for the inclusion of a predictor variable that is not quantifiable. Collection of additional data will allow for the indicator variable to be converted into a quantitative or numerical variable, once the new operating procedure has been utilized over a wider range of operating conditions.

Regression Statistics		(CN,Temp, discharge WAD CN, Cu concentration, and delayed determination dummy variable)
Multiple R	0.954	
R Square	0.909	
Adjusted R ²	0.892	
Standard Error	1,862.3	
Observations	32	

ANOVA					
	<i>df</i>	<i>SS</i>	<i>MS</i>	<i>F</i>	<i>Significance F</i>
Regression	5	905,432,674	181,086,535		
Residual	26	90,174,314	3,468,243		
Total	31	995,606,988			

	<i>Coefficients</i>	<i>Standard Error</i>	<i>t Stat</i>	<i>P-value</i>	<i>Lower 95%</i>	<i>Upper 95%</i>
Intercept	45,451.9	3,402.05	13.36	3.74E-13	38,458.9	52,444.9

Figure 5.10 contains a scatter plot of actual ABS addition rate vs. the 2000a Detox Model predicted ABS addition rate for the 32 observations included in the analysis. The reduction in the estimation error associated with the three months in which delayed readings were utilized (represented by the triangle observations) is an indication of the validity of using the indicator variable in the model.

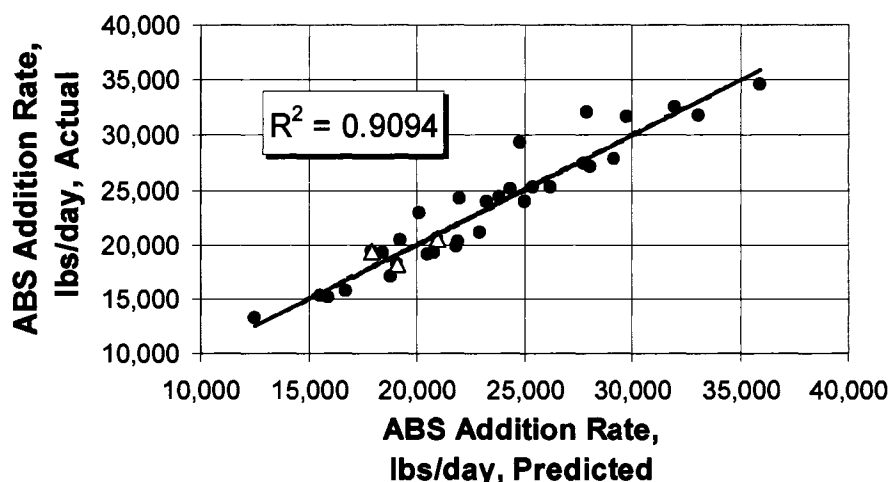


Figure 5.10 Actual ABS addition rate vs. ABS addition rate predicted by Detox Model 2000a.

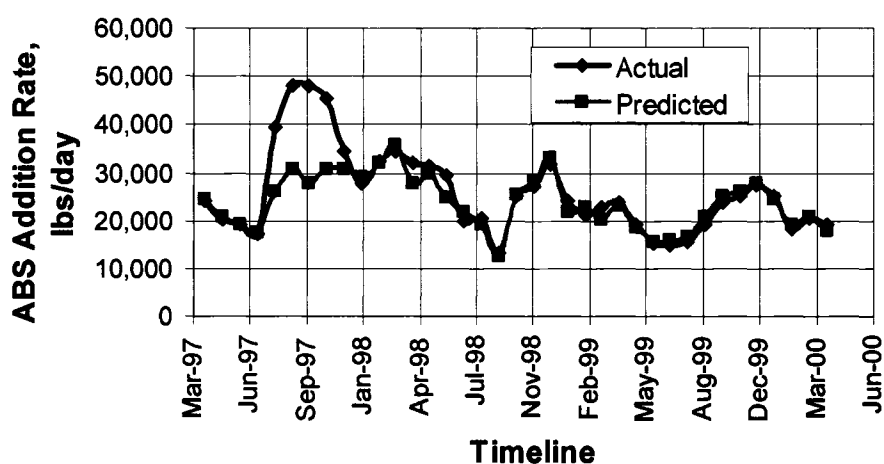


Figure 5.11 Trend line of actual and predicted ABS addition rates, lbs/day, Detox Model 2000a.

The timelines for the actual and predicted monthly ABS addition rates estimated by the 2000a Detox Model are displayed in Figure 5.11. Again the deviation in the 2000 observations has been reduced substantially by including the indicator variable in the model. However, April 98 and June 98 actual ABS addition rates appear to have an unusual deviation from the predicted values.

In Figure 5.12, the standardized residuals were plotted on a timeline and confirmed the abnormally high residuals. The other standard residual plots indicated no significant patterns. As mentioned previously, numerous plant regent test programs were conducted between April 1998 and June 1998 and it was assumed that the high actual ABS addition rates associated with this period was not representative of the normal operating conditions in the circuit. Although the value of the May 1998 standardized residual was not more than two, it seemed necessary to consider it part of the influential outlier group as the circuit was operated in a similar manner during the entire three month window.

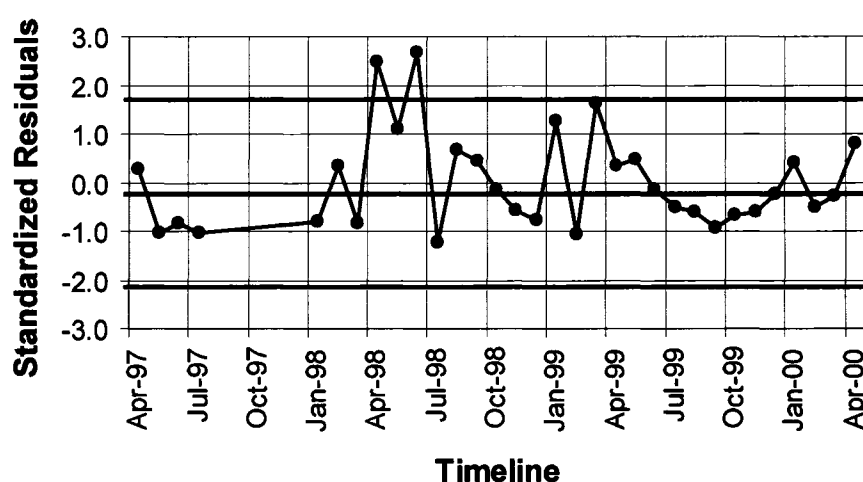


Figure 5.12 Standardized residual timeline, Detox Model 2000a.

With the three potential influential outliers removed from the data base, a multiple regression analysis was again performed on the remaining 29 observations. Table 5.4 contains the regression data analysis for the 2000b Detox Model, which included the indicator variable associated with delayed control cyanide determinations and eliminated the observations classified as influential outliers. Again the model utility test indicated that the overall model was highly significant and the adjusted R^2 value improved to 0.960; t tests also indicated high significance levels for each of the independent variable coefficients and all remained valid predictors.

Table 5.4 Regression statistics for the 2000b Detox Model.**SUMMARY OUTPUT**

(includes removal of 98 second quarter outliers)

Regression Statistics	
Multiple R	0.983
R Square	0.967
Adjusted R ²	0.960
Standard Error	1,059.9
Observations	29

ANOVA

	<i>df</i>	<i>SS</i>	<i>MS</i>	<i>F</i>	<i>Significance F</i>
Regression	5	761,620,757	152,324,151		
Residual	23	25,838,686	1,123,421		
Total	28	787,459,443			

	<i>Coefficients</i>	<i>Standard Error</i>	<i>t Stat</i>	<i>P-value</i>	<i>Lower 95%</i>	<i>Upper 95%</i>
Intercept	46,190.1	1,987.02	23.25	1.78E-17	42,079.6	50,300.5

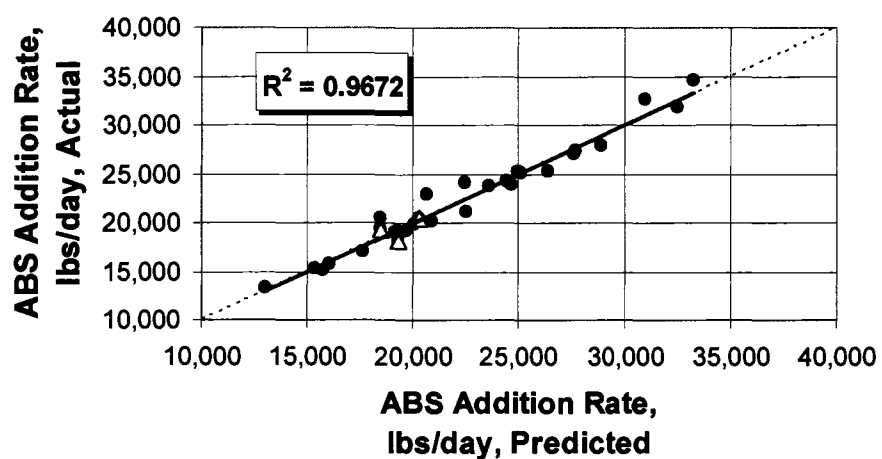


Figure 5.13 Actual ABS addition rate vs. ABS addition rate predicted by Detox Model 2000b.

As was done in the previous models, a scatter plot of the actual ABS addition rate vs. the 2000b Detox Model predicted ABS addition rate was generated for the remaining 29 data points, Figure 5.13.

The strong predictive power of the model is evident in the scatter plot. The timelines for the actual and predicted monthly ABS addition rates for the 2000b Detox Model are displayed in Figure 5.14.

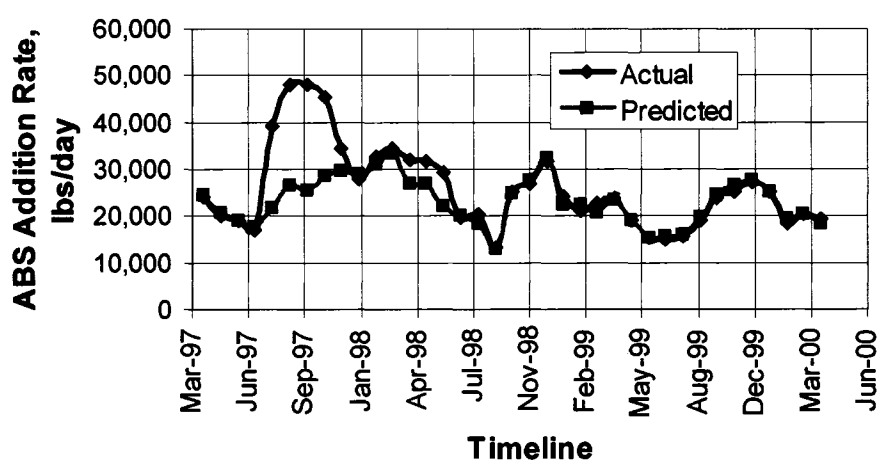


Figure 5.14 Trend line of actual and predicted ABS addition rates, lbs/day, Detox Model 2000b.

A timeline of the standardized residuals were again plotted (Figure 5.15). Although two observations were identified that had a standardized residual greater than 2, they were not in sequence and were either preceded or followed by a negative standardized residual and did not seem to represent influential outliers.

Figure 5.15 indicates two distinct periods of consistent negative residuals: 1) observations prior to the poor reagent quality period in 1997 and 2) the final 9 months of 1999. After further evaluation of the time periods, it became obvious that the consistent negative residuals were likely associated with ABS quality. Although mine site determinations of ABS strength were not available for the entire data set, the quality of the reagent delivered to the mine site by the new supplier was significantly higher than that received at any time after the reagent quality issues of 1997.

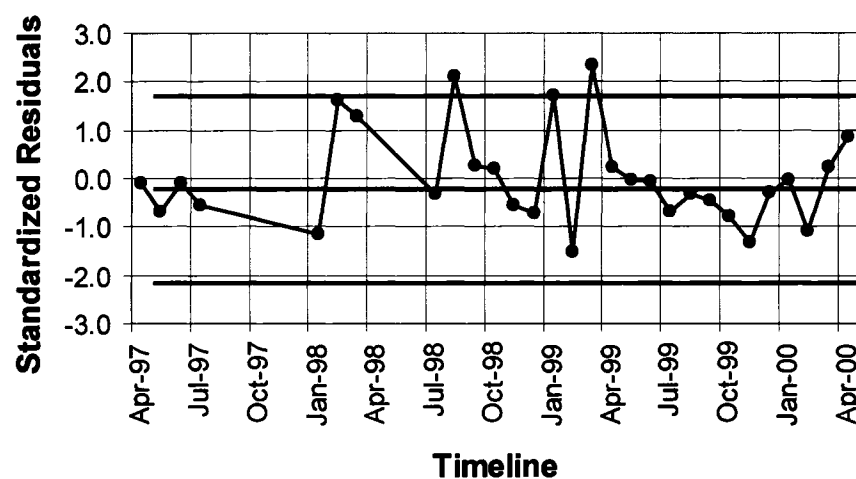


Figure 5.15 Standardized residual timeline, Detox Model 2000b.

The higher quality ABS was first tested in February 1999 and again in May 1999, then accounted for 100% of the ABS used in the plant after August 1999. The majority of these dates seem to coincide with the second period, when the model was consistently overestimating the actual consumption, but did not explain the period in 1997. Further evaluation identified factory produced QC reports for the early 1997 period, which confirmed that the ABS delivered during that time was of similar quality to that being provided by the new supplier.

It was decided to include a second indicator variable that represented supplier, or more specifically, ABS quality. The value was included as follows: 1 for new supplier (high quality) and 0 for low quality. The 29-observation data set utilized in the 2000b Detox Model was modified to include the second indicator variable and a regression analysis performed, utilizing a total of six independent variables; four quantitative (numeric) and 2 indicator.

Table 5.5 contains the regression data analysis for the 2000c Detox Model, which included the two indicator variables, but excluded the three data points classified as influential outliers.

Once again, a scatter plot of the actual ABS addition rate vs. the 2000c Detox Model predicted ABS addition rate was generated for the 29 data points, Figure 5.16. Also included in this scatter plot are the actual vs. predicted addition rate for the two time periods that were excluded from the 2000c Detox Model.

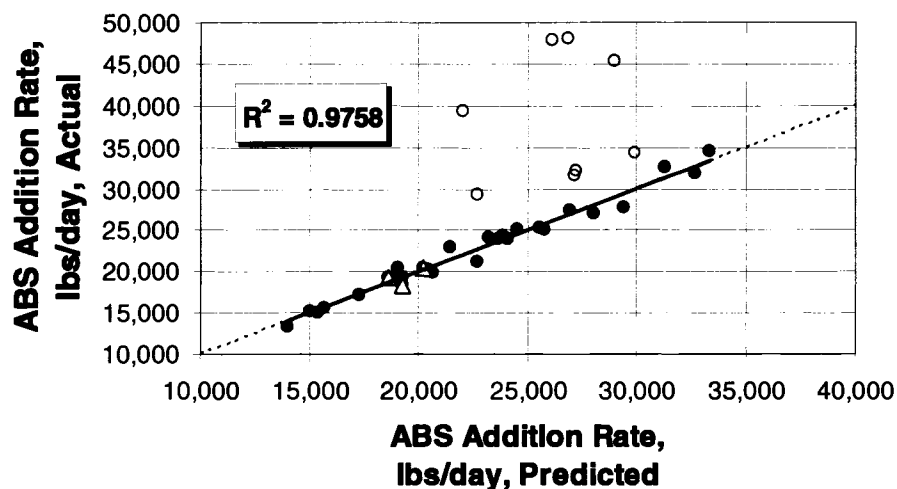


Figure 5.16 Actual ABS addition rate vs. ABS addition rate predicted by Detox Model 2000c.

A timeline of the standardized residuals was plotted, Figure 5.17. No visible improvement in the model is apparent in Figure 5.17 although the adjusted R^2 value increased slightly from 0.960 to 0.969.

Figure 5.17 indicates that the inclusion of the indicator variable associated with ABS supplier (ABS quality) in the 2000c Detox Model has eliminated the slight negative bias generated by the 2000b model.

The timeline of the standardized residuals from the 2000c Detox Model is plotted in Figure 5.18. No observations were identified that had a standardized residual greater than 2 and the inclusion of the second indicator variable has resulted in a more random pattern during the time period of concern, for the 2000b model.

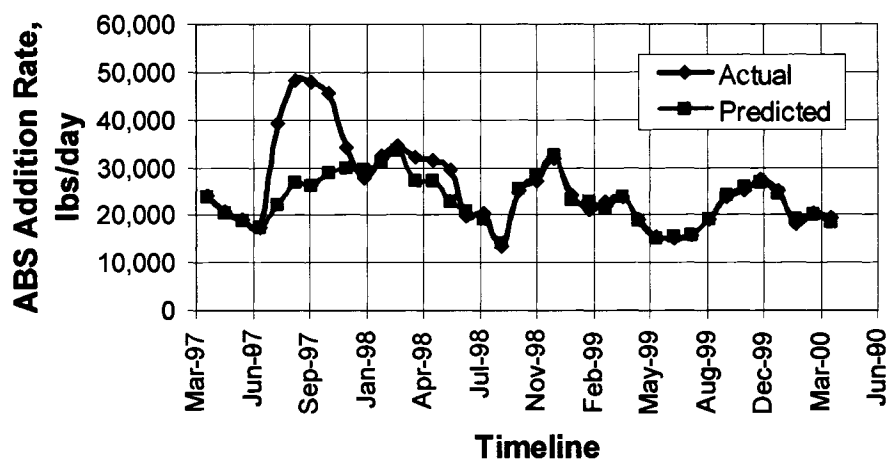


Figure 5.17 Trend line of actual and predicted ABS addition rates, lbs/day Detox Model 2000c.

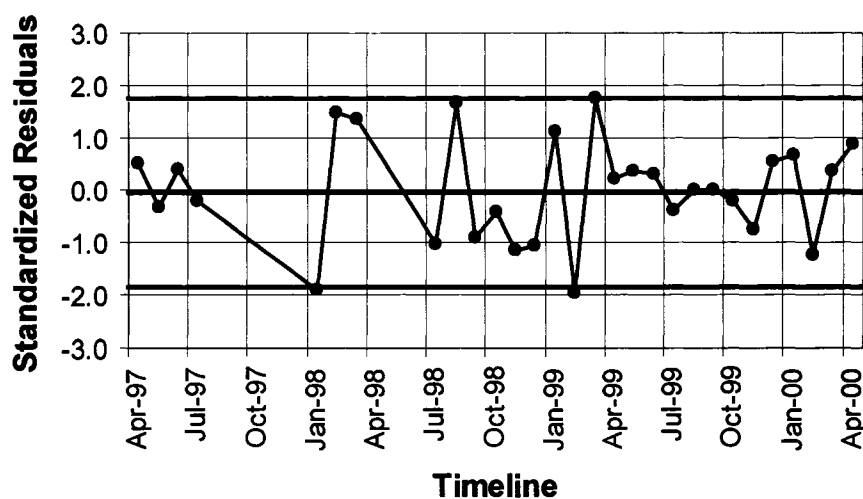


Figure 5.18 Standardized residual timeline, Detox Model 2000c.

5.4 CONCLUSSIONS AND RECOMMENDATIONS

A process model, that exhibits strong predictive power, has been systematically developed. The final 2000c Detox Model was a linear equation and represents the relationship between ABS addition rate (lbs/day) and the following independent variables:

- 1) cyanide load (CN_{WAD} lbs/day)
- 2) temperature (°F)
- 3) copper concentration (Cu^{2+} ppm)
- 4) reactor cyanide concentration (CN_{WAD} ppm)
- 5) delayed reactor control determinations, indicator variable
- 6) reagent supplier (ABS quality), indicator variable

The following equation contains the linear model that best fits historic operating history:

$$ABS = 46,472 + 7.4(CN_F) - 454(T) - 1,375(CN_D) - 339(Cu^{2+}) - 4,796(I_1) - 1,154 (I_2)$$

where:

ABS – ABS addition rate, lbs/day
 CN_F – $[CN^-]$ in detox feed slurry, ppm
 T – slurry temperature, °F
 CN_D – $[CN_{WAD}]$ in detox discharge slurry, ppm
 Cu^{2+} – Copper ion concentration in detox feed slurry, ppm
 I_1 – Indicator variable, delayed reactor control determinations
 I_2 – ABS quality

The inclusion of indicator variables compensated for the operational variations that had a measurable effect on circuit efficiencies. By including these indicator variables, the 2000c Detox Model has been able to considerably reduce the estimation error generated by previously developed detox models.

5.5 SUPPLEMENTAL WORK - 2001

The 2000c Detox Model was developed using monthly average values for all variables, since some of the data utilized to develop the relationship were not available on a daily basis for the period evaluated. With a better understanding of the circuit dynamics established, a fundamental change to the overall circuit operating philosophy was made mid year 2000. By operating the circuit using delayed $[CN_{WAD}]$ determinations and focusing on the compliance sample monthly average values, fluctuations in reagent addition rates, due to variations in reaction kinetics, were effectively eliminated.

Additionally, the SO_2 content of the ABS solution was measured daily as part of a quality control program and the value was input into the process control system used to determine the desired ABS addition rate. This allowed the elimination of the indicator variable, I_2 , from the model.

During the 2000c modeling efforts, it was determined that an economic $\text{Cu}^{2+}:\text{SO}_2$ ratio existed, that minimized circuit operating costs. This ratio was dependent on circuit slurry temperature due to variations in reaction kinetics. By delaying the $[\text{CN}_{\text{WAD}}]$ determinations by the operators, the influence of kinetics was eliminated and the optimum economic $\text{Cu}^{2+}:\text{SO}_2$ ratio was determined to be 0.16:1 (by weight). Beginning in October 2000, the ratio was fixed at that value and the copper sulfate solution addition was automatically adjusted by the control system, based on the ABS addition rate. This process control change eliminated the need for $[\text{Cu}^{2+}]$ as an independent variable for circuit modeling. Figure 5.19 shows the variation in the $\text{Cu}^{2+}:\text{SO}_2$ ratio evaluated at the Fort Knox mill.

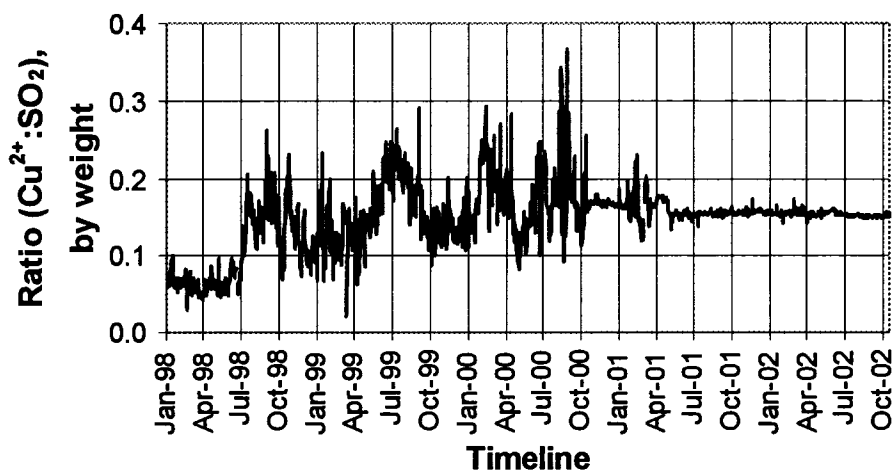


Figure 5.19 Trend line of $\text{Cu}^{2+}:\text{SO}_2$ addition rate ratio (by weight).

Multiple linear regression was applied to the daily plant data between October 1, 2000 and August 28, 2001 and a new detox model was established. In the 2001 Detox Model, the discharge $[\text{CN}_{\text{WAD}}]$ was input from the assay lab compliance values (determined using the perstorp analyzer) rather than from the operator determined values

(picric acid method). This eliminated the need for indicator variable, I_1 , in the model. Thus, the two indicator variables and the dependent variable for Cu^{2+} were all eliminated in the 2001 Model. However, temperature was still a statistically significant independent variable, indicating that fluctuations in slurry temperatures affects detox circuit performance through both reaction kinetics and reaction equilibriums. Table 5.6 contains the regression data analysis for the 2001 Detox Model.

Table 5.6 Regression statistics for the 2001 Detox Model.

SUMMARY OUTPUT

October 1, 2000 to August 28, 2001

<i>Regression Statistics</i>	
Multiple R	0.976
R Square	0.952
Adjusted R Square	0.952
Standard Error	2,216
Observations	509

<i>ANOVA</i>					
	<i>df</i>	<i>SS</i>	<i>MS</i>	<i>F</i>	<i>Significance F</i>
Regression	3	49516127106	16505375702		
Residual	505	2478920984	4908754.424		
Total	508	51995048090			

	<i>Coefficients</i>	<i>Standard Error</i>	<i>t Stat</i>	<i>P-value</i>	<i>Lower 95%</i>	<i>Upper 95%</i>
Intercept	12,786.9	661.0	19.35	8.3998E-63	11,488	14,085

The following equation contains the multiple linear regression model, developed on daily data, which best fits the operating data between October 2000 and August 2001 and is the form of the model currently in use:

$$\text{ABS} = 12,787 + 9.5(\text{CN}_F) - 180.7(T) - 416.9(\text{CN}_D)$$

where:

ABS – ABS addition rate, lbs

CN_F – $[\text{CN}^-]$ in detox feed slurry, ppm

T – slurry temperature, °F

CN_D – $[\text{CN}_{\text{WAD}}]$ in detox discharge slurry, ppm

A trend line of the predicted and actual ABS addition rates was plotted (Figure 5.20) and it indicates that the 2001 Detox Model produced an accurate estimate of the daily ABS requirements in the Fort Knox mill ($R^2 = 0.95$).

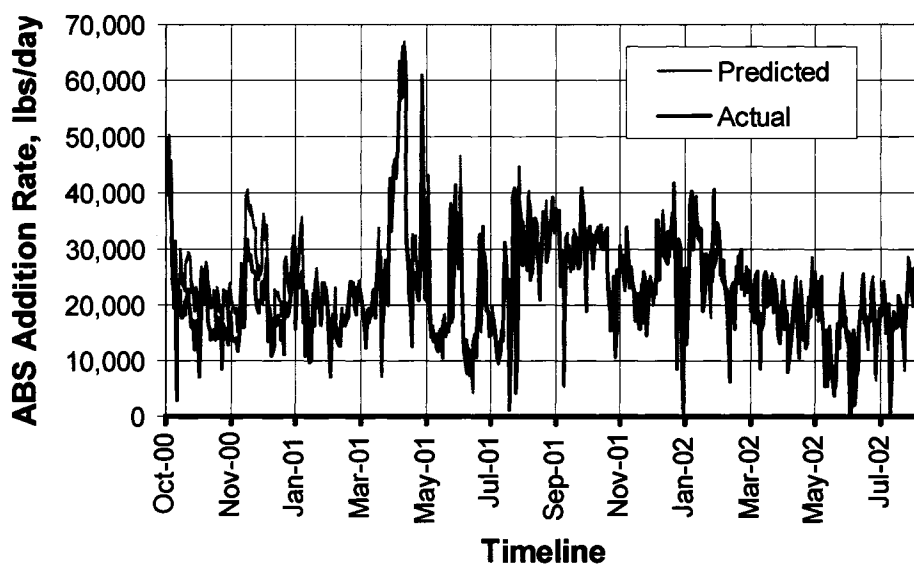


Figure 5.20 Trend line of actual and predicted ABS addition rates, lbs/day, 2001 Detox Model.

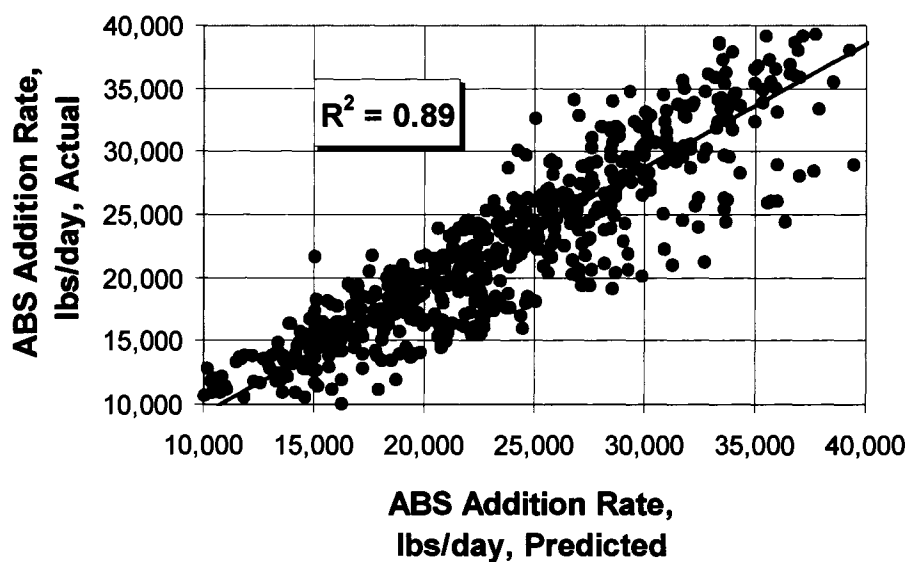


Figure 5.21 Actual ABS addition rate vs. ABS addition rate predicted by Detox Model 2001.

REFERENCES

- Hollow, J.T., Hill, E.M., Lin, H.K. and Walsh, D.E., 2005, *Modeling the influence of slurry temperature on gold leaching and adsorption kinetics at the Fort Knox Mine, Fairbanks, Alaska*, Minerals & Metallurgical Processing, Vol. 23, No. 3, pp. 151-159.
- INCO, 1992, *INCO SO₂/air process cyanide destruction operating manual for Lassen Gold Mining, Inc. Hayden Hill Mine*, Technical report prepared by INCO Exploration and Technical Services Incorporated, pp. 1-8.
- INCO, 1996, *INCO SO₂/air cyanide destruction operating manual, Fort Knox Mine, for Fairbanks Gold Mining, Inc. Alaska*, Technical report prepared by INCO Limited, pp. 15-20.
- Lin, H.K., Oleson, J.L., Hollow, J.T. and Walsh, D.E., 2002, *Characterization and flotation of gold in carbon fines at the Fort Knox Mine, Alaska*, Minerals & Metallurgical Processing, Vol. 19, No. 1, pp. 21-24.
- Marsden, J. and House, I., 1992, *The Chemistry of Gold Extraction*, Ellis Horwood, New York, pp. 275.
- Oleson, J.L., Lin, H.K. and Walsh, D.E., 2005, *Modeling of SO₂/air cyanide destruction process*, Minerals & Metallurgical Processing, Vol. 22, No. 4, pp. 199-204.

CHAPTER 6

THE DEVELOPMENT OF AN ENERGY BALANCE MODEL TO PREDICT THE ECONOMIC IMPACT OF INSTALLING A TAILINGS WASH THICKENER AT THE FORT KNOX MINE, FAIRBANKS, ALASKA¹

6.1 ABSTRACT

The Fort Knox Mine is located in Alaska's interior, where the average ambient air temperatures range from -24°C in January to 16°C in July. The mill processes a free milling gold ore utilizing both a gravity recovery circuit and conventional cyanide leach/carbon-in-pulp circuits. Mathematical models have been developed to accurately predict the impact of leach circuit slurry temperature on gold leach, carbon adsorption and cyanide destruction kinetics. Additionally, an energy balance approach has been used to model the seasonal variations in slurry temperatures throughout the Fort Knox mill. The energy balance model, combined with the kinetics models previously developed to predict plant performance, was used to justify a tailing thickener installation at the Fort Knox Mine. This paper describes the development of the energy balance model and its prediction of plant performance assuming a tailings wash thickener to reduce heat loss from the mill. Also presented is an analysis of the post project plant performance that validates the model and shows the mine produced an additional 596 kg (19,155 ounces) of gold, while reducing mill reagent costs by \$6,302,000 during the first 38 months of operation.

6.2 INTRODUCTION

The Fort Knox Mine, located in the Fairbanks Mining District, 40 km (25 miles) northeast of Fairbanks, Alaska, began commercial gold production in the first quarter of 1997. The mine site is approximately 150 km (94 miles) south of the Arctic Circle and experiences sub-Arctic climate conditions with the average ambient air temperature being

¹ Hollow, J.T., Lin, H.K., Walsh, D.E., and White, D.M., prepared for publication in *Minerals and Metallurgical Processing*, July, 2006.

slightly below 0°C. The Fort Knox gold deposit and process flowsheet have been previously described in detail (Lin *et al.*, 2002, Hollow *et al.*, 2003).

The primary source of mill makeup water is the decant pond within the tailings storage facility (TSF). The TSF is designed and operated as a zero discharge facility with a maximum operating capacity of 7.4 million m³ (6,000 acre-ft) of decant solution storage. The decant pond accumulates water due to surface runoff from the 17.4 km² (6.7 miles²) watershed upstream of the dam, mine dewatering activities, mill tailings slurry and precipitation. Water losses from the facility include water incorporated into the settled tailing (interstitial water) and evaporation. During dry, normal, and most wet years, the TSF is a net consumer of water and additional water is required to maintain operating volume. To supply this need, a water supply reservoir (WSR) was constructed down stream of the TSF.

The water supply reservoir was constructed approximately 3.4 km (2.1 miles) down gradient of the TSF and allows for collection of surface flow from an additional 36.0 km² (13.9 miles²) of drainage area. The WSR incorporates an earthen dam and concrete spillway system and has a normal operating capacity of approximately 4.9 million m³ (4,000 acre-ft). To ensure the availability of water during winter operation, water is reclaimed from the deepest point in the WSR via a stationary pump house.

As operating history was generated at the Fort Knox mill, seasonal fluctuations in the leach circuit slurry temperature were observed. Gold extraction and carbon adsorption efficiencies have been accurately predicted using temperature as an independent variable (Hollow *et al.*, 2006). In addition, variations in the consumption rate of lime for pH control in the grinding circuit, as well as copper sulfate and SO₂ used in the cyanide destruction circuit, were correlated to circuit operating temperature (Hollow, 2002). To better evaluate potential alternative gold ore processing scenarios, an energy balance model was developed to estimate average process circuit temperatures under varying mill throughput rates and flowsheet designs.

6.2.1 Ambient Air Temperature

The average annual temperature at the site is -0.5°C (31.2°F). Daily temperature is at a minimum in January, when the average daily value is -14.4°C (6.1°F) and has ranged from -20.6°C (-5.0°F) in 1999 to -9.8°C (14.4°F) in 2003. Daily temperature is at a maximum in July, when the average daily temperature is 15.2°C (59.4°F) and has ranged from 13.3°C (55.9°F) in 2001 to 18.6°C (65.5°F) in 2004. Table 6.1 contains the historic ambient air temperature data collected at the site.

Table 6.1 Fort Knox Mine average air temperature, $^{\circ}\text{C}$.

	1997	1998	1999	2000	2001	2002	2003	2004	2005	Mean
Jan	n.a	-15.4	-20.6	-17.3	-10.2	-10.4	-9.8	-18.6	-13.0	-14.4
Feb	n.a	-8.9	-23.0	-7.9	-9.3	-12.0	-5.5	-7.8	-9.8	-10.5
Mar	n.a	-4.8	-12.1	-5.3	-10.5	-8.8	-10.0	-11.6	-4.6	-8.5
Apr	n.a	1.6	-1.9	-1.7	-1.5	-4.7	1.0	2.8	0.4	-0.5
May	n.a	7.3	6.3	4.8	4.4	8.4	8.1	10.4	12.6	7.8
Jun	n.a	11.1	15.7	15.0	14.8	12.3	15.4	20.1	16.3	15.1
Jul	14.3	16.1	15.7	13.7	13.3	14.8	15.1	18.6	15.5	15.2
Aug	11.1	10.4	13.5	9.1	12.2	12.1	12.8	17.0	13.7	12.4
Sep	7.7	6.5	5.5	2.6	8.4	8.1	4.2	3.1	6.7	5.9
Oct	-10.0	-3.4	-6.8	-4.8	-5.8	-6.6	1.6	-1.4	-2.4	-4.4
Nov	-7.3	-11.0	-16.9	-8.0	-12.7	-2.9	-10.8	-7.4	-16.4	-10.4
Dec	-15.0	-17.8	-20.8	-12.2	-19.2	-8.8	-5.4	-12.8	-7.1	-13.2
Mean	n.a.	-0.7	-3.8	-1.0	-1.3	0.1	1.4	1.0	1.0	-0.5

6.2.2 Precipitation

The mine site receives an average of 46.7 cm (18.4 in.) of annual precipitation, with most falling in the summer and early fall. The 36.7 cm (14.5 in) minimum value was recorded in 2001 and the 58.8 cm (23.1 in.) maximum value recorded in 2002. Table 6.2 contains the historic precipitation data collected at the site.

6.2.3 Snow Fall

The average annual snow fall recorded at the Fort Knox Mine is 126.1 cm (49.9 in.). The minimum value recorded was 71.7 cm (28.2 in) in 2001 and the maximum of 168.0 cm. (66.2 in) in 2004. On average, the water content of the snow has been 0.320 cm water per 1.00 cm of snow (0.126 in. water per 1.0 in. of snow), which remains on the

ground from early October until early April. Table 6.3 contains the average snow fall data recorded at the mine.

Table 6.2 Fort Knox Mine average precipitation, cm.

	1997	1998	1999	2000	2001	2002	2003	2004	2005	Annual
Jan	n.a	0.3	2.4	5.4	1.0	2.6	0.9	0.8	6.6	2.5
Feb	n.a	0.4	0.5	0.0	1.2	1.8	2.6	1.6	1.2	1.2
Mar	n.a	0.3	0.1	0.1	1.0	0.4	0.3	1.2	0.1	0.4
Apr	n.a	0.3	1.6	0.0	0.5	8.0	0.0	0.0	0.9	1.4
May	n.a	4.2	3.3	5.4	2.7	2.2	0.8	7.2	5.0	3.8
Jun	n.a	3.8	5.1	4.0	5.3	6.8	3.0	1.8	10.6	5.1
Jul	7.2	12.5	3.7	6.1	8.6	12.6	19.6	3.9	10.2	9.4
Aug	5.9	10.7	7.2	16.3	9.1	13.3	9.1	2.7	2.0	8.5
Sep	2.2	5.4	7.2	9.3	0.7	5.0	6.8	3.1	8.6	5.4
Oct	9.6	0.4	6.7	4.4	4.6	4.7	3.6	2.6	0.9	4.2
Nov	0.9	1.9	5.7	2.1	0.4	0.1	7.1	2.0	3.3	2.6
Dec	2.6	3.1	4.0	1.0	1.5	1.3	3.8	2.9	0.3	2.3
Annual	n.a.	43.3	47.4	54.0	36.7	58.8	57.6	29.7	49.7	46.7

Table 6.3 Fort Knox Mine average snow fall, cm.

	1998	1999	2000	2001	2002	2003	2004	2005	Mean
Jan	n.a	12.2	71.6	12.4	39.4	13.8	8.9	44.5	29.0
Feb	n.a	4.1	0.0	17.8	12.4	19.6	12.2	11.9	11.1
Mar	n.a	10.4	5.3	4.1	4.6	3.8	23.6	7.6	8.5
Apr	n.a	8.6	0.0	7.4	37.5	2.5	0.0	7.1	9.0
May	n.a	21.1	0.0	0.0	0.0	0.0	0.0	0.0	3.0
Jun	n.a	0.0	0.0	0.0	0.0	0.0	0.0	0.0	0.0
Jul	n.a	0.0	0.0	0.0	0.0	0.0	0.0	0.0	0.0
Aug	n.a	0.0	0.0	0.0	0.0	0.0	0.0	0.0	0.0
Sep	n.a	6.4	5.1	0.0	0.0	0.0	3.1	9.4	3.4
Oct	4.8	20.8	30.2	12.8	12.8	2.8	46.5	13.0	17.9
Nov	15.2	24.2	14.0	5.1	1.3	59.1	30.9	46.2	24.5
Dec	25.4	25.4	3.8	12.2	19.1	24.6	42.9	3.6	19.6
Mean	n.a.	133.1	130.0	71.7	126.9	126.3	168.0	143.3	126.1

6.2.4 Water Supply Reservoir (WSR) Water Temperature

The 4.9 million m³ (4,000 acre-ft) WSR, constructed in 1996, is fed by a 36.0 km² (13.9 miles²) watershed. Water is reclaimed from the deepest point in the facility and supplies the 871 l/m (230 gpm) non-potable requirements for the mine site. In addition,

water can be transferred to the tailings storage facility when additional plant makeup water is required. The surface of the WSR is ice covered from early October through April. During this period, the water temperature remains below 4°C and reaches a minimum just prior to spring breakup in April.

After spring breakup, the WSR water temperature rises to maximum values in August, due to the increase in ambient air temperature and the extended solar radiation associated with the long summer days. These heat sources are slightly offset by summer precipitation events that reduce the pond water temperature. Table 6.4 contains the average monthly water temperatures at the Fort Knox WSR.

Table 6.4 Fort Knox Mine mean WSR water temperature, °C.

	1997	1998	1999	2000	2001	2002	2003	2004	2005	Mean
Jan	2.1	1.9	3.4	3.2	2.8	3.2	2.8	2.7	3.0	2.8
Feb	1.6	1.7	3.0	3.2	2.9	2.9	2.7	2.6	3.1	2.6
Mar	1.4	1.4	3.2	2.9	2.6	2.8	2.7	2.5	2.9	2.5
Apr	1.5	1.9	3.1	2.9	2.0	2.6	3.2	2.3	2.7	2.5
May	3.6	4.4	4.2	2.8	4.6	3.9	4.5	3.7	6.3	4.2
Jun	7.3	7.6	6.9	6.2	7.7	7.9	7.7	8.1	8.6	7.6
Jul	7.6	9.0	9.2	8.8	9.0	8.9	10.0	8.0	10.5	9.0
Aug	8.5	9.2	10.4	8.6	10.4	9.2	12.0	6.2	10.7	9.5
Sep	8.8	9.8	9.0	8.2	9.8	9.2	8.3	6.8	10.0	8.9
Oct	3.8	4.7	5.2	4.5	6.5	5.7	5.9	5.1	7.8	5.5
Nov	2.5	3.5	3.4	3.3	3.4	3.6	3.3	3.7	3.9	3.4
Dec	2.2	3.5	3.4	3.1	3.1	3.2	2.8	3.2	3.2	3.1
Mean	4.2	4.9	5.4	4.8	5.4	5.3	5.5	4.6	6.1	5.1

6.2.5 Tailings Storage Facility (TSF) Water Temperature

The majority of mill makeup water is reclaimed from a surface pond within the tailing storage facility (TSF). A temperature transmitter was installed in 2002, in order to provide continuous monitoring of the mill makeup water temperature.

An ice cover forms on the TSF in October, at which point the reclaim water temperature is approximately 4°C (39°F). The water temperature slowly drops during the course of the winter, reaching approximately 2°C (35°F) just prior to spring breakup in April. Water is reclaimed from the TSF surface pond via a floating barge containing

vertical turbine pumps. The suctions of these pumps are located approximately 2.4 m (8 ft) below the water surface, which results in slightly lower winter water temperatures compared to the WSR water that is reclaimed farther from the ice covered surface.

After breakup, the water temperature in the TSF increases to a higher level than that of the WSR water and reaches a maximum in July. The temperature of the TSF water is affected by ambient air temperature, solar radiation and precipitation events, and by the additional heat input from the placed mill tailings. During winter operation, the heat input from tailings slurry is dissipated into the ice cover and affects the thickness of the ice and not the water temperature. Additional variation in the TSF water temperature results from operational fluctuations in the surface area of the pond. Table 6.5 contains the average monthly water temperature at the Fort Knox TSF.

Table 6.5 Fort Knox Mine mean TSF water temperature, °C.

	1997	1998	1999	2000	2001	2002	2003	2004	2005	Mean
Jan	n.a	n.a	2.3	2.4	2.9	1.1	2.2	2.1	2.5	2.2
Feb	n.a	n.a	1.9	1.9	2.4	0.8	2.0	1.9	2.0	1.9
Mar	n.a	n.a	1.9	1.7	1.8	0.7	2.0	1.9	2.3	1.7
Apr	n.a	n.a	2.9	2.1	2.4	1.5	2.1	1.9	2.5	2.2
May	n.a	n.a	8.7	6.4	6.8	6.3	6.2	7.5	9.0	7.3
Jun	n.a	n.a	17.2	16.0	16.0	14.4	14.4	18.0	15.8	16.0
Jul	n.a	n.a	18.9	17.6	17.2	16.7	17.7	19.1	17.2	17.8
Aug	n.a	14.0	16.4	12.9	14.7	14.2	15.2	17.8	16.2	15.2
Sep	n.a	8.5	10.0	8.1	11.4	10.6	10.0	9.6	11.6	10.0
Oct	n.a	3.2	3.0	3.5	4.1	4.3	5.1	3.6	4.5	3.9
Nov	n.a	2.7	2.8	2.9	1.2	2.5	3.1	3.0	2.5	2.6
Dec	n.a	2.3	2.5	2.6	1.1	2.5	2.2	2.8	2.3	2.3
Mean	n.a.	n.a.	7.4	6.5	6.8	6.3	6.8	7.4	7.4	6.9

6.3 ENERGY BALANCE TEMPERATURE MODEL

In the Fort Knox grinding circuit, gold ore is combined with water and subjected to a significant amount of grinding energy (11.5 kw hr/ton) required to reduce the size of the ore to 80% passing 190 microns. Work has been presented that indicated an energy balance model can be used to estimate the rheology of the mill discharge slurry (Van Drunick and Moys, 2001). By utilizing a dynamic energy (enthalpy) balance model, a

better understanding of the circuit temperature variations can be developed and a model that successfully predicts plant slurry temperature can be utilized to evaluate alternative processing schemes that could be employed to improve plant performance.

In an energy balance model for a system in equilibrium, heat input to the system must equal heat removed from the system (Thomann and Mueller, 1987). Heat into the system is from the crushed ore, the fresh water, the reclaimed tailings water, and mechanical sources such as grinding mills, pumps, agitators and leach air compressors. Heat lost from the system includes convective heat losses from the unit processes into the buildings and from process streams leaving the system, such as SAG mill recycle material rejected from the grinding circuit and tailings slurry discharged to the TSF. Additional heat is lost from the leach/CIP circuit to the surrounding air by convection, conduction and radiation.

To develop the energy balance model, a water and ore mass balance must first be developed for the process streams throughout the plant. The heat content (W_H), which is a measure of the enthalpy or useful energy, is then calculated for each of the components being included in the model. The heat content can be estimated based on the following equation (Thomann and Mueller, 1987):

$$W_H = c_p Q T \quad (6.1)$$

where

W_H = heat content, J/day (BTU/day)

c_p = specific heat capacity, J/kg^{°K} (BTU/lb_m^{°F})

Q = mass flow of substance, kg/day (lb_m/day)

T = temperature of substance, ^{°K}, (^{°F})

The value c_p represents the specific heat capacity of a system at constant pressure. For the Fort Knox energy balance model, the specific heat capacity (c_p) of ore was assumed to be 0.879 J/g^{°K} (0.21 BTU/lb^{°F}) and is consistent with published values for

quartzite or high silica ores (Van Drunick and Moys, 2001, Henderson, 2000). The specific heat capacity of water was assumed to be 4.188 J/g^oK (1.0 BTU/lb^oF), which is accurate for water at 20°C (68°F). The values indicate that it requires nearly 5 times the energy to increase the temperature of 1 kg of water 1^oK as it does to produce the same temperature increase in 1 kg of ore. Based on this relationship and the typical water to solids ratio of the processes at the Fort Knox mill of approximately 1:1, the primary source of the seasonal slurry temperature variations is due to the variations in makeup water heat content.

Temperature measurements of key feed streams are also required to determine the heat content of each component throughout the flowsheet, and heat inputs into the milling system can be expressed as follows:

$$\text{Heat In} = \text{Heat}_{(\text{ore})} + \text{Heat}_{(\text{water})} + \text{Energy Input (electricity)} \quad (6.2)$$

$$\text{Heat}_{(\text{ore})} = \text{lbs}_{(\text{ore})} \times c_{p(\text{ore})} \times \text{Temp}_{(\text{ore})} \quad (6.3)$$

$$\text{Heat}_{(\text{water})} = \text{lbs}_{(\text{water})} \times c_{p(\text{water})} \times \text{Temp}_{(\text{water})} \quad (6.4)$$

$$\text{Energy Input} = g (\text{electric power input}) \quad (6.5)$$

where:

g = percent of total consumed power converted to heat

Once the total heat content of the system is known, the resulting temperature of the discharge slurry can be calculated. All values required for the input energy calculations are monitored continuously by plant instrumentation with the exception of mill feed ore temperature and moisture content.

6.3.1 Ore Temperature Determinations

Initial modeling was completed assuming an average annual ore feed temperature. However, the consistent pattern in the model error term indicated a more sophisticated approach would be needed. Periodic thermal scans were taken of the ore discharging the apron feeders with the results indicating that the ore temperature did cycle seasonally. A

mathematical model was developed that produced an estimated ore temperature on a daily basis, the results of which were integrated into the overall mill energy balance model. Figure 6.1 contains the actual thermal scan values and the mathematical model outputs.

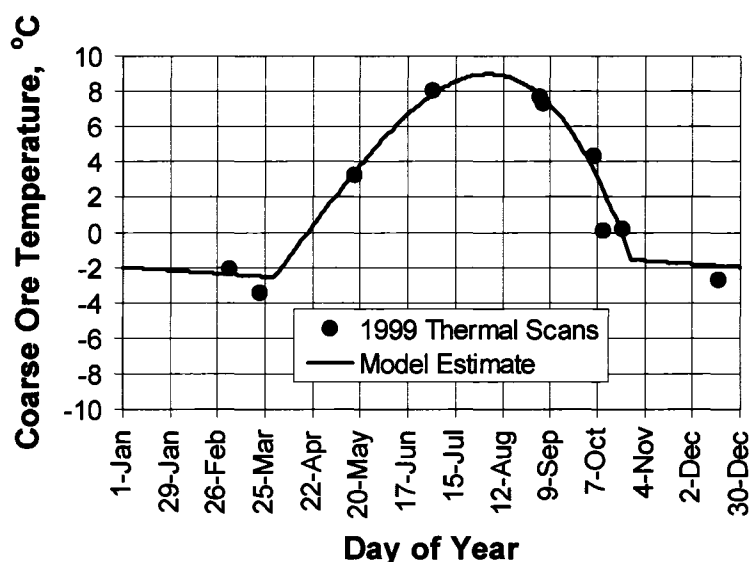


Figure 6.1 Ore temperature – model vs. thermal scan data.

6.3.2 Ore Moisture Content

An estimation of the ore moisture content was also required to eliminate some of the variance between actual and estimated leach circuit slurry temperatures. Numerous sampling campaigns have concluded that the average moisture content of the mill feed ore is approximately 3% by weight. This value is consistent through the months when average temperatures remain below freezing (approximately October to May). During the other months, the rainfall saturates the blasted ore in both the pit and stockpiles and increases the ore moisture content. A regression analysis was performed to develop the relationship between summer precipitation events and average ore moisture content. The model error term is minimized, when the effect of precipitation events is delayed 2 days before increasing the feed ore moisture content to account for the event. Figure 6.2

contains the seasonal trend of the estimated mill feed ore moisture. Figure 6.3 contains the relationship between precipitation and ore moisture content used in the energy balance model.

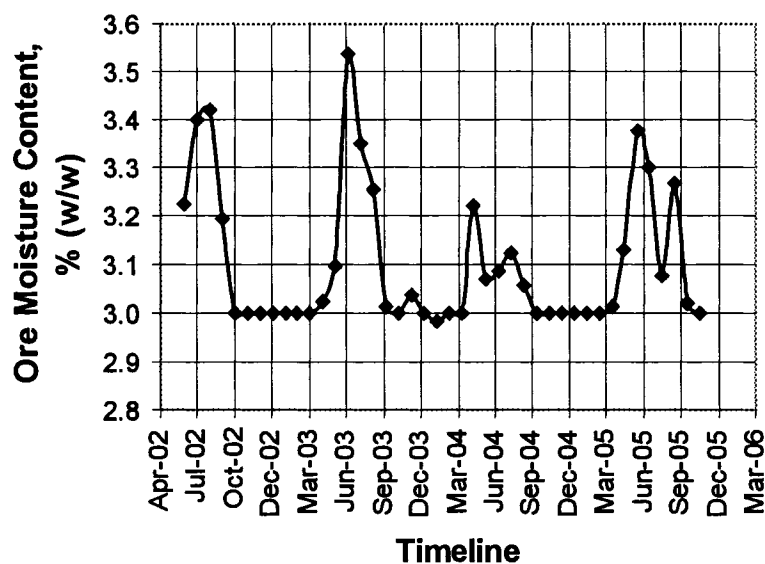


Figure 6.2 Model input - Ore moisture content.

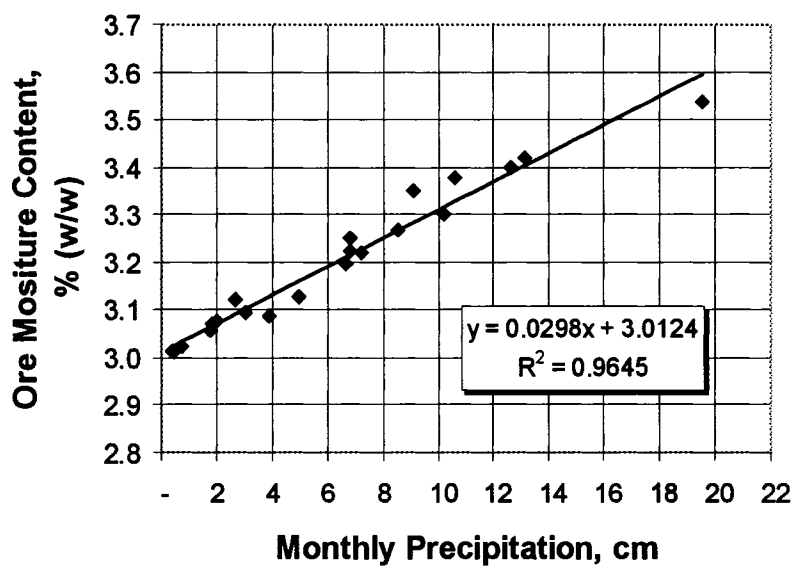


Figure 6.3 Ore moisture content vs. precipitation.

6.3.3 Grinding Circuit Heat Input

In the energy balance model, heat is added to the circuit in the form of mechanical energy from process equipment such as grinding mills, pumps and agitators. During model calibration, the value of the electrical power input converted to heat (g) was adjusted to maximize the coefficient of determination (R^2) of the predicted vs. actual temperature measurements from the data set.

The strongest correlation between model predicted and actual leach feed temperatures occurred when 98% of the grinding energy was converted to heat and added to the system. This value is consistent with published information indicating only about 1% of the energy input into grinding is utilized for particle fragmentation (Kelly and Spottiswood, 1989, Hukki, 1975). Through a similar process, it was determined that 75% of electrical energy consumed by pumps within the grinding circuit should be converted to heat and added to the system.

6.3.4 Grinding Circuit Heat Loss

In the energy balance model, heat is lost from the grinding circuit due to convective heat loss into the mill building interior. This source of heat loss is minimal and is ignored in the current model.

6.3.5 Model Versus Actual Leach Feed Temperature

The energy balance model was prepared and the daily leach circuit slurry temperatures predicted for the period May 2002 through December 2005. The temperatures predicted by the model showed good correlation with the actual leach feed slurry temperatures measured in the plant, as presented in Figures 6.4 and 6.5.

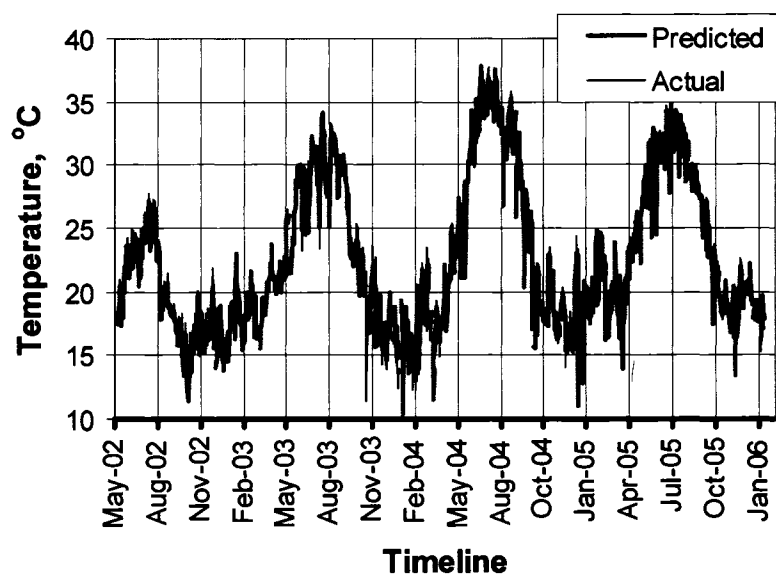


Figure 6.4 Actual and predicted leach feed slurry temperature.

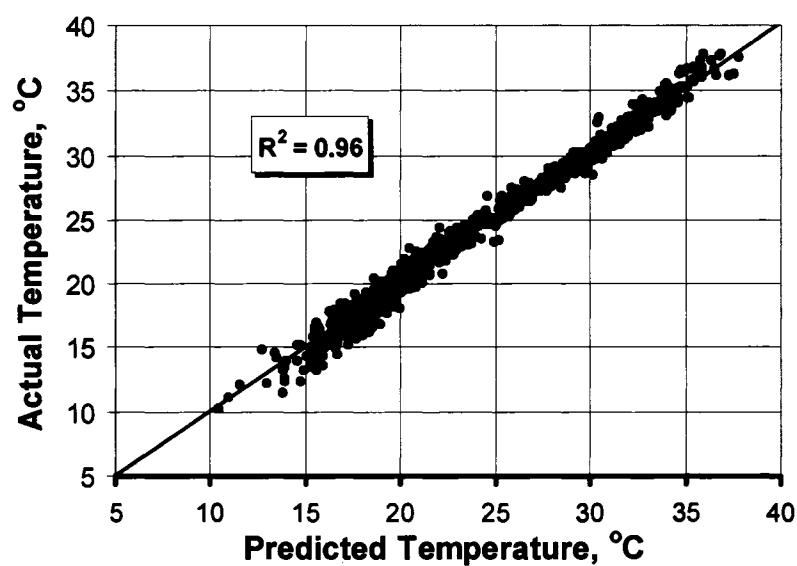


Figure 6.5 Actual vs. predicted leach feed slurry temperature.

6.3.6 Heat Transfer from Leach and CIP Tanks

There are 13 uninsulated leach/ CIP tanks in the Fort Knox circuit. Temperature transmitters were added in 2002 to allow for a continuous reading of leach feed slurry and CIP discharge slurry temperatures. The data collected from the transmitters indicate that the heat loss from the outside tankage results in a temperature drop of less than 1°C (2°F) in slurry temperature. Figure 6.6 contains a timeline of the actual leach feed slurry and CIP discharge slurry temperature. Figure 6.7 shows a timeline of the actual temperature drop in the leach/CIP circuit.

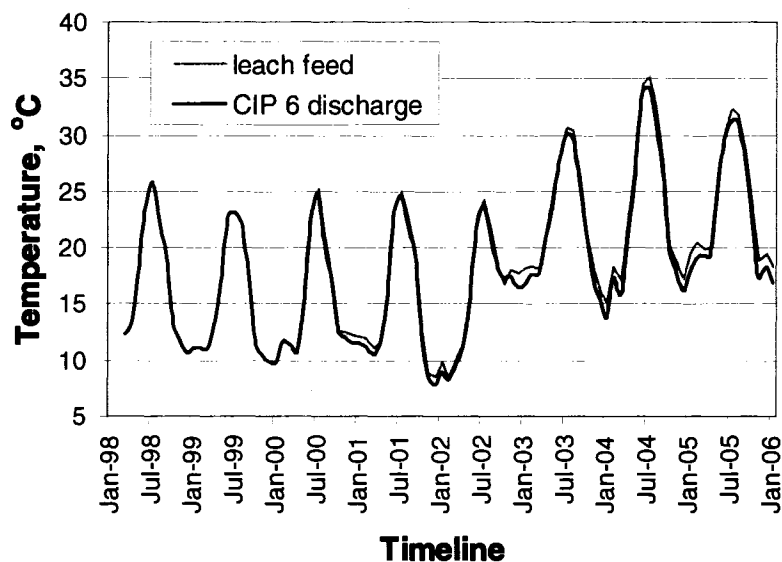


Figure 6.6 Historic leach/CIP circuit temperature.

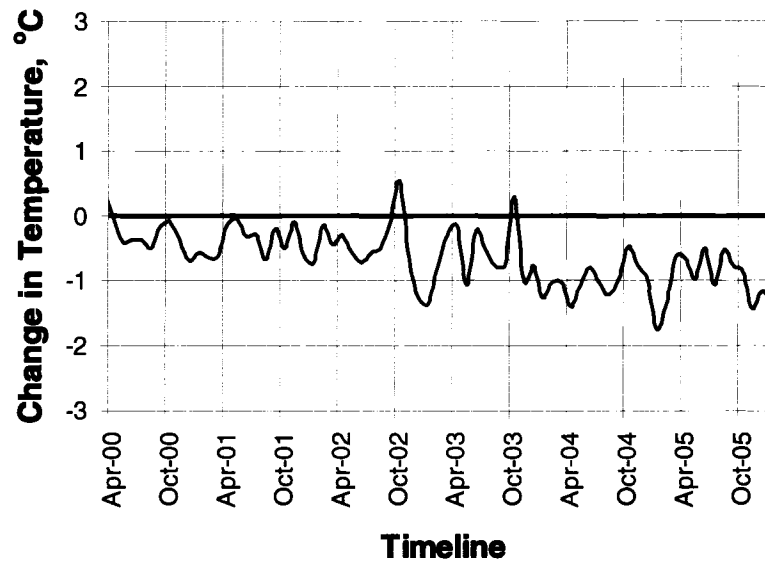


Figure 6.7 Historic temperature drop in leach/CIP tanks.

6.3.7 Heat Input to Leach/CIP Circuit

In the Energy Balance Model, heat is added to the slurry in the form of mechanical energy from electrical motors on equipment such as agitators and compressors. In the current model, it is assumed that 75% of the total motor capacity (Henderson, 2000) from these sources is converted to heat and added to the slurry heat content.

6.3.8 Heat Exchange Between the Atmosphere and Leach/CIP Circuit

A change in the heat content of the slurry also results from radiation (shortwave and longwave), convection and conduction as the slurry passes through the leach/CIP tanks. The net heat exchange per unit area between the air-tank surfaces can be calculated as follows (Thomann and Mueller, 1987):

$$\Delta H = [(H_s - H_{sr}) + (H_a - H_{ar})] - (H_{br} \pm H_c \pm H_e) \quad (6.6)$$

where:

ΔH = net heat exchange across the tank surface

H_s = shortwave solar radiation

H_{sr} = reflected shortwave radiation

H_a = longwave atmospheric radiation

H_{ar} = reflected longwave radiation

H_{br} = longwave radiation from tank surface

H_c = conductive heat transfer

H_e = evaporation/condensation heat transfer

The first group of terms in brackets, called the net absorbed radiation, is independent of the tanks' slurry temperature and can be measured directly or computed from meteorological observations. The second group of terms depends in various ways on the temperature differential between the tanks' surface and the ambient air. Calculating the various heat transfer coefficients and estimating the heat loss through the tanks mathematically is a relatively straightforward process. The initial modeling assumed an overall heat transfer coefficient could be used to estimate the heat loss from the circuit based on the temperature differential between the air temperature and the slurry temperature. Additionally, the gain or loss of heat is a function of slurry retention time. The following equation was used in the preliminary model:

$$\Delta H = U A (T_a - T_s) t \quad (6.7)$$

where:

ΔH = net heat exchange across the tank surface, J (BTU)

U = overall heat transfer coefficient, J/m² °K hr (BTU/ft² °F hr)

A = tank surface area, taken to be 13,000 m² (140,000 ft²)

T_a = ambient air temperature, °K (°F)

T_s = slurry temperature, °K (°F)

t = retention time, hrs

During model calibration, the value for the overall heat transfer coefficient was determined to be 42.8 kJ/m² °K hr (2.1 BTU/ft² °F hr), the value that maximized the R² of the predicted vs. actual temperature relationship for the data set. Figure 6.8 contains a trend of the error term from equation 6.7, and suggests a seasonal bias. Therefore, an

additional adjustment was needed to account for the solar and atmospheric radiation terms that are independent of the slurry temperature.

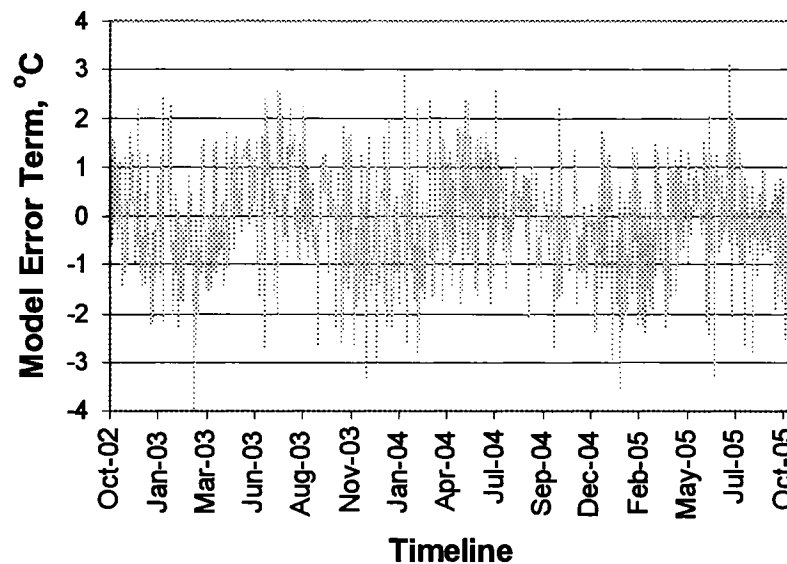


Figure 6.8 Heat transfer coefficient model error trend.

Incoming shortwave solar radiation H_s is partially reflected from the tank surface, H_{sr} , with the net solar radiation adsorbed by the tanks. The percentage reflected depends on the sun's altitude and cloud cover. The longwave atmospheric radiation can be derived from Stefan-Boltzman law and is found to be dependent on air temperature, T_a , and the saturated vapor pressure of water at air temperature, T_a . The reflected longwave radiation is generally small; about 3% of incoming longwave radiation. Since some of the meteorological observations required to calculate the net radiation term are not available, a simplified approach was used to account for this term in the model. A sinusoidal model was generated that fit the trend in the predicted vs. observed error term in the CIP discharge temperature. Figure 6.9 shows the sine wave fit to the error term from equation 6.7.

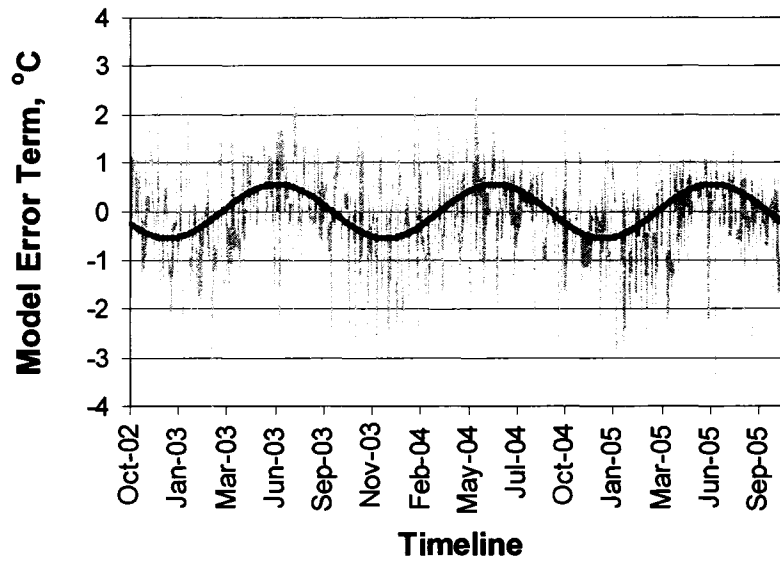


Figure 6.9 Error trend with model adjustment factor.

The final form of the leach/CIP heat transfer model can be expressed as follows:

$$\Delta H = U A (T_a - T_s) t + \Delta H_r \quad (6.8)$$

and

$$\Delta H_r = [\sin(2\pi(D/P + \pi/t_p))] A_{sw}/2 \quad (6.9)$$

where:

ΔH_r = net heat exchange across the tank surface from radiant heat, J/day (BTU/day)

D = day of year

P = period, (365 days)

A_{sw} = amplitude, 192,950,000 kJ/day (183 million BTU/day)

t_p = phase adjustment

The model provides a reasonable fit to the actual change in temperature as presented in the Figure 6.10. The remaining unexplained variance is likely the result of

not explicitly accounting for variations in meteorological conditions such as wind, humidity and cloud cover.

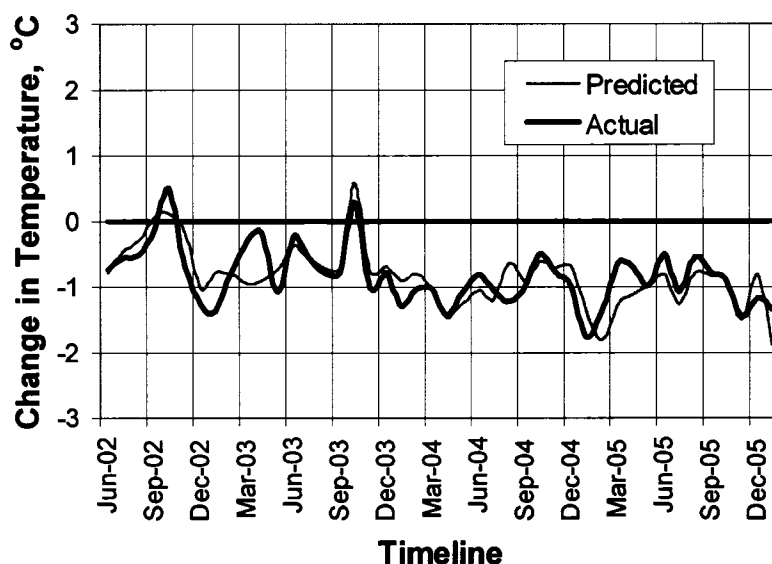


Figure 6.10 Actual and predicted temperature drop in leach/CIP tanks.

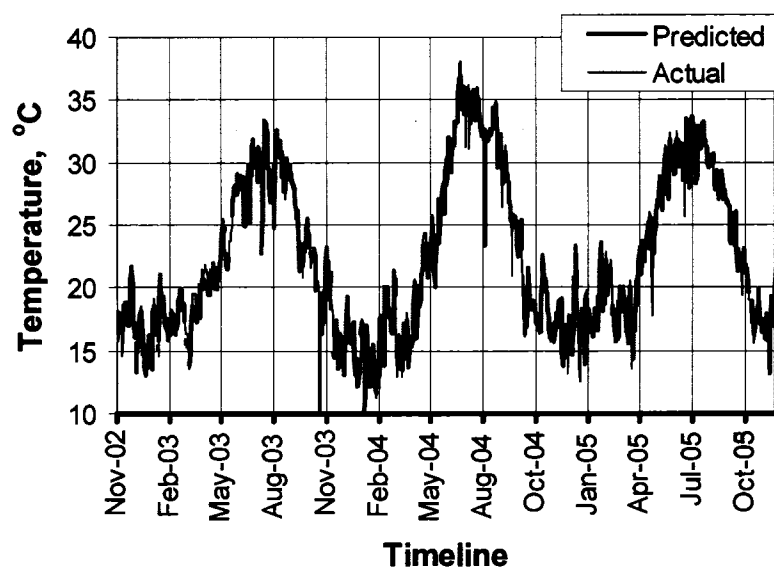


Figure 6.11 Actual and predicted CIP discharge slurry temperature.

Figures 6.11 and 6.12 contain the predicted and actual CIP discharge slurry temperature values. Figure 6.12 shows that although a higher error term exists in the daily

data ($\pm 2^{\circ}\text{C}$) when compared to the leach feed comparison (Figure 6.5), the model shows strong correlation over the entire temperature range measured in the plant over the last 3 years (Figure 6.11).

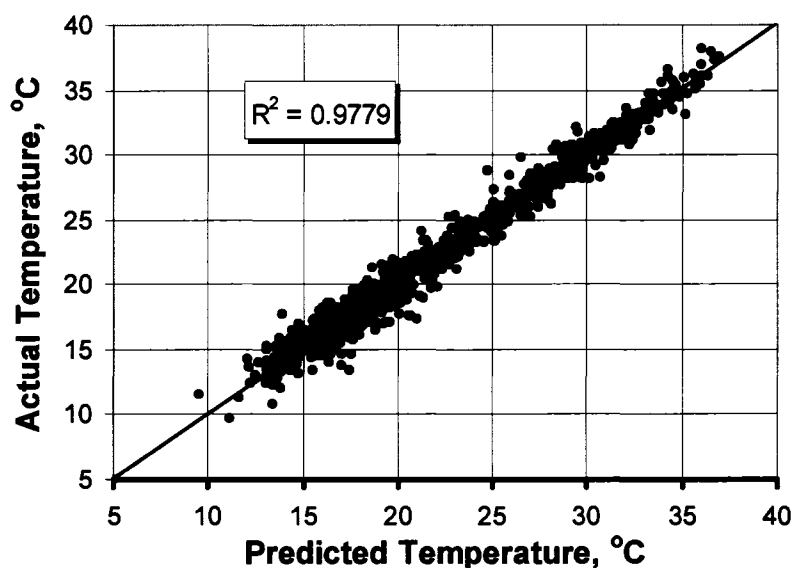


Figure 6.12 Actual vs. predicted CIP discharge slurry temperature.

Once an understanding of the heat balance around the Fort Knox mill was developed, it became apparent that the seasonal variation in the leach slurry temperature primarily resulted from the changes in the mill makeup water temperature. It was proposed that a significant increase in the leach slurry temperature could be realized, if the heat that is dissipated into the tailings storage facility could be used to preheat the mill makeup water prior to addition to the grinding circuit. A tailing thickener was evaluated as a possible mechanism to achieve this goal.

This proposed flowsheet modification would allow the decant water reclaimed from the TSF to be combined with tailings slurry and processed through a thickener. In the thickener, the total mass would reach an equilibrium temperature prior to the thickened underflow slurry being discharged to the TSF, with the thickener overflow

being pumped to the grinding circuit as mill makeup water. Figure 6.13 contains the simplified flowsheet of the proposed plant expansion.

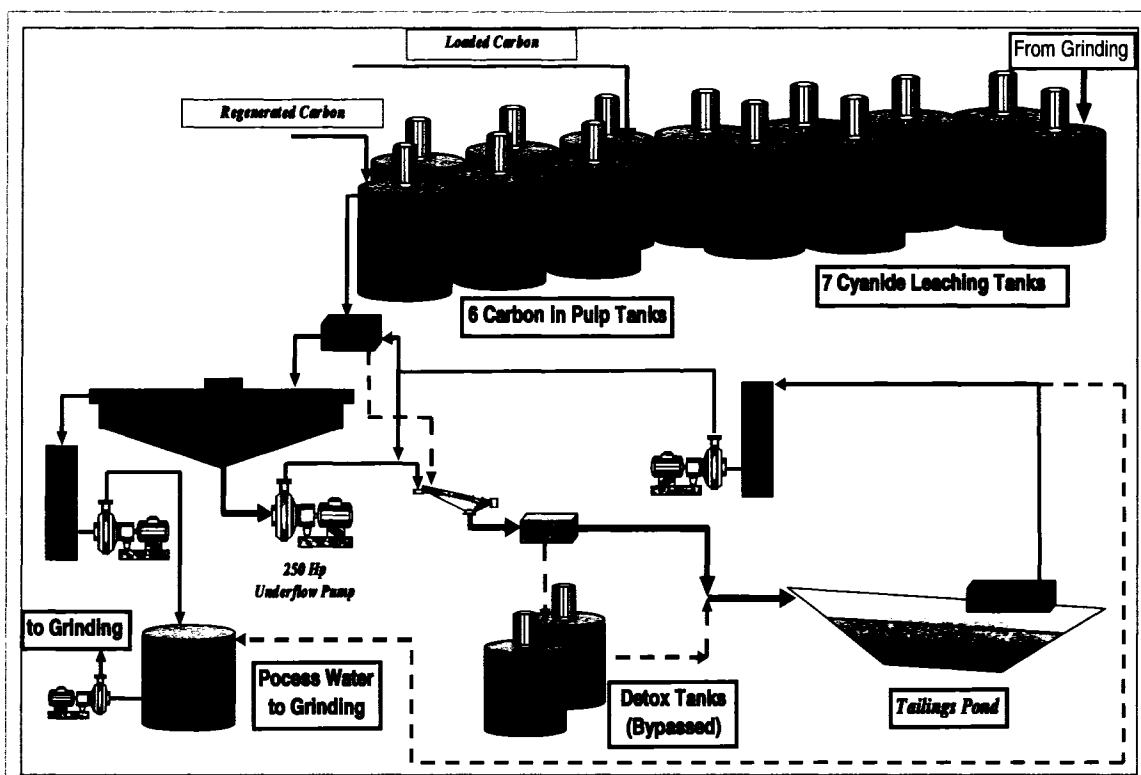


Figure 6.13 Simplified flowsheet for the proposed tailings thickener expansion.

6.4 RESULTS AND DISCUSSION

The energy balance model was run incorporating a tailings wash thickener after the last CIP tank and before the detox circuit. The average site data, contained in Table 6.6 and displayed in Figure 6.14, were used as the baseline model parameters for the evaluation.

A number of simulations were completed to establish the relationship between heat recovery and thickener underflow density. The results contained in Figure 6.15 indicate that the increase in mill makeup water temperature (ΔT_w) increases with

increasing thickener underflow density. Figure 6.15 also indicates that the increase in mill makeup water temperature (ΔT_w) will, ultimately, result in an increase to the leach/CIP slurry temperature (ΔT_s). It can be seen that substantial increases in mill operating temperatures and overall plant performance will be realized, if attempts are made to maximize thickener underflow density.

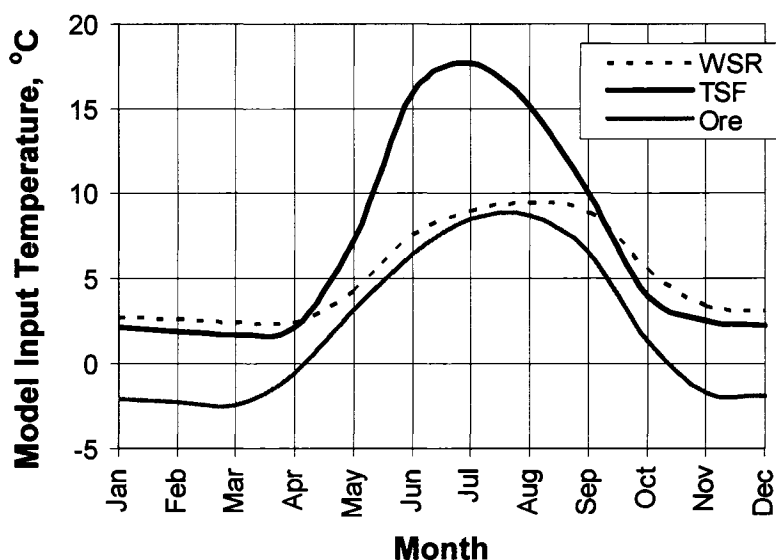


Figure 6.14 Baseline temperatures at the Fort Knox Mine.

The expected average annual makeup water temperature for the mill operated without a thickener, and at the baseline mill operating conditions shown in Table 6.7, is 6.9°C. The predicted average annual mill makeup water temperature with a thickener operated at 60% solids underflow is 16.5°C and represents an annual average increase of 9.6°C. Figure 6.16 contains the predicted daily mill makeup water temperature data with and without a TWT in the circuit.

Table 6.6 Baseline meteorological and water conditions used for the tailings wash thickener evaluation.

	Ambient Air Temp °C	Rainfall to ore moisture cm	Mill Feed		WSR Water Temp °C	TSF Water Temp °C
			Ore moisture % w/w	Ore Temp °C		
Jan	-14.4	0.0	3.0	-2.1	2.8	2.2
Feb	-10.5	0.0	3.0	-2.3	2.6	1.9
Mar	-8.5	0.0	3.0	-2.5	2.5	1.7
Apr	-0.5	0.0	3.0	-0.6	2.5	2.2
May	7.8	3.8	3.1	3.2	4.2	7.3
Jun	15.1	5.1	3.2	6.4	7.6	16.0
Jul	15.2	9.4	3.3	8.5	9.0	17.8
Aug	12.4	8.5	3.3	8.7	9.5	15.2
Sep	5.9	5.4	3.2	6.5	8.9	10.0
Oct	-4.4	0.0	3.0	1.3	5.5	3.9
Nov	-10.4	0.0	3.0	-1.7	3.4	2.6
Dec	-13.2	0.0	3.0	-1.9	3.1	2.3
Mean	-0.5	32.2	3.1	2.0	5.1	6.9

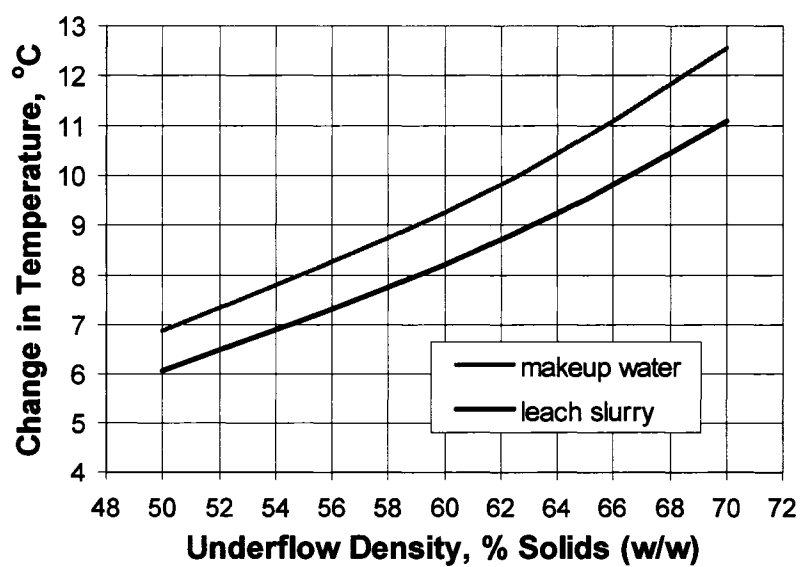


Figure 6.15 Effect of TWT underflow density on ΔT_w and ΔT_s .

Table 6.7 Baseline operating parameters – TWT evaluation.

Parameter	
mill feed rate, tpd	37,467
mill feed grade, mg/kg	0.96
gravity gold recovery, %	20.0
leach particle size P ₈₀ , microns	201
leach density, % solids (w/w)	55
leach [NaCN], ppm	75
carbon advance rate, tpd	12
SAG reject rate, tpd	0
mill availability, %	95.0
SAG mill density (w/w), %	75.0
cyclone feed density (w/w), %	58.0
preleach thickener U/F density (w/w), %	56.0
tailings wash thickener U/F density (w/w), %	60.0
grit screen spray water flow, l/s	31.5
detox/safety screen water flow, l/s	53.6
SAG mill power draw, kw	9,885
ball mill power draw (each), kw	5,073
cylone feed pump power draw (each), kw	700
preleach thickener U/F pump power draw , kw	300
tailings thickener U/F pump power draw, kw	100

The expected average annual leach feed temperature for the mill operated at baseline conditions without a thickener is 15.5°C. The estimated average annual leach feed temperature with a thickener operated under the same conditions is 23.7°C and represents an annual average increase of 8.2°C. Although the temperature of the mill makeup water will be increased by 9.6°C, other water sources such as fresh water and ore moisture content are not affected by the installation of a tailing thickener and the net result is only an 8.2°C increase in the estimated leach feed slurry temperature. Figure 6.16 contains the predicted daily leach circuit slurry temperature data with and without a TWT in the circuit.

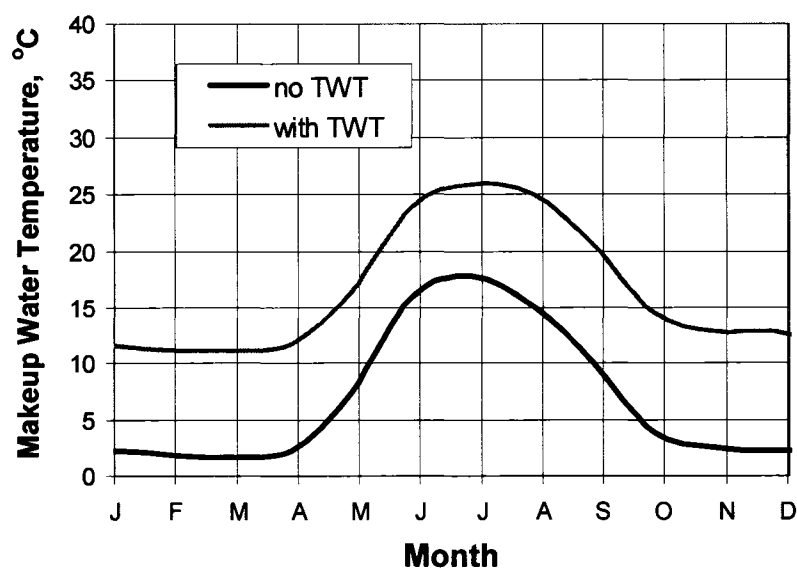


Figure 6.16 TWT effect on mill makeup water temperature.

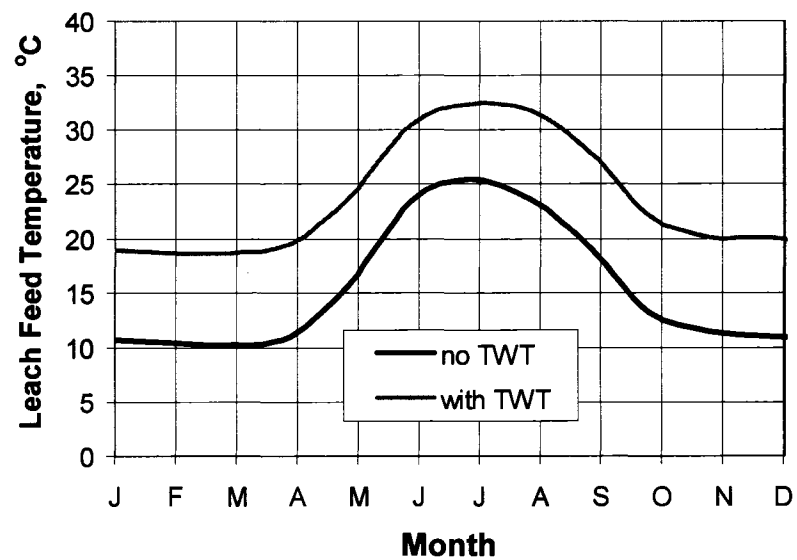


Figure 6.17 TWT effect on leach feed temperature.

6.4.1 Predicted Impact of TWT on Gold Recovery

Mathematical models have been developed that accurately predict leach gold kinetics and carbon adsorption efficiency as a function of temperature (Hollow *et al.*, 2006) at the Fort Knox Mine. The following summarizes the findings from that study and are used as the bases for work contained in this paper.

- The kinetic model (equation 6.10) provides an estimate of solid tailings gold content $[Au]_t$ that best fits the actual plant data, with $[Au]_o$ representing the leach feed gold content:

$$[Au]_t = \left[2.0k_{\text{leach}} t + \frac{1}{([Au]_o - [Au]_{\omega})^{2.0}} \right]^{-0.50} + [Au]_{\omega} \quad (10)$$

The unleachable gold content $[Au]_{\omega}$. Is estimated based on the leach particle size (P_{80}) and mill feed grade $[Au]_{HG}$, where $[Au]_{\omega} = 0.00033(P_{80}) + 0.0312[[Au]_{HG} + 0.0267]$. The retention time (t) is a function of mill throughput rates (tpd) and slurry density (% solids w/w).

- The leach rate constant (k_{leach}) is a function of leach circuit slurry temperature and leach cyanide concentration $[NaCN]$.

$$k_{\text{leach}} = \left\{ \frac{[NaCN]_{\text{actual}}}{[NaCN]_{\text{ave}}} \right\} 2.84 \times 10^{33} e^{-20,870(1/T)} \quad (11)$$

- The CIP circuit solution tailings gold concentration is best estimated by the first-order rate equation 6.12, where $[Au]_{L7}$ is the gold concentration in the CIP feed solution.

$$[Au]_t = [Au]_{L7} e^{-k_{\text{CIP}} t} \quad (12)$$

- The CIP rate constant (k_{CIP}) is a function of CIP circuit slurry temperature (T) and the carbon advance rate (AR), as presented in equation 6.13.

$$k_{\text{CIP}} = \left\{ \frac{AR_{\text{actual}}}{AR_{\text{ave}}} \right\} 0.22 e^{-918 (1/T)} \quad (13)$$

When the kinetics models were applied to the baseline mill conditions, the results in Figures 6.18 and 6.19 were obtained, showing the relationships between gold losses and leach slurry temperature.

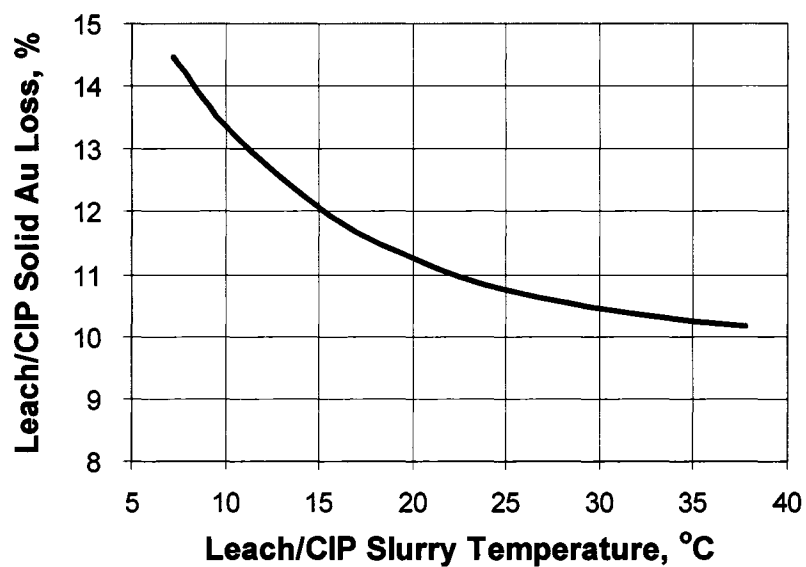


Figure 6.18 Temperature effect on solid gold loss.

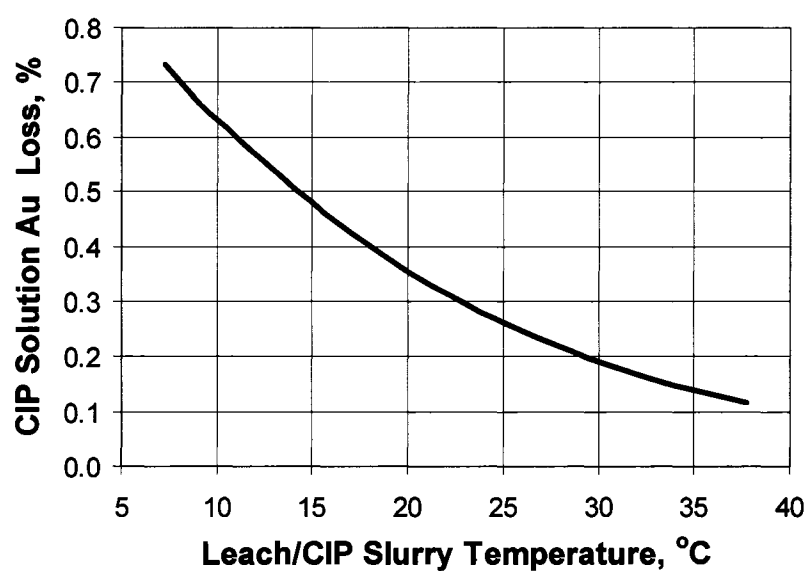


Figure 6.19 Temperature effect on solution gold loss.

Modeling indicated the installation of a TWT would increase slurry temperature by 8.2°C, resulting in a 1.68% increase in total leach gold recovery under the baseline mill operating parameters. This increase in estimated gold recovery was due to reduced

slurry viscosity associated with the increased slurry temperature, which improves both gold leach kinetics and carbon adsorption rates. Assuming the gold concentration in the water reclaimed from the TSF is zero, 55% of the gold remaining in the CIP discharge solution would be recycled back to the grinding circuit in makeup water. Therefore, 87% of the increase in gold production would be a consequence of the TWT project, as the result of the leach/CIP temperature increase, with the remaining 13% due to recycle of solution gold values.

The expected gold recovery vs. temperature relationship for the circuit operated with and without a tailings wash thickener, producing a 60% solid (w/w) underflow slurry, is shown in Figure 6.20, which also shows the expected operating range under each scenario. The offset between the two curves represents the additional benefit from recycling solution gold values, via the thickener overflow, back to the grinding circuit. This benefit is independent of temperature and varies based on available thickener feed dilution water and thickener underflow density.

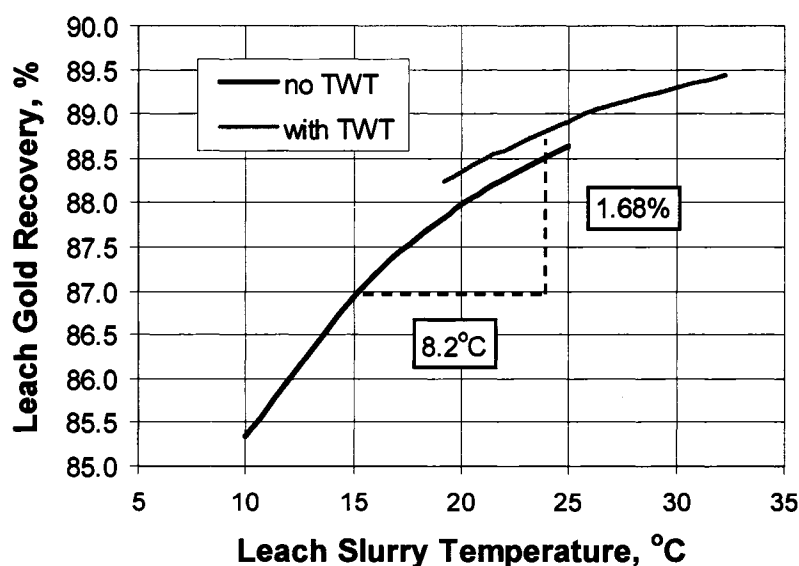


Figure 6.20 TWT effect on total leach gold recovery.

6.4.2 Predicted Impact of TWT on Reagent Usage

Similar to the mechanism by which gold in the CIP discharge solution is recovered to the overflow, free cyanide is also recovered. Approximately 60% of the free cyanide discharging the CIP circuit is recovered to the thickener overflow and returned to the grinding circuit in makeup water at baseline mill conditions. Assuming 100% of the cyanide returned in the makeup water is available to the leach circuit, a 1 to 1 reduction in new cyanide addition would be expected. The remaining 45% of the free cyanide discharging the CIP circuit reports to the thickener underflow. Figure 6.21 shows the impact of the TWT installation on new cyanide addition to leach #1, as leach #1 [NaCN] varies, over the expected operating range.

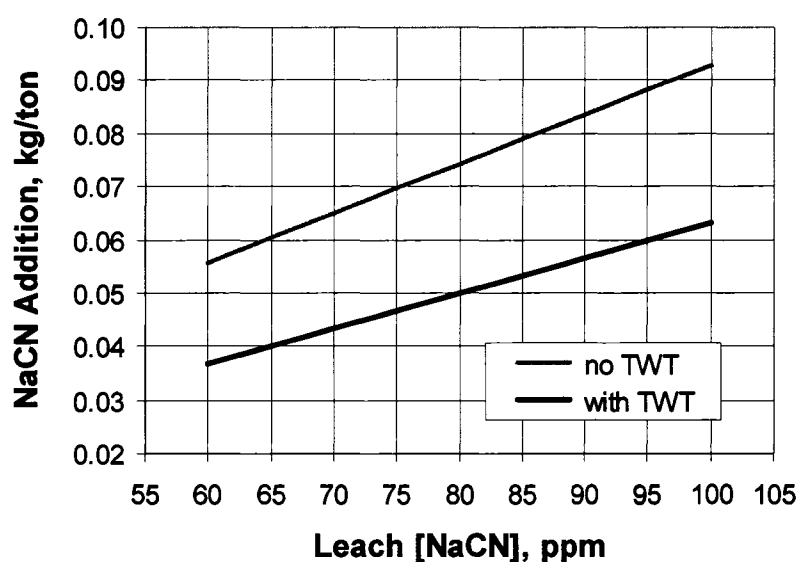


Figure 6.21 TWT effect on NaCN addition in leach circuit

The concentration of the cyanide remaining in the TWT underflow must be reduced to less than 10 ppm prior to discharge into the tailings storage facility. A cyanide destruction circuit, utilizing the Inco SO_2 /Air process, has been used since mill startup in 1996 to meet this requirement. The reaction kinetics and thermodynamic equilibria have been shown to be temperature dependent (Oleson *et al.*, 2005, Hollow, 2002) with increased reagent requirements with decreasing temperature. The installation

of the thickener was not expected to significantly change the slurry temperature in the cyanide destruction circuit, however, it would reduce the cyanide load feeding the destruction circuit substantially. When the baseline mill conditions were run through the model, the impact of the TWT installation on weak acid dissociable cyanide (CN_{WAD}) in the detox feed slurry would be predicted. Figure 6.22 shows the impact of the TWT installation on CN_{WAD} in the detox feed slurry, as leach #1 $[NaCN]$ varies, over the expected operating range.

The expected reagent usage in the cyanide destruction circuit, assuming no change in circuit slurry temperature, was related to the cyanide load in the destruction circuit. Because this cyanide load would be expressed as a function of the concentration of cyanide in leach solution, the impact of the TWT on detoxification reagent usage, ammonium bisulfite (ABS) and copper sulfate ($CuSO_4$), was estimated (Hollow, 2002). Figures 6.23 and 6.24 show these relationships, respectively.

After completion of the economic evaluation, a decision was made in December 2001 to install a tailings wash thickener at the Fort Knox mill.

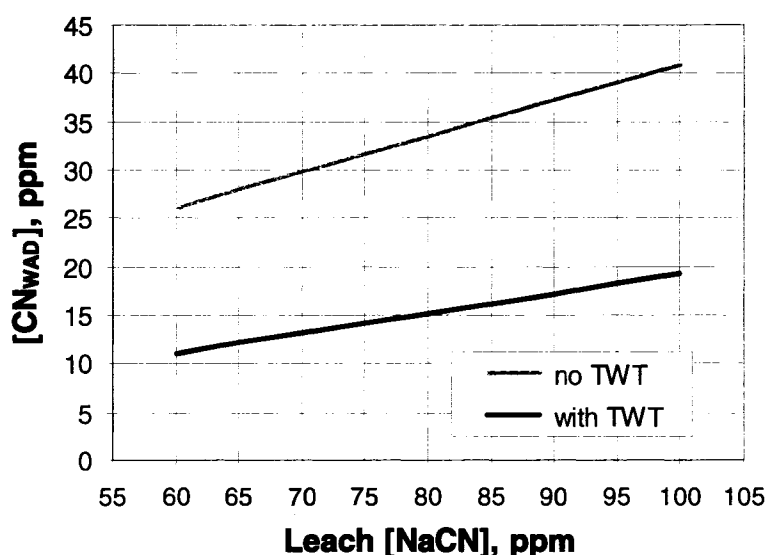


Figure 6.22 TWT effect on detox circuit feed slurry $[CN_{WAD}]$.

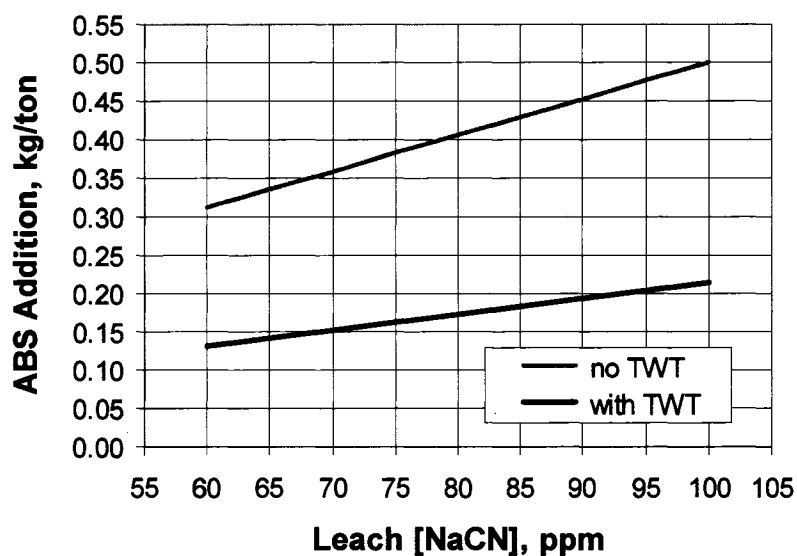


Figure 6.23 TWT effect on detox circuit ABS addition.

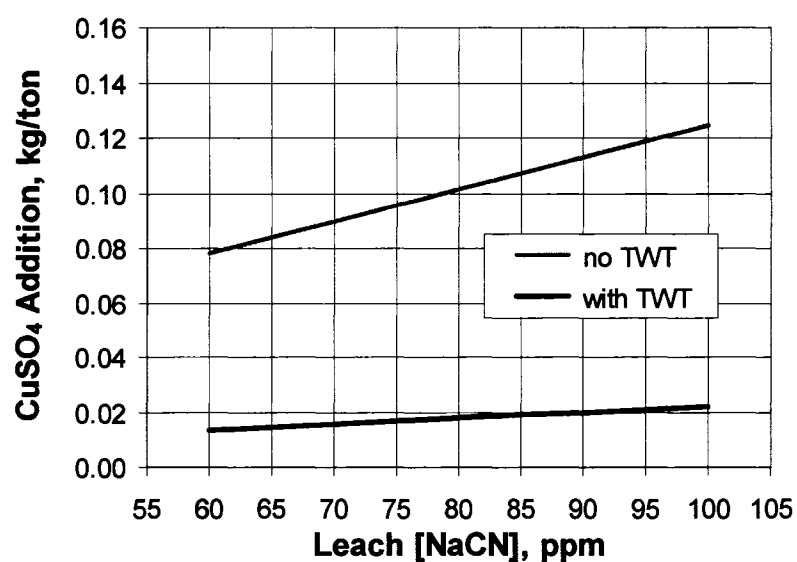


Figure 6.24 TWT effect on detox circuit copper sulfate addition.

6.5 TWT PROJECT SCHEDULE

Total construction from mobilization to demobilization was 157 days. The first concrete was placed 20 days after mobilization. No mill downtime was attributed to the

construction project, as the thickener was operationally tied into the existing circuits during scheduled mill downtime. .

The detailed design of the 90-foot diameter, high-compression thickener, selected for the Fort Knox application, began on December 14, 2001. The vendor was ultimately contracted to supply, fabricate, and erect the thickener on February 19, 2002. Total time required for the design, fabrication and erection of the thickener was 227 days and was the critical path task in the overall project schedule. The project schedule and key milestones are shown in Table 6.8.

Table 6.8 Project schedule and key milestones.

<u>DESCRIPTION</u>	<u>date</u>	<u>day</u>
Begin thickener detailed engineering	12/14/01	0
Begin facility detailed engineering	01/29/02	46
Begin thickener fabrication	02/19/02	67
Begin construction	04/29/02	136
Rough excavation by mine	05/23/02	160
General contractor mobilized	06/05/02	173
First concrete placed	06/25/02	193
Thickener contractor mobilized	07/08/02	204
Thickener erection complete	08/13/02	227
Tie into existing plant	09/11/02	246
Hydro-test thickener, etc.	10/02/02	264
Begin start-up	10/17/02	279
Building complete	11/07/02	300
General contractor demobilized	11/08/02	301
Attain normal production	11/10/02	303

<u>KEY ACTIVITY DURATION</u>	<u>DAYS</u>
Total thickener fabrication	120
Total thickener erection	38
Total building erection	58
(14 days lost to weather delays)	
Total construction to startup	143
Total construction contract duration	165

6.6 TWT PROJECT COST

Total project spending was \$6,624,000. FGMI direct purchases accounted for \$3,308,000 of the total spending with the remaining \$3,317,000 being the construction contract. The project cost summary is shown in Table 6.9.

Table 6.9 Project cost summary.

Total civil, \$US	22,000
Total concrete, \$US	947,000
Total steel, \$US	307,000
Total architectural, \$US	560,000
Total mechanical, \$US	1,994,000
Total piping, \$US	1,358,000
Total electrical, \$US	375,000
<u>Total instrumentation, \$US</u>	<u>198,000</u>
Total direct cost, \$US	5,761,000
Engineering services, \$US	298,000
Const. mgmt. & procurement. services, \$US	479,000
Mobilization. & demobilization., \$US	inc. above
Heavy construction equipment, \$US	inc. above
Freight, \$US	81,000
<u>Startup & commissioning, \$US</u>	<u>5,000</u>
Total indirect cost, \$US	863,000
Total project costs, \$US	6,624,000

Total project spending was \$1,161,000 (21%) over budget. In general, the variances were \$231,000 over budget spending on indirect costs and \$930,000 over budget on direct costs. Some post budget reengineering was required to address changes

to the Alaska building code and to add the thickener underflow dilution system. The following is a break down of the major spending variances from budget for the project.

1) Engineering and design changes after the budget was approved accounted for \$101,000 in additional project costs. The major changes occurred in concrete (\$38,000), building internal structural steel (\$32,000), and piping detail (\$27,500).

2) Items not included in the definitive cost estimate accounted for an estimated \$219,000; primarily the reclaim water line tie in (\$46,000) and no allocation for pipe supports (\$144,000).

3) Spending for contractor supplied equipment was underestimated by approximately \$150,000, since mine equipment, originally planned for use, was unavailable.

4) Spending for contractor supplied materials was approximately \$323,000 over budget; primarily internal structural steel (\$105,000) and piping (\$159,000).

5) The contract labor spending was estimated to be \$311,000 over budget. This resulted from underestimation of labor hours required to complete the project; primarily mechanical and piping.

6.7 POST TWT EXPANSION LEACH GOLD RECOVERY

The leach kinetics model (Hollow *et al.*, 2006) was applied to actual plant data for 2002 through 2005 and calibrated to account for monthly variation in the unleachable gold concentration $[Au_o]$ of the mill feed. Predicted and actual data for solid gold loss is presented in the Figure 6.25. The results indicate the model accurately estimated plant performance throughout that period.

With the solid tailings $[Au]$ model calibrated and the leach discharge solution gold concentration $[Au_{L7}]$ estimated, the CIP solution $[Au]$ model as originally defined (Hollow *et al.*, 2006) underestimated actual plant performance. Significant changes to the rate constants were observed and had to be redefined to match actual plant performance, after the TWT installation. It was hypothesized that the changes to the baseline rate

constants were the result of higher carbon activity, which was likely the result of the conditioning of the TSF reclaim water through the tailings thickener, resulting in a reduction of carbon fouling. Figures 6.26 shows this change and Figure 6.27 shows a timeline of the estimated effect of the TWT installation on solution gold concentrations in the CIP discharge.

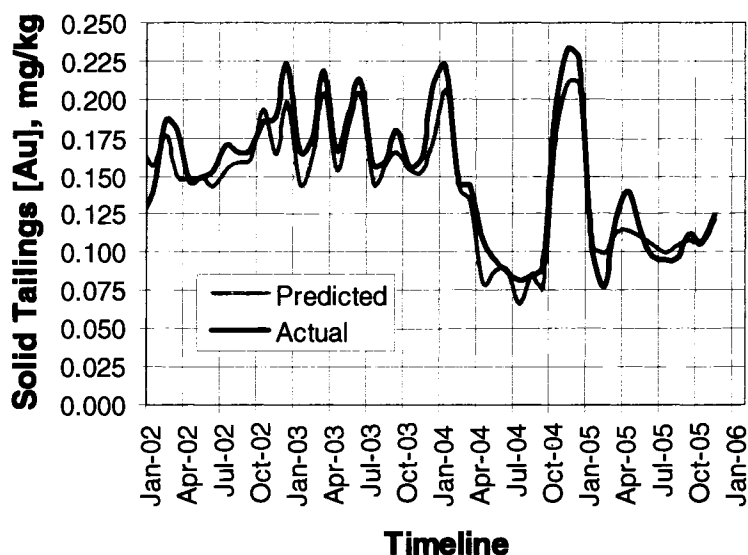


Figure 6.25 Actual vs. predicted solid tailings [Au].

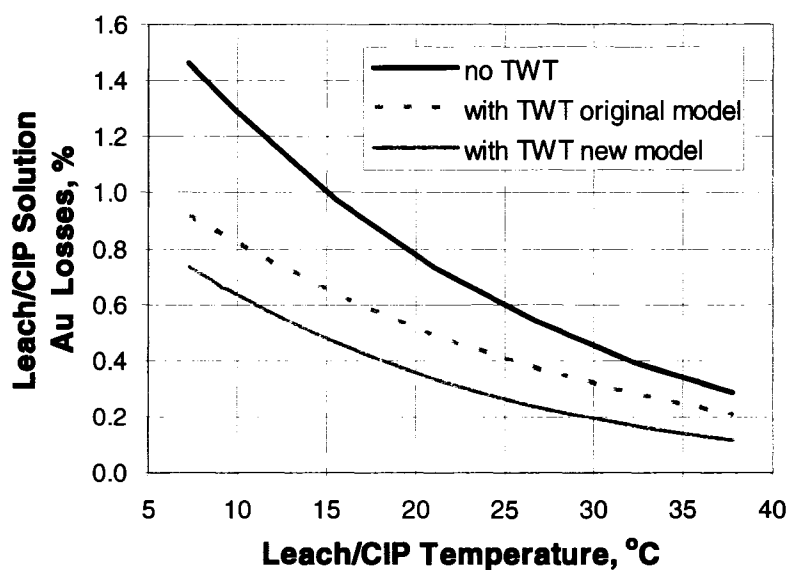


Figure 6.26 TWT effect on solution gold loss.

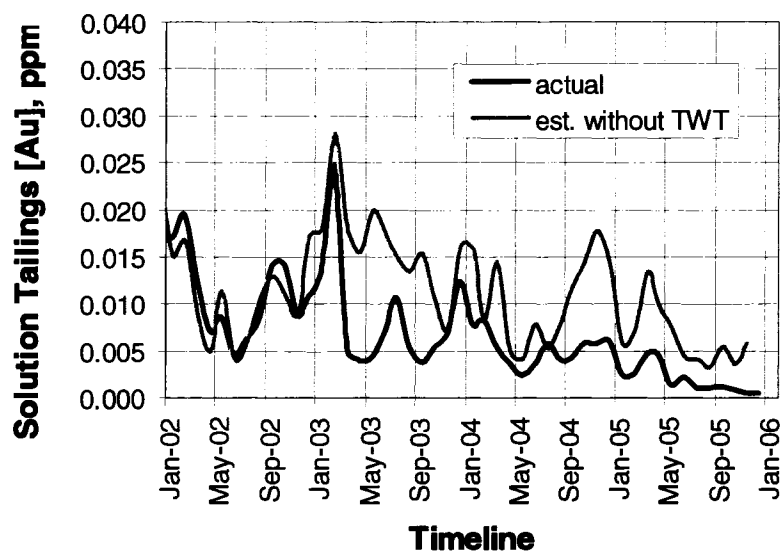


Figure 6.27 TWT effect on solution tailings [Au].

The increased gold production associated with the thickener expansion was estimated by comparing model predictions (for a circuit operated without a TWT) to actual operating data, for the circuit with a TWT. Figure 6.28 shows a timeline of the estimated effect of the TWT installation on leach gold recovery. Table 6.10 shows the estimated increases in gold production and revenues from adding the TWT.

Table 6.10 Estimated increase in gold production and revenue from adding a TWT.

	<u>2002</u>	<u>2003</u>	<u>2004</u>	<u>2005</u>	<u>Total</u>
Months in service	2	12	12	12	38
Leach feed ounces	84,034	406,681	360,100	306,484	1,157,299
Change in solid tails ounces (temperature)	-992	-4,009	-3,729	-3,083	-11,813
Change in CIP solution ounces (temperature)	-450	-1,437	-701	-396	-2,984
<u>Change in solution tails ounces (recycle)</u>	<u>-824</u>	<u>-2,202</u>	<u>-852</u>	<u>-480</u>	<u>-4,358</u>
Total change in tails ounces	-2,266	-7,648	-5,282	-3,959	-19,155
Increased revenue-gold sales, \$US	720,588	2,753,280	2,160,338	1,730,083	7,364,289
	<u>2002</u>	<u>2003</u>	<u>2004</u>	<u>2005</u>	<u>Average</u>
Mill throughput rate, tpd	37,028	36,772	35,854	35,537	36,105
Increase in leach gold recovery, %	2.70	1.88	1.47	1.29	1.66
Realized gold price, \$US/oz	318	360	409	437	384

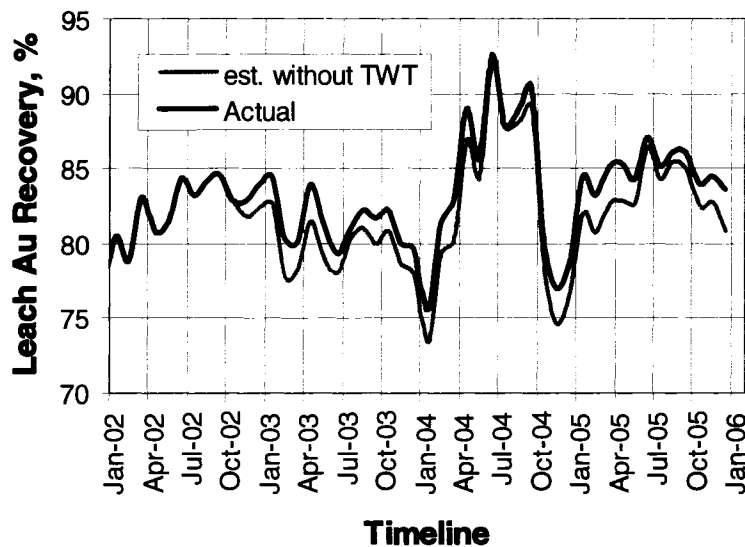


Figure 6.28 TWT effect on leach gold recovery.

The model predicted that gold in CIP solid tails would be reduced by 367.4 kg (11,813 oz) during the first 38 months following the TWT installation in October 2002. This change in gold recovery was due only to the change in slurry temperature, all other variables being held constant, and represents an increase in leach gold recovery of 1.02%. In addition, the increase in slurry temperature resulted in increased CIP efficiency, thus solution gold loss was reduced by 92.8 kg (2,984 oz) during the same period. This change in solution gold tails represents an increase in leach gold recovery of 0.26%.

Solution gold tailings were also reduced through recycling of the gold from the CIP tails to the thickener overflow tank. During the same 38 month time period, the makeup water recycled back to the grinding circuit contained an additional 135.6 kg (4,358 oz) of gold that would have been discharged to the TSF without the thickener operating. This represents an increase in leach gold recovery of 0.38%.

The actual improvement in total leach gold recovery associated with the thickener installation was 1.66% for the first 38 months of operation and compares favorably with the predicted value of 1.68% shown in Figure 6.20. However, due to above average solution gold losses in 2002 and 2003 nearly 23% of the total change in leach gold

recovery was associated with recycled solution gold ounces and 77% due to the increased temperature. The model predicted the values to be 13% and 87%, respectively.

6.8 POST TWT EXPANSION REAGENT USAGE

The original evaluation estimated 55% of the free cyanide discharging the CIP circuit would be recovered to the TWT overflow and returned to the grinding circuit as makeup water at baseline mill conditions. It was also assumed that a 1 to 1 reduction in new cyanide addition would be expected. However, when this assumption was compared to actual 2005 mill data, a period when only Fort Knox ore was processed and the TWT was being operated, the predicted new cyanide addition was overestimated (Figure 6.29).

No significant change in average ore characteristics was measured in 2005. Therefore, it is likely that the TSF water was being conditioned, when mixed with the CIP tails, and cyanide consuming constituents were neutralized prior to addition of new cyanide after grinding. This was also apparent in the cyanide consumption measured through the leach and CIP circuits.

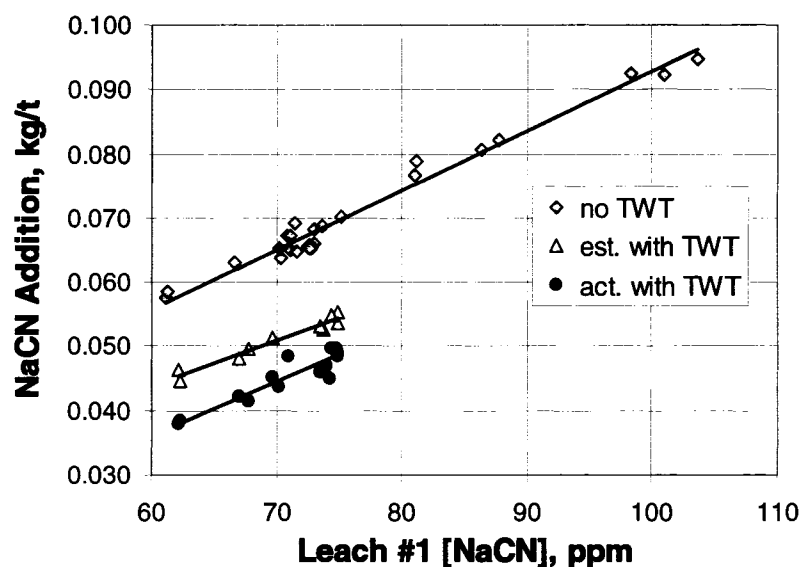


Figure 6.29 NaCN addition vs. leach [NaCN].

The average cyanide concentration in the CIP discharge changed significantly after the installation of the tailings thickener (Figure 6.30), while the average concentration leaving the leach circuit (Figure 6.31) remained consistent to pre-expansion performance, across the range of cyanide concentrations [NaCN] maintained in the leach circuit. This was attributed to higher overall carbon circuit activity and an increase in the carbon-catalyzed oxidation of cyanide to cyanate (Adams, 1990). The increased activity can, in part, be explained by the increase in slurry temperature (Hollow *et. al.*, 2006). However, the remaining increase in activity may be due to less carbon fouling by conditioned mill makeup water, since the carbon regeneration circuit was operated consistently throughout this time period.

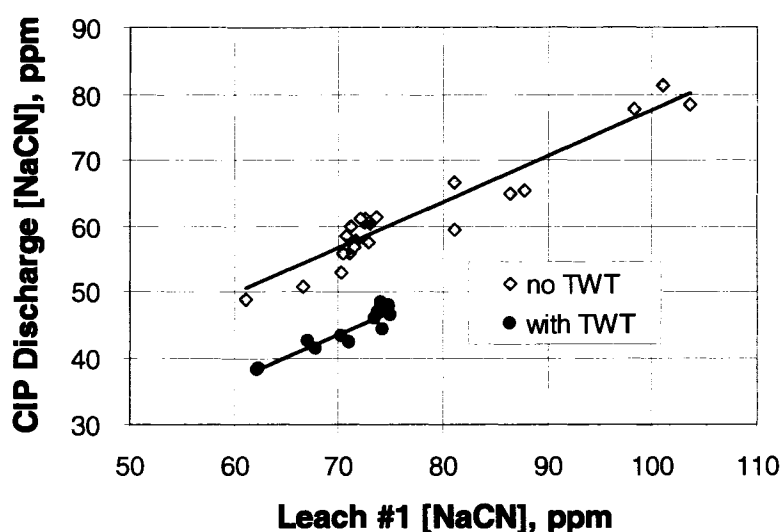


Figure 6.30 TWT effect on detox circuit feed [NaCN].

The effect of the TWT installation was also measurable in the lime addition required for pH control. Historically, slurry pH was maintained between 10.0 and 10.6 with no significant correlation between lime addition rate and the slurry pH set point. A weak correlation exists between slurry temperature and lime addition. It is likely that the temperature is an indicator variable with the actual increase in lime addition being attributed to the increase in organic acids in the TSF water, resulting from runoff into the

TSF during breakup and summer precipitation events. Figure 6.32 contains the relationships between the lime addition rate and circuit slurry temperature both with and without the TWT.

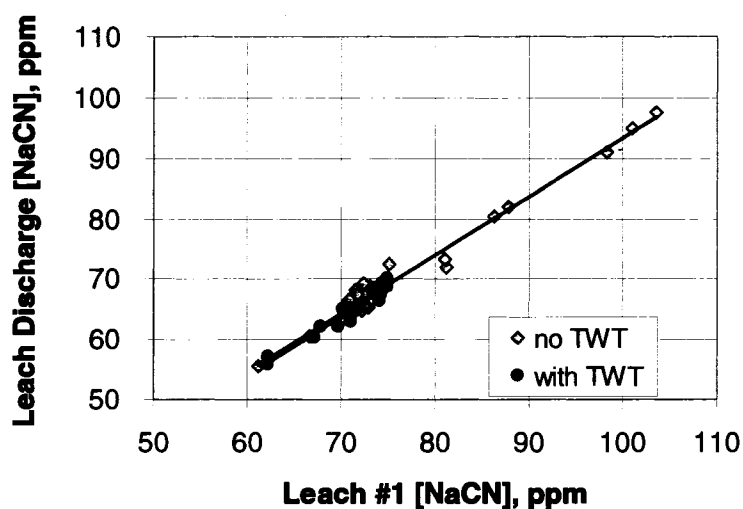


Figure 6.31 TWT effect on leach discharge [NaCN].

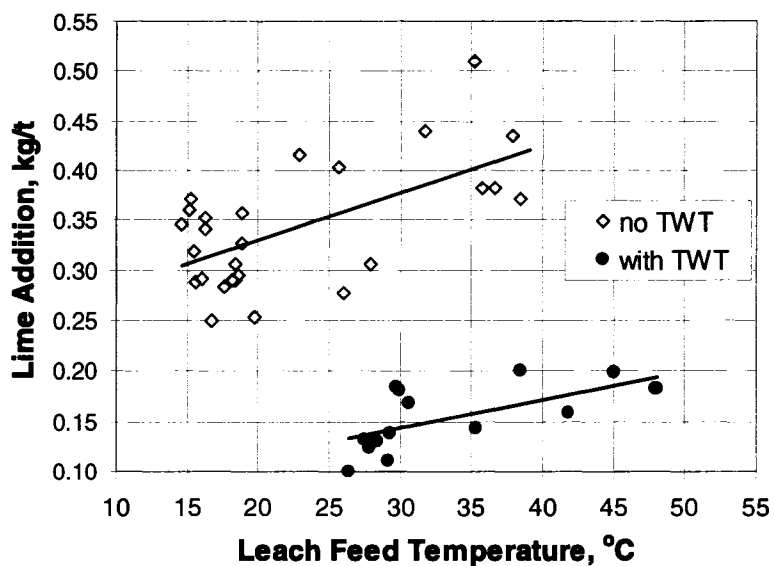


Figure 6.32 Lime addition vs. slurry temperature.

The data indicate that a significant reduction in lime addition resulted from the installation of the tailings thickener. This reduction is the result of lime (alkalinity) being recycled, similar to gold and cyanide, and it is theorized that additional benefit is realized due to the conditioning of the TSF water in the TWT prior to being added as makeup water in the grinding circuit. The reduction in lime usage was not thought to be significant originally and was not included in the original project justification.

As originally predicted, the installation of the TWT did not increase the slurry temperature in the cyanide destruction circuit, however, the reduction in the cyanide load in the TWT underflow was reduced in excess of the predicted values. This additional reduction was due to the increase in carbon catalyzed oxidation of cyanide in the CIP circuit. The recycling of cyanide to the thickener overflow occurred as predicted, with the percentage of cyanide recycled being a function of thickener underflow slurry density. Additionally, the percentage of cyanide recycled is a function of the weak acid dissociable cyanide concentration $[CN_{WAD}]$ in the water reclaimed from the TSF.

The percentage of cyanide recycled from the TWT decreased as the $[CN_{WAD}]$ of TSF water increases. This increase in concentration occurred during the period when the TSF was ice covered, typically from October through April. Figure 6.33 shows the seasonal variation in the TSF water $[CN_{WAD}]$. Figure 6.33 also contains a trend of the average $[CN_{WAD}]$ in the tailings slurry discharged to the TSF. The original project economics did not include this variable in the analysis.

When the baseline mill conditions are incorporated into the model, the TWT installation and the effect of TSF water $[CN_{WAD}]$ can be predicted. Figures 6.34 and 6.35 show the $[CN_{WAD}]$ in the CIP discharge and the TWT underflow as leach #1 $[NaCN]$ and TSF water $[CN_{WAD}]$ were varied over the expected operating ranges.

In addition to the reduction in $[CN_{WAD}]$ in the thickener underflow, the TWT expansion included a dilution loop that allowed the underflow slurry to be diluted with additional TSF water, in order to further reduce the $[CN_{WAD}]$, prior to discharge into the

TSF. This dilution loop allowed permit discharge limits to be met without operating the cyanide destruction circuit.

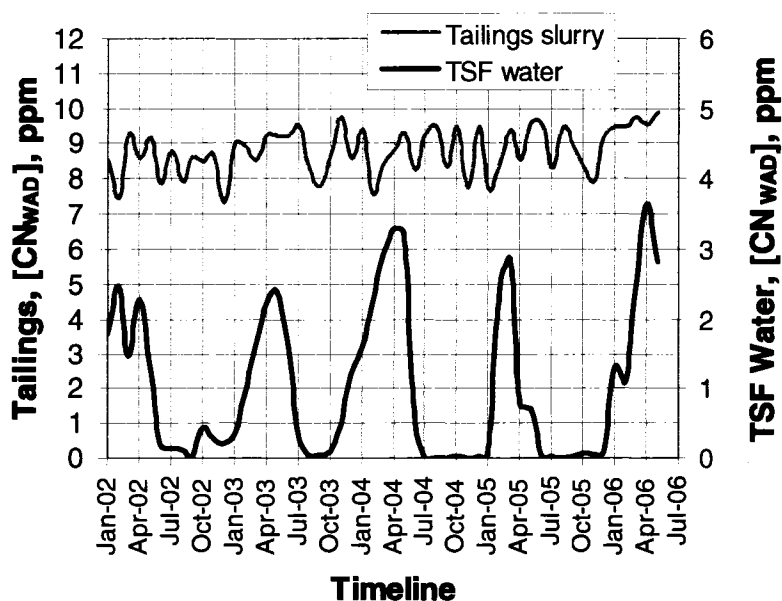


Figure 6.33 Historic TSF water and final plant tailings $[CN_{WAD}]$.

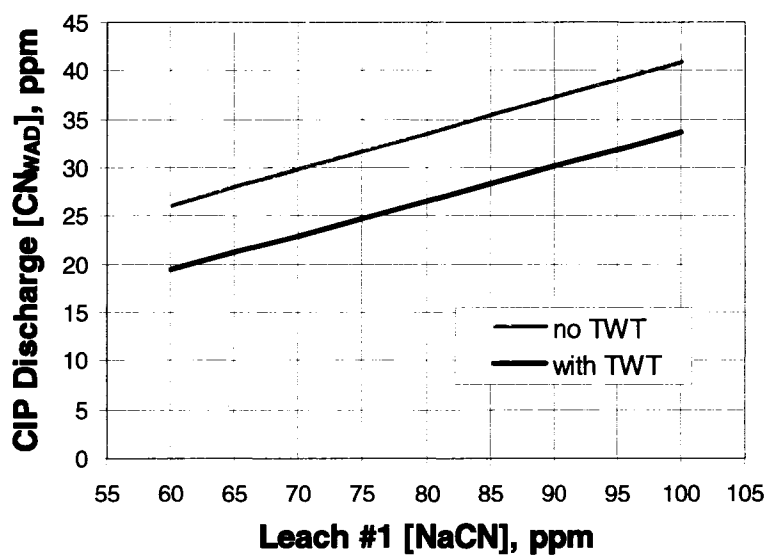


Figure 6.34 TWT effect on CIP discharge $[CN_{WAD}]$.

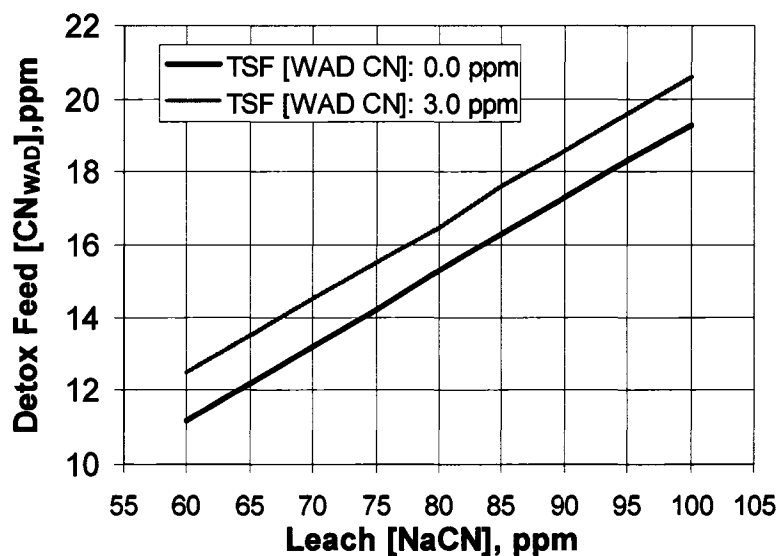


Figure 6.35 Effect of TSF [CN_{WAD}] on detox feed slurry [CN_{WAD}] with TWT.

The TWT flocculant requirements represent the only increase in mill reagents. Initial flocculant consumption was approximately 1.2 times that required at the preleach thickener. However, the consumption rate dropped substantially as operating experience was gained and reached 0.8 times the preleach thickener consumption rate in 2005. Table 6.11 contains a summary of the changes in reagent usage in the plant and the associated changes in reagent costs attributed to the TWT installation.

Expenditures for operating labor, maintenance labor and maintenance supplies required to run the tailings wash thickener/reclaim water system were more than offset by reductions in spending for the same categories in the cyanide destruction plant. In addition, the 375 kw load associated with the expansion and the 300 kw increase in the TSF water pumping requirements, due to water used to dilute TWT underflow slurry, were offset by the reduction in power required to operate the cyanide destruction circuit (575 kw for compressed air and 115 kw for the reactor agitation). A net cost savings was realized from these sources. However, no attempt was made to quantify these individual items and they were not included in the project financial analysis.

Table 6.11 Changes in reagent usage and reagent spending due to TWT installation.

	<u>2002</u>	<u>2003</u>	<u>2004</u>	<u>2005</u>	<u>Average</u>
Change in NaCN addition, %	-35	-35	-22	-32	-30
Change in lime addition, %	-23	-23	-23	-52	-33
Change in ABS addition, %	85	-85	-95	-100	-92
Change in copper sulfate addition, %	-80	-80	-95	-100	-90
Change in flocculant addition, %	117	117	54	55	82
	<u>2002</u>	<u>2003</u>	<u>2004</u>	<u>2005</u>	<u>Total</u>
Months in service	2	12	12	12	38
Change in NaCN spending, \$US	-104,015	-672,704	-331,831	-427,800	-1,536,350
Change in lime spending, \$US	-37,806	-229,438	-221,972	-587,249	-1,076,465
Change in ABS spending, \$US	-151,733	-910,395	-795,528	-759,054	-2,616,711
Change in copper sulfate spending, \$US	-122,272	-733,631	-675,252	-648,461	-2,179,615
<u>Change in flocculant spending, \$US</u>	<u>94,601</u>	<u>567,606</u>	<u>261,459</u>	<u>183,366</u>	<u>1,107,033</u>
Total change in spending, \$US	-321,224	-1,978,562	-1,763,124	-2,239,198	-6,302,108

6.9 PROJECT FINANCIAL ANALYSIS

After an initial investment of \$6,624,000 the TWT project generated \$11,453,000 in additional revenue through the first 38 months of operation. Cash flow analysis indicates the project had an 83.7% IRR, a payback period of 1.8 years, and a NPV of \$2,139,518, when evaluated at a 10% discount rate. The project will continue to generate positive value for the remaining life of the mine, currently estimated at seven years. A summary of the project financial analysis is contained in Table 6.12.

Table 6.12 Summary of project financial analysis

	<u>2002</u>	<u>2003</u>	<u>2004</u>	<u>2005</u>
Initial investment, \$US	-6,624,000			
Operating cost, \$US	-94,601	-567,606	-261,459	-183,366
Operating cost savings, \$US	226,623	1,410,956	1,501,665	2,055,832
<u>Additional revenue, \$US</u>	<u>720,546</u>	<u>2,753,413</u>	<u>2,160,592</u>	<u>1,730,472</u>
Net cash flow, \$US	-6,624,000	852,568	3,596,763	3,400,798
Cum cash flow, \$US	-6,624,000	-5,771,432	-2,174,669	1,226,129
Present value of cashflow, \$US	-6,624,000	775,062	2,972,531	2,555,070
Annual discount rate, %		10.0		
Project NPV (at 38 months), \$US		2,139,518		
IRR (at 38 months), %		83.7		
Paypack period, yrs		1.8		

6.10 CONCLUSIONS

- An equilibrium energy balance model was developed assuming, heat input to the system must equal heat removed from the system. The model includes a water and ore mass balance for the process streams throughout the plant. Heat content (W_H) for each of the components was calculated based on the following equation:

$$W_H = c_p Q T$$

- Results suggest that 98% of grinding energy was converted to heat, with $\leq 2\%$ being utilized for the fragmentation of ore particles. Additional results suggest that 75% of slurry pumping energy was converted to heat.
- The model-predicted leach feed slurry temperature correlated strongly ($R^2=0.96$) with actual plant data between May 2002 and December 2005, over the temperature range experienced at the Fort Knox Mine (10°C to 38°C).
- Leach and CIP tank heat transfer was minimal, in general less than 1°C during the average 20 hour retention time of the circuit. The net heat exchange per unit area between the air-tank surfaces was calculated as follows:

$$\Delta H = [(H_s - H_{sr}) + (H_a - H_{ar})] - (H_{br} \pm H_c \pm H_e)$$

The first group of terms in brackets, called the net absorbed radiation is independent of the tanks (slurry) temperature and can be measured directly or computed from meteorological observations. The second group of terms depends in various ways, on the temperature differential between the tanks surface and the ambient air.

- Heat recovery, and the increase in mill makeup water temperature, increased with increasing thickener underflow density. Substantial increases in leach/CIP and slurry temperatures will be realized if attempts are made to maximize the TWT underflow density.

- During the initial 38 months of operation with the TWT in the circuit, gold production was increased by 595.8 kg (19,155 oz), a 1.66% increase in leach gold recovery. Nearly 77% of the increased gold production was due to the increased leach/CIP slurry temperature, while the remaining 23% resulted from recycle of solution gold values back to the grinding circuit.
- Spending for mill reagents was reduced by US\$ 6,302,000, during the same 38 month period. This saving was the result of a reduction in the required lime addition to grinding, increased cyanide consumption in the CIP circuit, recovery of NaCN prior to destruction, and dilution of the remaining cyanide to below permit levels without destruction.
- The initial investment of US\$ 6,624,000 had a pay back period of 1.8 years. At the end of 38 months, the project had an IRR of 83.7% and a NPV of \$2,139,518 at a 10% discount rate.

REFERENCES

- Adams, M.D., 1990, *The chemical behaviour of cyanide in the extraction of gold. 2. Mechanisms of cyanide loss in the carbon-in-pulp process*, J.S. Afr. Inst. Min. Metall., Vol. 90, No. 3, pp. 67-73.
- Henderson, R., 2000, HATCH Engineering, personal communication.
- Hollow, J.T., 2002, *Modeling the influence of slurry temperature on the cyanide destruction plant at the Fort Knox Mine, Fairbanks, Alaska*, Internal FGMI report.
- Hollow, J.T., Hill, E.M., Lin, H.K. and Walsh, D.E., 2003, *The effect of $Pb(NO_3)_2$ addition on the processing of blended Fort Knox and True North ores at the Fort Knox Mine*, Minerals and Metallurgical Processing, Vol. 20, No. 4, pp. 185-190.
- Hollow, J.T., Hill, E.M., Lin, H.K. and Walsh, D.E., 2006, *Modeling the influence of slurry temperature on gold leaching and adsorption kinetics at the Fort Knox Mine, Fairbanks, Alaska*, Minerals and Metallurgical Processing, Vol. 23, No. 3, pp. 151-159.

- Hukki, R.T., 1975, *The principles of comminution: An analytical summary*, Eng. Min. J., Vol. 176, pp. 106-110.
- Kelly, E.G. and Spottiswood, D.J., 1989, Introduction to Mineral Processing, John Wiley and Sons, p. 113.
- Lin, H.K., Oleson, J.L., Hollow, J.T. and Walsh, D.E., 2002, *Characterization and flotation of gold in carbon fines at the Fort Knox Mine, Alaska*, Minerals & Metallurgical Processing, Vol. 19, No. 1, pp. 21-24.
- Oleson, J.L., Lin, H.K. and Walsh, D.E., 2005, *Modeling of SO₂/air cyanide destruction process*, Minerals & Metallurgical Processing, Vol. 22, No. 4, pp. 199-204.
- Thomann, R.V. and Mueller, J.A., 1987, Principles of Surface Water Quality Modeling and Control, Harper Collins Publishers, Inc., New York, pp. 599-613.
- Van Drunick, W.I. and Moys, M.H., 2001, *The use of an energy balance to measure and control the rheology of mill discharge slurry*, Third International Conference on: Autogenous and Semiautogenous Grinding Technology 2001, Editors: D.J. Barratt, M.J. Allan, and A.L. Mular, Vol. 2, pp. 304-316.

CHAPTER 7

RECOMMENDATIONS FOR FUTURE WORK

In Chapters 2 and 3, it was proposed that a passivating film on free gold particles reduced gold recovery when Fort Knox and True North ores were blended, and processed through the Fort Knox mill. It was also proposed that the passivating film was the result of stibnite dissolution and that the level of reduced gold extraction was a function of gold particle size. The retarding effect of the passivating film was substantially reduced through the addition of lead nitrate. The following research would further define the proposed surface chemistry mechanisms:

- Determine the chemical speciation of the passivating film and the mechanism of the film formation.
- Determine the dissolution kinetics of both oxide and sulfide antimony minerals.
- Evaluate the kinetics of film formation and gold leaching as a function of gold particle size.
- Determine the gold particle surface reactions and the mechanism by which lead nitrate dissolution products interfere with the passivating film formation.

In Chapter 4, it was proposed that variations in slurry rheology result in measurable impacts to reactions controlled by diffusion, and these impacts can be predicted using temperature as the independent variable. Models were developed that predict gold dissolution in cyanide solution, gold-cyanide complex adsorption onto activated carbon and cyanide oxidation in the SO_2/O_2 reactors, utilizing temperature as an independent variable. The following research would further define the proposed slurry viscosity effect on cyanidation plant efficiencies:

- Evaluate the influence of slurry temperature and viscosity on reactor mixing efficiencies.
- Evaluate the influence of slurry viscosity and reactor mixing efficiency on cyanidation reaction kinetics.

- Evaluate the relationship between slurry temperature and slurry viscosity.
- Evaluate the relationship between slurry temperature and the efficiency of power usage in grinding mills.
- Evaluate the relationship between slurry temperature and cyclone separation efficiency.

In Chapter 6, an energy balance approach was used to accurately model slurry temperatures throughout the process facility at the Fort Knox mine. Results suggested that 98% of grinding energy and 75% of slurry pumping energy was converted to heat that increased the slurry temperature. The following research would further define the proposed energy conversion to heat:

- Measure the effect of grinding energy input on the increase in milled slurry temperature.
- Measure the effect of pumping energy input on the increase in slurry temperature through a pumping system.

Also in Chapter 6, it was proposed that processing of reclaimed tailings storage facility water through the tailings wash thickener (TWT), prior to use in the grinding circuit, resulted in an unanticipated reduction in operating costs. The added benefit was thought to result from the water being conditioned by the plant tailings slurry when mixed in the TWT. The following research would further define the proposed conditioning effect of the TWT operation:

- Research the impact to plant water chemistry, due to the installation of the TWT
- Research the impact to cyanidation reagent consumptions, due to changes in water chemistry.
- Evaluate the impact to activated carbon activity, due to variations in solution water chemistry